MICRODIALYSIS COUPLED ON-LINE WITH CAPILLARY ELECTROPHORESIS: IN VIVO MONITORING IN THE RAT STRIATUM

By

MARK WITOLD LADA

A DISSERTATION PRESENTED TO THE GRADUATE SCHOOL
OF THE UNIVERSITY OF FLORIDA IN PARTIAL FULFILLMENT
OF THE REQUIREMENTS FOR THE DEGREE OF
DOCTOR OF PHILOSOPHY

UNIVERSITY OF FLORIDA

1997

To my parents for their wisdom and guidance and my wife for her continuous encouragement and boundless love and support.

ACKNOWLEDGMENTS

I would like to thank Dr. Robert T. Kennedy for his scientific guidance and support as my graduate research advisor and mentor. I would also like to thank all of the members of the Kennedy Research Group, both past and present, for their scientific advice and camaraderie. I would also like to express my gratitude to Dr. Thomas Vickroy for his expertise and assistance regarding our *in vivo* studies. Financial support was granted from NSF, NIH, and the Herbert Laitinen Fellowship.

TABLE OF CONTENTS

page

LIST OF ABBREVIATIONS

AMPA	α-amino-3-hydroxy-5-methylisoxazole-4-propionate
ACPD	(1S,3R)-1-aminocyclopentane-trans-1,3-dicarboxylic acid
aCSF	artificial cerebral spinal fluid
AP	anterior-posterior
Asp	aspartate
β-ME	beta-mercaptoethanol
BP	band pass
CE	capillary electrophoresis
CHES	2-(N-cyclohexylamino)ethanesulfonic acid
Cys	cysteine
CZE	capillary zone electrophoresis
Da	dalton
DV	dorsal ventral
EAA	excitatory amino acid
EGTA	bis-(aminoethyl)glycoether-N,N,N',N'-tetraacetic acid
ED	electrochemical detection
GABA	γ-aminobutyric acid
Glu	glutamate
GSH	glutathione
He-Cd	helium-cadmium
HEPES	N-(2-hydroxyethyl)piperazine-N'-(2-ethanesulfonic acid)
HPLC	high performance liquid chromatography
i.d.	inner diameter
Ile	isoleucine
KA	kainate

LC	liquid chromatography
Leu	leucine
LIF	laser induced fluorescence
LP	long pass
Lys	lysine
mBBr	monobromobimane
MCPG	(RS)-α-methyl-4-carboxyphenylglycine
MD	microdialysis
MEKC	micellar electrokinetic chromatography
Met	methionine
ML	medial-lateral
mGluR	metabotropic glutamate receptor
MS	mass spectrometry
NMDA	N-methyl-D-aspartate
NDA	naphthalene dicarboxyaldehyde
o.d.	outer diameter
OPA	ortho-phthaldialdehyde
PDC	L-trans-pyrrolidine-2,4-dicarboxylic acid
PFC	prefrontal cortex
Phe	phenylalanine
PMT	photomultiplier tube
PTFE	teflon
SEM	standard error of the mean
Tau	taurine
TTAB	tetradecyl trimethyl ammonium bromide
TTX	tetrodotoxin
Tyr	tyrosine
Val	valine

Abstract of Dissertation Presented to the Graduate School
of the University of Florida in Partial Fulfillment of the
Requirements for the Degree of Doctor of Philosophy

MICRODIALYSIS COUPLED ON-LINE WITH CAPILLARY ELECTROPHORESIS: IN VIVO MONITORING IN THE RAT STRIATUM

By

Mark Witold Lada

December 1997

Chairman: Robert T. Kennedy
Major Department: Chemistry

A fully automated analytical method for monitoring biologically significant chemicals in the extracellular space of the rat striatum was developed using capillary electrophoresis (CE) with both UV-Vis absorbance and laser-induced fluorescence (LIF) detection. Microdialysis probes placed in the striatum of anesthetized rats were coupled on-line with the CE system by an automated flow-gated interface. Analytes not detectable by absorbance were derivatized on-line with either o-phthaldialdehyde/β-mercaptoethanol or monobromobimane and detected by LIF using the 354 nm line of a 2 mW helium-cadmium laser for excitation. The relative recovery was nearly 100% for all analytes at 79 nL/min and quantitative monitoring was possible. The basal and stimulated concentration levels of ascorbate, lactate, primary amines including the neurotransmitters glutamate, aspartate, and taurine, and thiols including glutathione and cysteine were monitored with 45-180 s time resolution. This system was the first to obtain high relative recoveries of

biologically active analytes and high time resolution simultaneously with microdialysis sampling.

By incorporating a strategy for rapid CE separations, which included increasing electric field strength and detector sensitivity while decreasing separation capillary length and injection time, it was possible to monitor the neurotransmitters glutamate and aspartate *in vivo* with 5-s sampling intervals. Rapid CE separations coupled with high dialysis flow rates (1.2 μL/min) allowed for 12-14 s temporal resolution. With such high temporal resolution, it was possible to monitor rapidly occurring events *in vivo*. For example, first-ever measurement of electrically stimulated overflow of the neurotransmitters glutamate and aspartate in the rat brain using microdialysis sampling was accomplished with this system. These substances were confirmed to be of a neuronally derived origin. In addition, observance of uptake inhibitor effects on glutamate/aspartate dynamics as well as functional metabotropic autoreceptors *in vivo* was achieved. Finally, this was the first separation-based system using microdialysis sampling that exhibited sensor-like monitoring *in vivo* while maintaining multi-analyte detection capabilities.

CHAPTER 1
INTRODUCTION

Traditionally, most neurochemical studies of the brain have been performed by analyzing postmortem brain tissue slices and homogenates for various endogenous and exogenous chemicals (Tossman et al., 1986a). This provided for crude, yet reliable, measurements reflective of intracellular contents of the tissue, but not of the extracellular space. It is in the extracellular space, however, where communication between the cells of the nervous system transpire and where most drugs interact with nervous system function. In fact, due to the presence of the blood-brain barrier, the extracellular space is a separate entity between the blood and the cytoplasm of the cells. This space, comprising approximately 20% of the total tissue volume, is the intersection of an incredible number of chemical substances on their way between cells, nerves, and blood vessels (Ungerstedt, 1984). Body nutrients diffuse from the blood vessels to the cells, while metabolites migrate in the opposite direction. Neurotransmitters leave neural synapses, ions travel rapidly over cell membranes and ion channels, and various chemical messengers circulating in the blood enter the extracellular space through the blood-brain barrier. Therefore, in part because of the limitations associated with primitive *in vitro* methods and in part because of the fascination of relating neurochemical phenomena with behavior and physiology, there has been considerable interest in the development of *in vivo* neurochemical methods capable of monitoring the intricate and information-filled extracellular space of the brain.

In vivo methods that were developed to sample from the extracellular space of the brain, such as push-pull perfusion, have been in existence for many years (Gaddum, 1961; Myers, 1972; Delgado et al., 1972). However, push-pull perfusion requires extracellular fluid to be simultaneously delivered and withdrawn at high flow rates from the tissue sampled, thus creating numerous disadvantages, such as tissue disturbance and damage. More recently, *in vivo* microdialysis has emerged as a powerful bioanalytical tool for closely monitoring not only the extracellular environment of the brain, but also a variety of other organs, tissues, and bodily fluids *in vivo* (Ungerstedt, 1984). As a result, microdialysis has grown to become an important sampling technique for biomedical, pharmaceutical, and neuroscience applications (Ungerstedt, 1984; Lunte et al., 1991).

The Microdialysis Probe

In vivo microdialysis involves the implantation of a microdialysis probe into living tissue. Upon stereotaxic placement of the probe, essentially every chemical event taking place in the sampling region can be monitored. This all-inclusive type of sampling is mainly due to the tip of the dialysis probe, which is typically constructed from semipermeable membranes, such as cellulose (MW cutoff of 6 kDa), cuprophan (12 kDa), polycarbonate (20 kDa), polyacrylonitrile (40 kDa), or cellulose acetate (70 kDa). Substances in the extracellular fluid diffuse through the pores of the membrane and into the perfusate, while substances in the perfusate diffuses into the tissue. The diffusion of chemical substances will occur in the direction of the lower concentration. In this way, substances may be recovered from an organ or added to the organ depending upon their relative concentration. Beside concentration gradients, diffusion of substances into the

membrane are also affected by steric characteristics of substances. For instance, if the molecular weight of a particular substance is less than the MW cutoff of the membrane, it will diffuse across the membrane and into the probe. If the MW of the substance is greater than the MW cutoff, the molecule will be excluded. As a result, samples are protein-free and ready to analyze without further cleanup. The resulting perfusate is then collected and analyzed by the appropriate analytical technique. The dialysate collected is a measure of the extracellular fluid surrounding the membrane of the microdialysis probe.

Three types of probe geometries are commonly used in microdialysis. They include loop, concentric, and side-by-side style probes (Ungerstedt, 1984). A loop-style probe, which is used in this work, is illustrated in Figure 1-1. It consists of two parallel fused silica capillaries connected by a hollow dialysis fiber. The tip diameter is typically 0.5 mm while the tip length is typically 1-4 mm. An isotonic perfusion fluid flushes the interior of the membrane at a constant flow rate, usually 0.5-2.0 μL/min, and is then collected and analyzed.

Microdialysis Features

Compared with the other *in vivo* sampling methods, microdialysis provides cleaner samples for the analytical method and minimizes tissue damage since the flowing sample stream is not in direct contact with the tissue. Microdialysis distinguishes itself from other *in vitro* and *in vivo* techniques in other ways as well. For example, microdialysis directly collects a representative sample in almost every organ and tissue of the body, including blood. It can sample from intact tissue while recovering and/or introducing endogenous and exogenous substances in the tissue continuously for hours or days in a single animal.

In addition, it carries collected samples out of the body and makes them accessible to conventional analytical techniques. As a result, microdialysis provides the most convenient and practical method for sample collection.

Recovery Characteristics of the Probe

The recovery of substances from the extracellular fluid depends on several factors, including length of dialysis membrane, perfusion rate, temperature, molecular weight of the substance, molecular shape of substance, and binding to the membrane and tubing. For example, recovery is directly proportional to the size of the dialysis membrane surface area. As the length of the membrane increases, more surface area is available for substances to diffuse into the probe. Recovery is also inversely proportional to perfusion rate. Low perfusion rates allow more time for the substances to diffuse into the probe, resulting in increased recovery. Temperature is also important; recovery may increase as much as 30% if the temperature of the sampling medium is increased from 23°C to 37 °C (Menacherry et al., 1992). Therefore, it is extremely important to perform *in vitro* probe calibrations at temperatures identical to the *in vivo* conditions, typically 37 °C.

As mentioned in the previous section, if the molecule is larger than the membrane pore size or if the molecular weight of the analyte is more than the molecular weight cutoff of the probe, it simply will not diffuse through the membrane pores. It is advantageous to select a dialysis membrane with a MW cutoff at least 5-10 times the molecular weight of the sample to be analyzed, thus ensuring adequate diffusion through the membrane pores. Finally, non-specific binding of analytes are also problematic, especially when dealing with peptides and proteins. Typically, the recoveries of peptides

and proteins are substantially less than the recoveries of small molecules such as amino acids and monoamines.

Quantification

A fundamental problem of microdialysis is the quantification of the extracellular concentration of the analytes in the tissue. Quantification is made difficult by the fact that the analyte never equilibrates across the probe membrane because the interior of the probe is continuously perfused. Thus, the relative recovery of the probe, defined as the ratio of the concentration in the dialysate to the actual concentration outside the probe, must be known in order to quantify substances. It has been demonstrated that the relative recovery measured *in vitro* can differ significantly from that obtained *in vivo*, making *in vitro* calibrations unreliable for quantitative purposes (Benveniste et al., 1989; Bungay et al., 1990; Parsons and Justice, 1992). In the brain, this difference has been attributed to an altered diffusional environment and active supply and consumption of compounds *in vivo* (Benveniste et al., 1989; Bungay et al., 1990; Morrison et al., 1991). The active supply and consumption refers to metabolic processes, high-affinity uptake, and release.

Three mathematical methods for *in vivo* calibrations have been derived; they include the no-net flux, zero-flow, and near-equilibrium dialysis methods. In the no-net flux method, the loss or gain of an endogenous compound is measured while that compound is added to the perfusion solution at several different concentrations. Linear regression is then used to calculate the point where diffusion no longer occurs, that is, when the concentration at the probe inlet is the same as the outlet. Although a very accurate method, this calibration model can be long and cumbersome, resulting in day-

long calibrations before any *in vivo* experiments can be performed. In the zero-flow method, dialysate concentrations are measured at several perfusion flow rates. Non-linear regression is then used to estimate the extracellular concentration at zero flow rate, that is, at 100% recovery. Finally, the near equilibrium method uses as low a flow rate as practically possible so that the diffusion time is long enough to allow equilibration of the concentrations on both sides of the membrane. Calculations are unnecessary and the true extracellular concentration is measured. This is the easiest and fastest calibration method to perform, and can be accurate and precise if an on-line system is developed to handle the small samples collected at low flow rates.

Temporal Resolution

Of course, microdialysis is only a sampling technique, and must be coupled to an appropriate analytical method. In most cases, microdialysis has been used for chemical monitoring by collecting dialysate in fractions and then analyzing the fractions by HPLC (Wages et al., 1986), mass spectrometry (Menacherry and Justice, 1990), immunoassay (Maidment et al., 1989), or capillary zone electrophoresis (Hogan et al., 1994; O'Shea et al., 1992; Hernandez et al., 1993a; Hernandez et al., 1993b). The temporal resolution, typically defined as the time necessary to collect a detectable quantity of analyte, ranges from 10 to 30 min for the off-line case. For example, it would take 30 min to collect 30 μL of dialysate using a perfusion rate of 1 μL/min. It is therefore of interest to use analytical methods with high mass sensitivity. It also possible to couple the microdialysis probe on-line to an analytical method for convenient monitoring of concentration changes in close to real time (Wages et al., 1986; Hogan et al., 1994; Kuhr and Korf, 1988;

Caprioli and Lin, 1990; Zhou et al., 1995; Chen and Lunte, 1995; Church and Justice, 1987). The temporal resolution now becomes limited by the analytical method, and not the time necessary for adequate sample collection. The analysis time is just too long to keep pace and utilize the continuous stream of sample; as a result, it has become desirable to couple fast analytical methods, whether separation, mass spectrometric, or electrochemically based, to microdialysis. Indeed, microdialysis is powerful since it can be coupled with a variety of analytical methods, resulting in the ability to simultaneously monitor a large variety of endogenous and exogenous compounds.

Spatial Resolution

Another limitation of microdialysis sampling involves poor spatial resolution and the damaging effect of sampling on tissue. Although less obtrusive than push-pull perfusion, the dialysis probes are large enough to cause damage and poor spatial resolution in small sampling environments such as rodent brain structures. In addition, when probes are operated to maximize absolute recovery, typically at 1-10 μL/min flow rates, they will remove compounds from a relatively large area around the probe. The concentration gradients that develop can extend for several millimeters away from the probe thus decreasing spatial resolution. This distance will also depend on the *in vivo* regulation of the compound. The continual removal of analytes and other compounds by the dialysis probes can also alter or adversely affect the tissue under investigation.

Microdialysis Coupled On-Line with Capillary Electrophoresis.

In this work, an automated analytical method for monitoring physiologically significant chemicals in the rat brain has been developed by coupling microdialysis on-line with capillary electrophoresis (CE), and using both UV-Vis absorbance and laser-induced fluorescence (LIF) for detection. Although small volume techniques with high mass sensitivity such as CZE and capillary LC have already been interfaced on-line to microdialysis (Hogan et al., 1994; Menacherry et al., 1992), it has been our emphasis to produce a convenient and practical method for quantification of analytes using microdialysis and to improve temporal resolution by decreasing sampling times. As a result, we have created a multi-analyte, separation-based system with sensor-like characteristics, that is, fast temporal responses. The interfaces that have been previously designed not only are incompatible with low perfusion flow rates, but also exhibit poor analyte transfer efficiencies and temporal resolution (Zhou et al., 1995; Hogan et al., 1994).

The use of low dialysis flow rates which are compatible with this flow-gated interface, combined with a technique which has high mass sensitivity, would eliminate or ameliorate many of the disadvantages associated with quantification, temporal resolution, spatial resolution, and tissue disturbance. With low dialysis flow rates, the relative recovery approaches 100% which makes *in vitro* calibration reliable. In fact, low flow rates have been used as a calibration method; however, the sampling time was so long that it was not practical to operate the system continuously (Menacherry et al., 1992). The increased concentration of sample that is removed at low flow rates also improves the

detection limit for concentration sensitive measurements. With low flow rates, the concentration gradients developed by the probe would be less which would improve the spatial resolution and decrease the disturbance to the tissue (Morrison et al., 1991). Finally, a system which could utilize low flow rates would be compatible with smaller probes, which could further improve the spatial resolution.

Alternatively, high dialysis flow rates (1.2 µl/min) coupled with high-speed separations can also be used with this system, thus further improving the temporal resolution. Although advantages due to low flow rates, such as simple quantification and higher analyte concentrations, would be sacrificed with high flow rates, superior temporal resolution can be gained. As a result of higher time resolution, it would be possible to monitor rapidly occurring events, such as electrically stimulated release of neurotransmitters from neurons in the rat brain, and quite possibly would allow for future measurements not previously possible with microdialysis.

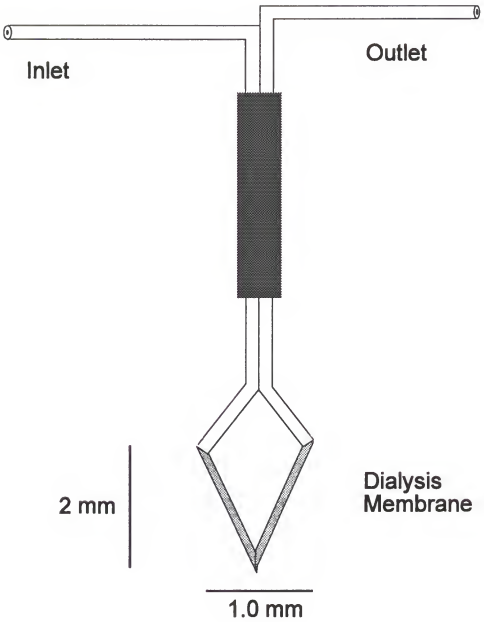

Figure 1-1. Diagram of a loop-style microdialysis probe. The microdialysis probe (ESA, Bedford, MA) is of a flexible loop design with a 0.5 mm tip diameter and a 2 mm tip length. The probes utilized fused silica tubing (150 μm o.d.) as inlet and outlets to the probes. The probe tip is made of cellulose fibers and has a molecular weight cutoff of 6 kDa.

CHAPTER 2
ON-LINE INTERFACE BETWEEN MICRODIALYSIS AND CAPILLARY ZONE ELECTROPHORESIS

Introduction

In this chapter, an interface between microdialysis and CZE that allows the probe to be operated at flow rates as low as 79 nL/min while maintaining sampling times of 85 s is described and characterized. The flow-gated interface design that is used in this work was first reported by Lemmo and Jorgenson for the coupling of capillary LC to CZE in a two-dimensional separation system (Lemmo and Jorgenson, 1993). This work demonstrates, for the first time, a method for utilizing low microdialysis flow rates without sacrificing time resolution. As a demonstration of the system, ascorbate was monitored in the striatum of a rat brain. Ascorbate is a convenient test analyte because it is present in high concentrations in the brain (Grunewald, 1993). Ascorbate is of interest because of its putative role in consciousness (Crespi et al., 1992), aging (Svensson et al., 1993), glutamate uptake (Grunewald, 1993), and as an antioxidant (Lyrer et al., 1991). It may also play a role as a neuromodulator or neuroprotective agent in the brain. It has been monitored *in vivo* by both voltammetry (Basse-Tomusk and Rebec, 1991; Boutelle et al., 1990) and microdialysis (Brazell et al., 1990; Clemens and Phebus, 1984; Grunewald, 1993).

Experimental

Electrophoresis Conditions

All separations were performed in 25 μm inner diameter (i.d.) by 360 μm outer diameter (o.d.) fused silica capillaries coated with polyimide (Polymicro Technologies, Phoenix, AZ). The capillaries were 50 to 60 cm long with 15 cm from point of injection to the detector cell. Each day, capillaries were treated with successive ten-minute rinses of 0.1 M NaOH, distilled water, and electrophoresis buffer. The electrophoresis buffer consisted of 25 mM sodium phosphate dibasic and 0.52 mM tetradecyltrimethylammonium bromide (TTAB) at pH 7.0. A Spellman 1000R CZE Reversible HV power supply (Plainview, NY.) was used to apply the voltage. On-column detection was accomplished using a Spectra 100 variable wavelength detector equipped with a capillary flow cell (Spectra-Physics, San Jose, CA). The CZE capillary had a small length of the polyimide coating (approximately 5 mm) removed to allow UV absorbance measurements to be made. The detector was set at 265 nm and 0.1 s rise time. Data acquisition and voltage control was accomplished through a National Instruments AT-MIO-16F-5 data acquisition board programmed using LabWindows (National Instruments, Austin TX). Data were collected at 10 Hz.

Microdialysis

The microdialysis probes (ESA, Bedford, MA) were a flexible loop design with a 450 μm tip diameter and a 2 mm tip length. The probes utilized fused silica tubing (100 μm o.d.) as inlet and outlets to the probes. The probe tips were made of cellulose fibers

and had a molecular weight cut-off of 6 kDa. Before use, all probes were conditioned according to manufacturers specifications. During experiments, the probe was perfused with artificial cerebral spinal fluid (aCSF) with a microliter syringe pump (Harvard Apparatus model 2274, South Natwick, MA) equipped with a 500 μL gas-tight syringe. Artificial CSF consisted of 145 mM NaCl, 2.68 mM KCl, 1.01 mM $MgSO_4$, and 1.22 mM $CaCl_2$.

Interface Design and Operation

The dialysate was sampled on-line using an interface previously used for coupling capillary LC and CZE (Lemmo and Jorgenson, 1993). A block diagram of the microdialysis/CZE system is shown in Figure 2-1. Since low perfusion flow rates were used, it was necessary to minimize the dead volume in all connections after the probe tip. The outlet of the dialysis probe was connected to the interface inlet line using a butt-type connection with Teflon tubing (1 cm long, 1/16" o.d., 0.01" i.d. from Alltech Associates, Deerfield, IL) as the sleeve. The line connecting the dialysis probe outlet to the interface consisted of a 5 cm piece of 25 μm i.d. by 360 μm o.d. fused silica tubing. To ensure a snug, leak-free seal between the dialysis probe outlet and the inlet to the interface it was necessary to modify the dialysis probe outlet. Approximately 2 cm of the probe outlet was slid into a fused silica capillary with 150 μm i.d. with 360 μm o.d. and sealed in place with cyanoacrylate cement. This modification effectively increased the o.d. of the dialysis probe outlet, thus making a better seal with the Teflon sleeve.

A detailed cross-section of the interface is shown in Figure 2-2. This interface consisted of a 1"x 1"x 1/2" Lucite block, a material chosen because of its transparency.

Channels 1/64" in diameter were perpendicularly drilled into the block, as shown in the figure. It was crucial that the resulting intersection be perfectly aligned with each other and that it remained transparent after drilling, otherwise it would be difficult and/or impossible to perform the desired experiments. Then, holes 1/16" in diameter were drilled into each channel outlet 7/16" from the outer edge of the block to allow for teflon tubing inserts. These inserts firmly held the separation and transfer capillary (360 μm o.d.) in place inside two of the ports while allowing for gating flow and waste connections in the other two ports. The waste port tubing was made of a stainless steel material which allowed for electrical grounding connections. Then, 10-32 taps were placed inside each channel 5/16" from the outer edge of the block. The taps allowed for finger tight nuts and ferrules to be placed into the interface to securely hold all tubing in place.

The flow-gated interface held the outlet of the dialysis probe and the inlet of the CZE capillary directly opposite each other with a distance of approximately 75 μm. The interface was also equipped with two other ports which allowed a gating-flow of electrophoresis buffer perpendicular to the dialysis and CZE capillaries to be introduced into the chamber. During a CZE run, the gating-flow was maintained by a syringe pump (Sage 341B, Orion Research Inc., Boston, MA) at sufficient level to rinse the dialysate away and prevent it from reaching the inlet of the CZE. The electrophoresis buffer flowing across the CZE inlet provided buffer to support the electrophoresis. To perform an injection, the gating flow was stopped using the valve (Valco, model C6W, Houston, TX) and the electrophoresis voltage turned off which allowed the dialysate to build up near the CZE inlet. Unless stated otherwise, an injection voltage of +1 kV was applied

for 10 s after a delay time of 10 s. The voltage was then turned off, the cross-flow resumed by opening the valve, and a final run voltage of +30 kV applied for separation.

It will be shown in later chapters that the high voltage can be constantly applied throughout the experiments. To inject a sample onto the column, the gating flow is stopped by a pneumatically-actuated valve equipped with a high speed switching assembly. Thus, the injected amount would be determined by the separation voltage and valve close time (20-100 ms). Unfortunately, this technology was not available for work in Chapters 2-5.

Surgical Procedure

Male Sprague-Dawley rats weighing 250-350 g were anesthetized with a subcutaneous injection of 100 mg/mL ketamine HCl, 20 mg/mL xylazine, and 10 mg/mL acepromazine maleate. The dosage of the initial injection was 0.7 mL/kg. This initial injection was boosted with injections of half the initial dosage every 15 min until the animal no longer exhibited limb reflex. After surgery, the animal was kept unconscious by tail-vein infusion of 10 mg/mL propafol. The flow rate was varied to maintain unconsciousness. The rats were mounted in a Kopf 900 stereotaxic apparatus (Tujunga, CA). During the experiment, the rat's body temperature was maintained with a heating pad. To insert the probes, the skull was exposed and a hole was drilled in the appropriate location using a dental drill and the dura removed. The dialysis probe was slowly lowered to the following coordinates: +.02 AP, -0.30 ML, -0.65-0.71 DV from bregma (Pellegrino et al., 1967).

Once the probe was in position, electrophoresis injections were made approximately every 5 min until the basal level of ascorbate had stabilized. Once a stable reading was obtained, samples were taken every 60 to 120 s. To test the effect of amphetamine, the drug was injected subcutaneously at 3 mg/mL (dosage of 1 mL/kg). To demonstrate the effect of an anesthetic overdose, rats were injected with 1 mL of the same mixture used for the initial anesthesia. After the animals were sacrificed, the brain was removed and placement of the dialysis probe verified by visual inspection.

Chemicals

Sodium phosphate dibasic, L-ascorbic acid, sodium chloride, potassium chloride, magnesium sulfate heptahydrate, and calcium chloride dihydrate were purchased from Fisher Scientific (Fairlawn, NJ). Tetradecyltrimethylammonium bromide (TTAB) was obtained from Sigma Chemical Co. (St. Louis, MO). All of these reagents were used as received. All solutions were prepared with purified deionized water (18 MΩ) using a Millipore Milli-Q water purification system (Milford, MA) and filtered through 0.2 μm nylon membrane filters.

Results and Discussion

Capillary Zone Electrophoresis

Since the assay was performed on-line, it was important that the separation step was performed as quickly as possible to maintain a high sampling rate. In CZE with bare fused silica capillaries, the electroosmotic flow runs in a direction opposite the migration of ascorbate. This unnecessarily delays the migration of ascorbate from the CZE capillary.

In this work, we utilized the positively charged surfactant TTAB at 0.520 mM, well below the critical micelle concentration, in the migration buffer to change the charge state on the capillary wall. This changed the direction of the electroosmotic flow so that it was the same as the ascorbate migration direction. Utilizing 0.520 mM TTAB in the migration buffer and an electric field strength of 419 V/cm allowed ascorbate to migrate in 85 s with 125,000 theoretical plates as shown in Figure 2-3. The analysis time decreased to 42 s and the plates to 65,000 when the electric field was increased to 600 V/cm and TTAB was increased to 0.523 mM as shown in the upper portion of Figure 2-3. The decrease in theoretical plates was presumably an extra-column effect due to a greater effect of injection volume on the faster electropherogram. Thus, the electric field and TTAB concentration could be adjusted to give the desired migration times for a given experiment.

Interface Characterization

Any interface between the dialysis probe and CZE must minimize extra-column band broadening and dilution of the sample. In addition, the interface should be easy to use and should not degrade the reproducibility of the assay. It was found that several variables in the operation of the interface could affect these characteristics, so it is useful to consider these variables. The most important variables were the distance between electrophoresis inlet and dialysis outlet, the gating flow rate, and the delay time between stopping gating-flow and starting the electrophoresis injection.

The distance between the dialysis outlet capillary and the CZE inlet within the interface was critical in determining the proper gating-flow rates and the delay time

between the stopping of flow and the beginning of the injection. The closer the capillaries, the higher the gating-flow that was needed and the shorter the delay time. If the capillaries were too close, then the gating-flow could not prevent breakthrough of the dialysate into the CZE capillary and uncontrolled injections would occur. If the capillaries were too far apart, then very long delay times were required, and in some cases, no detectable quantities could be injected. Therefore, each time the system was assembled, the distance between the capillaries was different and proper gating-flow and delay time had to be determined. Fortunately, this was easily done by positioning the capillaries and then increasing the gating-flow to slightly above the rate that prevented spontaneous injections due to breakthrough of the dialysis solution. If the gating-flow was too high, it caused parabolic flow in the CZE capillary and decreased resolution. Gating-flow rates varied between 0.3 and 1.0 mL/min.

The delay time could be varied to optimize different results as illustrated in Figure 2-4 and Figure 2-5 which show the theoretical plates and peak area as a function of delay time. For fast sampling times and higher separation efficiency, the delay time should be kept as short as possible. To optimize the signal to noise ratio, longer delay times could be used to give larger peaks. These results are due to the dynamics of the injection system. Immediately after the gating-flow was stopped, the flow from the dialysis probe began to increase the concentration of ascorbate around the CZE inlet. However, the first dialysate that reached the capillary was diluted by diffusional mixing with the migration buffer left in the gap between the two capillaries. Therefore, the area of the injected peak was lower. In addition, during the delay time analyte could diffuse into the CZE capillary

which would also cause an increase in the apparent amount injected. The theoretical plates decreased because of analyte diffusion during the delay time and because the concentration of salt that was injected would increase during the delay time. The higher ionic strength of the injected solution caused electric field inhomogeneities which led to lower efficiencies. Using a delay of 10 s, the injections made on-line with the probe removed from the flow system yielded peaks with nearly identical areas and theoretical plates to those obtained off-line. Thus, the interface could be used without diluting the sample and without causing extra-column band broadening.

In Vitro Testing

The relative recovery of the probe as a function of the dialysis flow rate is illustrated in Figure 2-6. The data was obtained with the probe placed in a quiescent solution of 200 μM ascorbate in aCSF maintained at 37 °C. This data was obtained by adjusting the flow rate to the desired value and allowing the system to stabilize for 45 min. Eight electropherograms were obtained at each flow rate and the points represent the mean for those values.

To calculate relative recovery, the peak areas were divided by the peak area obtained with the probe removed from the system and the same solution of ascorbate pumped into the interface. The relative recovery increased to 98% at a perfusion flow rate of 79 nL/min under these conditions. The high relative recoveries show that the analyte had time to nearly reach equilibrium across the dialysis membrane.

The high relative recovery possible with this system resulted in several advantages over operation at higher perfusion flow rates and lower relative recovery. First of all, it

made recovery less susceptible to changes in diffusional environment and allowed reliable quantitation based on *in vitro* calibration as demonstrated previously (Menacherry et al., 1992). In addition, the probe disturbed the tissue less by removing less material per unit time. For example in this experiment, at 79 nL/min ascorbate was removed at a rate of 16 pmol/min, whereas at 400 nL/min it was removed at 42 pmol/min. The use of low flow rates also improved the concentration detection limit of the system by an order of magnitude. At 79 nL/min, the concentration detection limit for ascorbate was 6 μM while at 1.0 μL/min it was 82 μM. The mass detection limit of ascorbate, on the other hand, was 3.7 fmol at 79 nL/min and 11.4 fmol at 1.0 μl/min. The detection limit was calculated as the concentration or mass of ascorbate outside the probe that would generate a signal three times the root mean square noise in the electropherograms.

The system also exhibited good quantitative characteristics. With a flow rate of 155 nL/min, a linear response was obtained from the detection limit up to 500 μM ascorbate (correlation coefficient = 0.9999). The relative standard deviation of the peak height for the calibration curve was 3.8%. Relative standard deviations of the peak height for all experiments varied between 3% and 8% and were independent of the dialysis flow rate. It is expected that complete automation of the system would improve the reproducibility.

The time resolution of the measurement was evaluated *in vitro* by making step changes in the ascorbate concentration at the probe while sampling the dialysate with the CZE system at regular intervals. Step changes were induced by moving the probe to a beaker containing a different ascorbate concentration. Figure 2-7 illustrates data from one

of these experiments where the dialysis flow rate was 79 nL/min. As seen in the figure, step changes in concentration were not observed in the electropherograms until 6 min after the concentration change around the probe had been made. For this experiment, the dead volume of the probe plus the tubing connecting to the interface was approximately 506 nL. Therefore, at a flow rate of 79 nL/min, the expected delay in response would be 6.4 min. Thus, the delay in response can mainly be accounted for by the time required to flow through the dead volume from the probe to the interface.

Since the delay in response due to dead volume is easily accounted for, it is not critical in terms of the information generated by system unless an instantaneous readout is necessary. The delays could be reduced by reducing the dead volume of the system. Since shorter connecting capillaries are not practical for *in vivo* studies, the best approach would be to decrease the i.d. of the capillaries that are used for connection. However, this approach would also increase the back pressure which would increase the likelihood of leaks and damage to the probe.

Although the delay itself is not problematic, it does lead to a decrease in temporal resolution. Temporal resolution, in this case, refers to the accuracy with which a step change in concentration at the probe could recorded. As shown in Figure 2-7, at dialysis flow rates of 79 nL/min, electropherograms could be obtained every 85 s and the step change in concentration could be faithfully recorded. It was possible to increase the sampling to every 65 s by using conditions that allowed for faster electrophoresis as discussed above. However, if sampling was increased to every 65 s, the ascorbate was observed to decrease over the period of two electropherograms. This suggests that

sufficient diffusional mixing occurred during the time the sample flowed from the probe to the interface to limit the temporal resolution to about 85 s. At a perfusion flow rate of 155 nL/min; however, it was possible to follow step changes with sampling every 65 s. This improvement was due to the decreased time allowed for diffusional mixing.

In Vivo Testing

To demonstrate the use of this technique *in vivo*, ascorbate was monitored in the striatum of an anesthetized rat. A typical electropherogram is shown in Figure 2-8 and is compared to the electropherogram obtained for the same column with a standard solution. As seen, the electropherogram was remarkably clean with only the ascorbate peak apparent. Several factors contributed to the high selectivity of the system. The most important being the combination of poor sensitivity of UV detection on a 25 μm i.d. capillary and the high concentration of ascorbate relative to most other UV absorbing species. In addition, the sample clean-up caused by the dialysis probe helped to remove some compounds. Finally, the electrokinetic injection combined with the reversed electroosmotic flow meant that the injection was strongly biased towards anionic substances.

The basal level of ascorbate was 47 ± 17 μM ($n = 3$) under the anesthesia conditions used. This agrees well with the value of 48 μM obtained using voltammetry in the striatum of anesthetized rats (Crespi et al., 1992). Figure 2-9 illustrates the peak area of ascorbate from a series of electropherograms obtained with the probe implanted *in vivo* and operated at a flow rate of 155 nL/min. In response to injections of amphetamine, ascorbate increased by 50% over a period of 14 min. Similar results have been previously

reported by voltammetric measurements (Wilson and Wightman, 1985; Mueller and Kunko, 1990; Basse-Tomusk and Rebec, 1990). Once the amphetamine began to take effect, a lethal dosage of anesthetic was given. As shown in the figure, the injection of anesthetic caused initially a drop in the ascorbate level as expected due to the decrease in consciousness (Crespi et al., 1992). At death, a massive release of ascorbate was observed which is again consistent with other *in vivo* measurements (Hillered et al., 1988; O'Neill et al., 1982).

Conclusion

The data presented in this chapter demonstrate the utility of the interface for allowing low perfusion flow rates while allowing temporal resolution of 65-85 s. This is the first report of high temporal resolution measurements from a dialysis probe where the perfusion flow was below 100 nL/min. The low perfusion rates improved the relative recovery which in turn facilitated quantification, minimized removal of compounds from the extracellular fluid, improved spatial resolution, and lowered the concentration detection limit. Although ascorbate is a useful test analyte, it is also readily detected by voltammetry. The true power of the technique will be realized as it is extended to compounds which are not readily detected by existing sensors. Improvements in UV-detection sensitivity, either by use of other wavelengths, larger bore capillaries, or more sophisticated detectors, will allow this method to be used for other chromophores including aromatic amino acids, purines, and pyrimidines. Incorporation of other detectors, such as laser induced fluorescence or electrochemistry, and derivatization schemes will allow the method to be further extended. Finally, with this system, the

possibility exists for scaling down the size of the dialysis probe which would further improve the spatial resolution and minimize tissue damage.

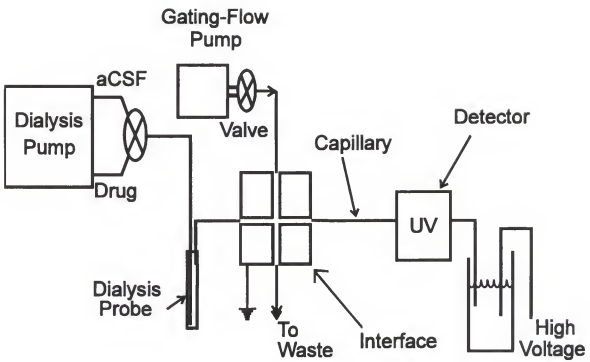

Figure 2-1. Block diagram of microdialysis/CZE system. Description of operation is given in text.

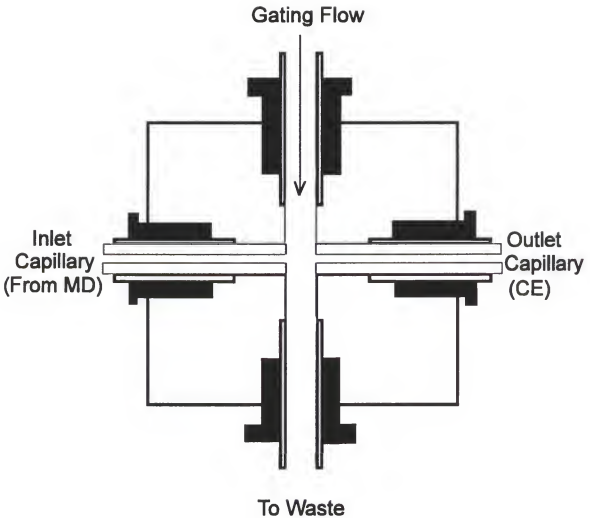

Figure 2-2. Cross-section of the interface between the microdialysis flow and the CE. Description of operation is given in the text. Dimensions and materials are also given in the text.

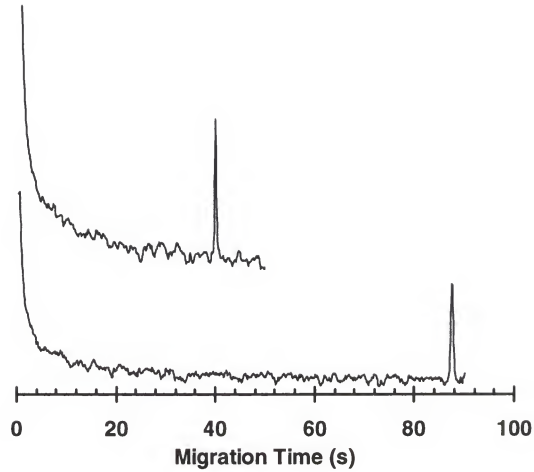

Figure 2-3. Electropherograms obtained using the microdialysis/CZE system with the probe in 100 μM ascorbate standard dissolved in aCSF. The upper electropherogram was obtained with an electric field strength (E) of 600 V/cm and a TTAB concentration of 0.523 mM. The lower was obtained with E of 419 V/cm and a TTAB concentration of 0.520 mM. In both cases the injection was +1 kV for 10 s. The dialysis flow rate was 155 nL/min and the dialysis probe was at 37 °C.

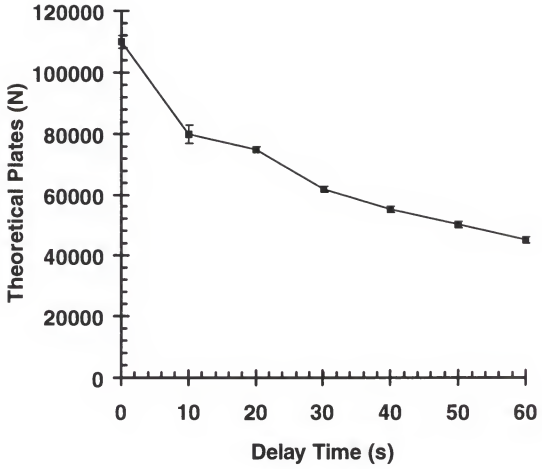

Figure 2-4. The effect delay time on theoretical plates (N) of ascorbate. The error bars are 1 standard deviation and each point represents the mean of 4 runs.

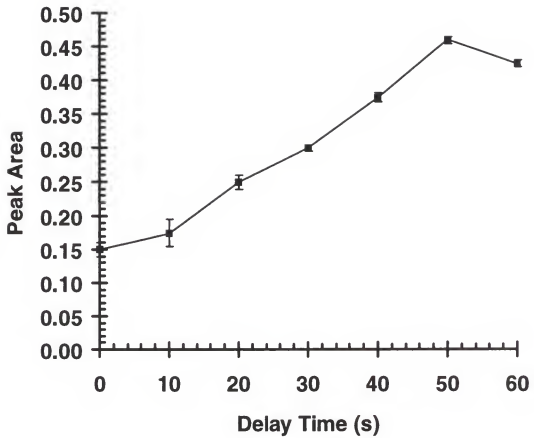

Figure 2-5. The effect delay time on peak area of ascorbate. The error bars are 1 standard deviation and each point represents the mean of 4 runs.

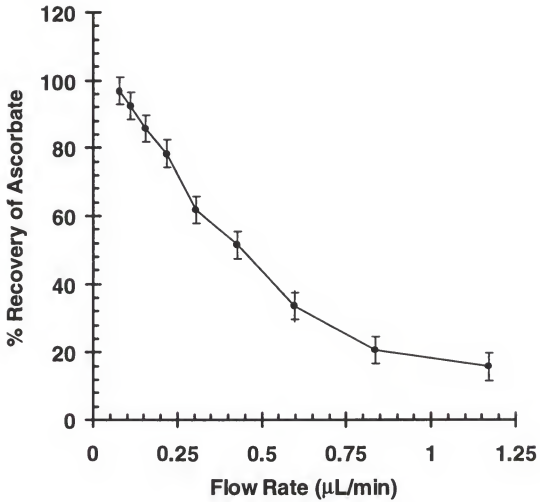

Figure 2-6. Relative recovery of probe for 200 μM ascorbate at 37 °C. Data obtained as described in the text.

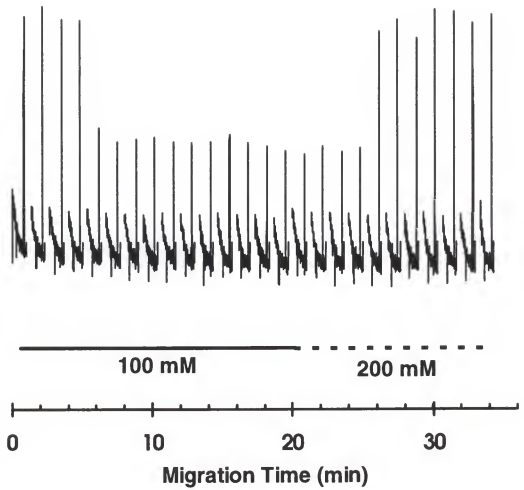

Figure 2-7. Series of electropherograms illustrating the response of the system to step changes in ascorbate concentration. Initially the probe was equilibrated with 200 μM ascorbate. At time = 0 the probe was changed to a beaker with 100 μM ascorbate. The probe switched back to 200 μM as indicated by the bars. Injections were performed every 85 s which includes a 10 s delay, a 10 s injection (+1 kV) and a 65 s electropherogram (at +30 kV). The initial 5 s of all electropherograms was removed for clarity since there were large shifts associated with the application of the voltage. discussed above.

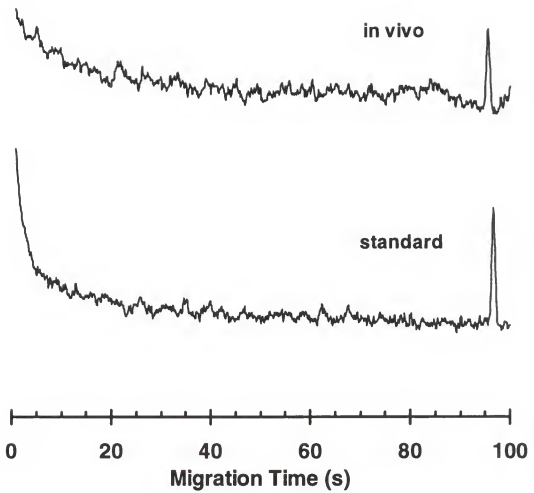

Figure 2-8. Comparison of electropherograms obtained *in vivo* and from 50 μM standards using the same dialysis probe and column. The *in vivo* electropherogram was obtained with ascorbate at basal levels. (The following conditions were used: separation voltage = +25 kV, injection voltage = +1 kV, delay time = 10 s.)

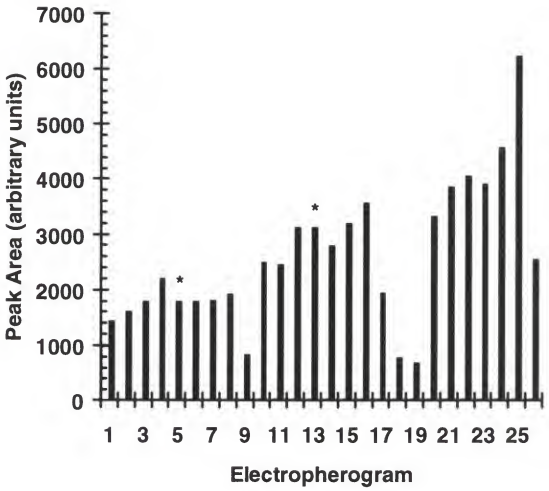

Figure 2-9. Peak area for ascorbate during an *in vivo* experiment. Injections were made every 110 s. The first asterisk indicates amphetamine injection while the second asterisk denotes anesthetic overdose. Amount of drugs injected are indicated in the Experimental Section. The decrease at the ninth electropherogram was an artifact due to a mis-timed injection.

CHAPTER 3
QUANTITATIVE *IN VIVO* MEASUREMENTS OF ASCORBATE AND LACTATE IN THE RAT STRIATUM

Introduction

A recurrent issue in microdialysis sampling is quantitative analysis. Constant perfusion of the probe results in a concentration gradient across the membrane. As a result, the concentration of analyte in the dialysate is always lower than the extracellular concentration. The ratio of dialysate concentration to extracellular concentration is the relative recovery. Absolute quantification of analytes requires that the relative recovery be known. It has been demonstrated that the relative recovery measured *in vitro* can differ significantly from that obtained *in vivo,* making *in vitro* calibrations unreliable for quantitative purposes (Benveniste et al., 1989; Bungay et al., 1990; Parsons and Justice, 1992). In the brain, this difference has been attributed to an altered diffusional environment and active supply and consumption of compounds *in vivo* (Benveniste et al., 1989; Bungay et al., 1990; Morrison et al., 1991). A number of *in vivo* calibration methods have been devised, including point of no-net-flux (Lonnroth et al., 1987), extrapolation to zero flow rate (Jacobson et al., 1985), and low flow rate (Menacherry et al., 1992). Although these methods are accurate, they are time-consuming.

The principle of the low flow rate method is that if the perfusion flow rate is low enough, then equilibrium across the probe is approximated and recovery is essentially 100%. Once the concentration of an analyte is determined *in vivo* by a measurement at

100% recovery, then the relative recovery at the actual flow rate for analysis can be determined. This can only be performed in cases where the analyte concentration is not under active control and does not change concentrations between changes in flow rate. The low flow rate method is cumbersome when the analytical method is not compatible with the low volume samples that are generated. For example, at 50 nL/min, a flow rate that may be expected to give approximately 100% recovery for small analytes under many conditions, 200 min would be required to generate a 10 μL sample. In contrast, if the analytical method has a high mass sensitivity and is compatible with small volume samples, then the low flow rate method may be practical. Furthermore, if the probe is appropriately coupled with the analytical method, it may be possible to obtain good time resolution and maintain *continuous* operation at low flow rates so that the probe operates at essentially 100% relative recovery. Thus, quantitative measurements could be obtained without an *in vivo* calibration.

In a Chapter 2, a method of interfacing CZE to microdialysis probes was described. CZE is ideally suited for analyzing low volume dialysates generated during perfusion at low flow rates since it is a rapid, microscale separation method that is compatible with automated, nanoliter scale sample analysis. We demonstrated that the on-line interface allowed sampling of the dialysate stream by CZE at 60 s time intervals at flow rates as low as 79 nL/min. In this chapter, we utilize this system to investigate the possibility of making quantitative measurements at low flow rates. Ascorbate and lactate are monitored as test compounds in the striatum.

Experimental

Capillary Zone Electrophoresis Conditions

All separations were performed in either 25 or 50 μm inner diameter (i.d.) by 360 μm outer diameter (o.d.) fused silica capillaries coated with polyimide (Polymicro Technologies, Phoenix, AZ). The capillaries were 50 cm long with 15 cm from injection inlet to the detector cell. The electrophoresis buffer consisted of 25 mM $Na_2HPO_4 \cdot 7H_2O$ and 0.53 mM tetradecyltrimethylammonium bromide (TTAB) at pH 7.0. The voltage source was a Spellman 1000R CZE Reversible HV power supply. On-column UV absorbance detection at 210 and 260 nm was accomplished by using a Spectra 100 variable-wavelength detector (Spectra-Physics, San Jose, CA). The CZE was coupled to the microdialysis probe using the same interface described in the previous chapter. The only differences was that the system was operated automatically by a computer for this work.

Briefly, the interface allowed approximately 1 nL samples to be injected periodically to the CZE capillary without dilution. The dialysate was shunted to a waste when it was not being injected. A +1 kV (5 s duration) injection voltage and a +30 kV separation voltage was applied when using the 25 μm capillary while a +5 kV (10 s duration) injection voltage and a +20 kV separation voltage was applied when using the 50 μm capillary. Data acquisition and automated control of the system was accomplished through a National Instruments AT-MIO-16f-5 data acquisition board programmed using LabWindows (National Instruments, Austin, TX).

Microdialysis

Flexible loop microdialysis probes (ESA, Bedford, MA) with a 2 mm tip length and 450 μm tip diameter were used. The probe tips were made of cellulose fibers and had a molecular cut-off of 6 kDa. Artificial cerebral spinal fluid (aCSF) used in perfusion of the dialysis probe consisted of 145 mM NaCl, 2.68 mM, KCl, 1.01 mM $MgSO_4$, and 1.22 mM $CaCl_2$. For high K^+ infusion, an isotonic perfusate solution consisting of 2.68 mM NaCl, 145 mM KCl, 1.01 mM $MgSO_4$, and 1.22 mM $CaCl_2$ was used in the dialysis probe. The flow rate was 155 nL/min unless stated otherwise.

Surgical and Pharmacological Procedures

Male Sprague-Dawley rats weighing 250-350 g were anesthetized with a subcutaneous injection of 100 mg/mL of chloral hydrate. The dosage of the initial injection was 4.0 mL/kg. This initial injection was boosted with injections of half the initial dosage every 30 min until the animal no longer exhibited limb reflex. After surgery, the animal was kept unconscious with subcutaneous administration 2 mL/kg dosages of chloral hydrate as needed. Once the rat was secured in the stereotaxic apparatus, the dialysis probe was placed in the striatum to the coordinates of +0.02 AP, -0.30 ML, -0.67-(-0.73) DV from bregma (Pellegrino et al., 1967). Once the probe was in position, basal level readings for analytes were taken until they stabilized.

For amphetamine treatments, the drug was administered subcutaneously at 5 mg/mL (dosage of 2 mL/kg). After the initial increase in amphetamine was observed, a 0.7 mL/kg injection of a mixture of 100 mg/mL ketamine HCl, 20 mg/mL xylazine, and 10 mg/mL acepromazine maleate was given to lower ascorbate levels and prevent animal

waking. For K^+ stimulation, the aCSF was replaced with elevated K^+ buffer (see above) for perfusion through the microdialysis probe. Charts indicate the time of K^+ infusion corrected for the dead volume of the system. During ascorbate monitoring with K^+ infusion, the ketamine/ xylazine/ acepromazine mixture was administered after ascorbate levels had stabilized.

Chemicals

Chloral hydrate and TTAB were purchased from Sigma (St. Louis, MO). L-ascorbic acid, $Na_2HPO_4 \cdot 7H_2O$, $MgSO_4 \cdot 7H_2O$, and $CaCl_2 \cdot 2H_2O$ were obtained from Fisher Scientific (Fairlawn, NJ). All reagents were used as received. Ketamine, xylazine, acepromazine, and amphetamine were donated by Professor Thomas Vickroy of the University of Florida Veterinary School. All solutions were prepared with purified deionized water (18 MΩ) using a Millipore Milli-Q water purification system (Milford, MA) and filtered through 0.2 μm nylon membrane filters.

Results and Discussion

Detection of Ascorbate and Lactate *In Vivo*

In Chapter 2, we demonstrated that when using CZE with absorbance detection at 260 nm, it was possible to obtain electropherograms from striatal dialysates containing a single peak which was due to ascorbate. A typical electropherogram obtained *in vivo* from an automated, on-line injection of dialysate from the striatum of an anesthetized rat compared with that obtained for 250 μM *in vitro* standard is shown in Figure 3-1. Under these conditions, ascorbate migrated to the detector window in 39 ± 0.4 ($n = 5$) seconds

with a separation efficiency of 64,500 theoretical plates. The simplicity of the electropherogram is due to several factors including the wavelength used, the high concentration of ascorbate relative to other anions, and the poor sensitivity of the detector. The concentration detection limit was 5.4 μM while the mass detection limit was 1.7 fmol. The detection limits were calculated as the concentration or mass of ascorbate outside the probe that would generate a signal three times the root mean square noise in the electropherograms

Although the clean electropherogram at 260 nm is useful for detection of ascorbate, it is of interest to determine if other endogenous compounds could also be monitored using the separation and detection system. Figure 3-2B illustrates an electropherogram obtained *in vivo* with a more general absorbance wavelength of 210 nm. In this case, the column i.d. was 50 μm in order to increase detector sensitivity. UV absorbance detection was accomplished on-column, therefore the path length, which is proportional to absorbance, was increased with the larger bore capillary. The concentration detection limit was 0.3 mM and the mass detection limit was 4.0 pmol. The detection limits were calculated as the concentration or mass of lactate that would generate a signal three times the root mean square noise in the electropherograms.

Identification of compounds detected was attempted by comparing electropherograms of standards to *in vivo* data, as shown in Figure 3-2. Only anions were tested since the *in vivo* electropherogram indicated only anions had been detected. This is shown by observing that the electrophoresis conditions are such that the migration order is anions, neutrals (carried by electroosmotic flow), and then cations (also carried by

electroosmotic flow but slowed by their electrophoretic mobility). The last peak detected *in vivo* matched the migration time of a neutral compound, therefore all of the detected substances were anions. It is not surprising that only anions were detected since the electrokinetic injection technique strongly discriminates against cations.

The following compounds were tested: pyruvate, lactate, adenosine 5'-monophosphate, adenosine 5'-diphosphate, adenosine 5'-triphosphate, 5-hydroxyindole-3-acetic acid, uric acid, 3,4 dihydroxyphenylacetic acid (DOPAC), and homovanillic acid. Of these compounds, only lactate (peak 3 in Figure 3-2A) was consistently found to have a matching peak in the *in vivo* electropherograms (peak 4 in Figure 3-2B). In addition to a matching migration time, peak 4 in Figure 3-2B had the same unusual peak shape as the peak due to standard lactate. Finally, spiking of the dialysate with lactate increased the peak identified as lactate. Peaks which matched the mobility of pyruvate, DOPAC, uric acid, and HVA were occasionally observed (for example peaks 3, 5, 6 in Figure 3-2B); however, they were inconsistent and their identity was not established. The inconsistency is probably because the basal levels of these compounds are near the detection limit of the system. For example, extracellular DOPAC concentration is 18-21 μM (Basse-Tomusk and Rebec, 1991) and the detection limit for DOPAC was 11 μM.

Calibration of Probe

One of the goals of this work was to investigate quantitative aspects of microdialysis at low flow rates. *In vitro* calibration showed that the relative recovery of ascorbate was 97.0% at 79 nL/min and 85.8% at 155 nL/min. Nearly identical values were obtained for lactate. Since the relative standard deviation for the peaks was 3.7%,

the recovery at 79 nL/min is within experimental error of 100%. This suggested that it may be possible to monitor compounds while obtaining quantitative recovery at the probe. To test this idea *in vivo*, the peak area for ascorbate and lactate was determined as a function of the perfusion flow rate as shown in Figure 3-3. As shown, for both ascorbate and lactate, the peak area is essentially unchanged by decreasing the perfusion flow rate from 79 nL/min to 40 nL/min. This result suggests, in agreement with the *in vitro* calibrations, that recovery is nearly 100% at a flow rate of 79 nL/min. In the previous chapter, we demonstrated that the system could be used to monitor ascorbate with 60 s time resolution while perfusing at 79 nL/min. Therefore, the system can now be used for quantitative monitoring *in vivo* without calibration of the probe once the 100% relative recovery point is determined for an analyte.

In Vivo Monitoring of Ascorbate

We determined the basal level of ascorbate to be 333 ± 16 μM (n = 3) using low flow rate correction. This value correlates well with the measured extracellular levels of 200-500 μM obtained by using voltammetry (Gonon et al., 1981; Ewing et al., 1982; Schenk et al., 1982). In the previous chapter, with rats anesthetized by a injections of ketamine/acepromazine/xylazine, we had observed a much lower level of ascorbate. Given the results obtained here, it is apparent that chloral hydrate did not depress ascorbate levels like the other anesthesia.

To demonstrate quantitative time-resolved monitoring, ascorbate was measured after systemic injection of amphetamine, as illustrated in Figure 3-4. Ascorbate increased by 24.0 ± 5.7 % (n = 3) within 7 min of administration. Once the amphetamine took

effect, injections of anesthesia (ketamine/ xylazine/ acepromazine) lowered ascorbate levels as expected. Amphetamine takes 30-70 min to have its maximum effect on ascorbate; therefore, the increases reported here are lower than the maximum increases reported in other studies; however, the initial increase is similar to that observed previously (Basse-Tomusk and Rebec, 1990; Mueller and Kunko, 1990).

It was also possible to monitor changes in ascorbate induced by infusions of elevated K^+ through the dialysis system as illustrated in Figure 3-5. A 142% increase in ascorbate was observed over a 9 min time period with this treatment. Again, injection of ketamine/xylazine/acepromazine was found to reduce ascorbate. It is difficult to quantitatively compare the increases in ascorbate seen here with other studies since the perfusion rate is different. However, the increase in ascorbate with K^+ treatment is expected (see Grünewald, 1993 for review). At least part of the increase is due to exchange of intracellular ascorbate with extracellular glutamate during reuptake of glutamate which is released by the K^+ depolarization. Some of the ascorbate may be directly released as well since it has been found to be co-secreted with catecholamines found in the striatum. The use of perfusion at low flow rates for stimulation may be of interest because it should provide better spatial resolution than perfusions at higher flow rates. At low flow rates, less material is delivered to the region under study and therefore a smaller region is affected.

In Vivo Monitoring of Lactate

As indicated above, using detection at 210 nm it was possible to detect lactate. The basal level of lactate was found to be 5.6 ± 2.3 mM (n = 3). This is significantly higher than the value of 1.1 mM obtained by Kuhr and Korf (1988) using a calibrated probe and an enzyme assay for lactate. The discrepancy in values may be due to differences in experimental conditions. The value of 1.1 mM was obtained on awake, freely moving animals and our value was obtained on heavily anesthetized animals. Another possibly critical difference in experimental conditions was that glucose was not provided in the perfusion fluid in our case, unlike the previous work. Finally, it may be possible that lactate may have co-migrated with an unknown component in the CZE system causing a falsely large peak area. However, attempts to improve resolution by using longer columns did not reveal new peaks.

Infusion of K^+ through the dialysis probe for 40 min caused a distinct pattern of two increases in lactate as illustrated in Figure 3-6. During infusion, lactate concentration initially rose an average of 72% ± 44 (n = 3). This agrees well with the value of 67% obtained by microdialysis coupled to on-line fluorometric analysis (Taylor et al., 1994). This rise in lactate concentration results from an increase in metabolic activity caused by depolarization. After the perfusion fluid was returned to normal K^+ levels, a second increase of lactate concentration was observed in 2 of the 3 animals tested. This increase averaged 42% over over 4 min which agrees well with previous observations of 42% over 8 min (Taylor et al., 1994). This increase is attributed to the increase in metabolic activity following repolarization of cell membranes (Taylor et al., 1994).

For monitoring lactate, the time resolution was approximately 125 s. This is lower than the 45 s resolution attained with ascorbate measurements. In this system, the time resolution depends on the speed of the separation. For ascorbate, since the electropherogram was so simple, it was possible to perform fast electrophoresis with little regard for separation resolution. In contrast, at 210 nm several peaks were observed which necessitated allowing all of them to migrate through the capillary prior to the next injection. In addition, lower electric field strengths were used with the 50 μm capillary to prevent excessive Joule heating, which also slowed the electrophoresis.

Conclusions

The system described here is readily operated at flow rates from 40 to 155 nL/min which allows either continuous operation at nearly 100% relative recovery or simplified calibration by the low flow rate method. Because of the microscale analysis system, these flow rates can be used without sacrificing temporal resolution. Ascorbate and lactate were monitored with time resolution of 45 and 125 s, respectively. Other approaches for monitoring these particular compounds may be preferred from a practical standpoint; however, the data indicate the potential utility of CZE interfaced to microdialysis for quantitative monitoring. Several other compounds can apparently be detected at 210 nm; however, they are as yet unidentified.

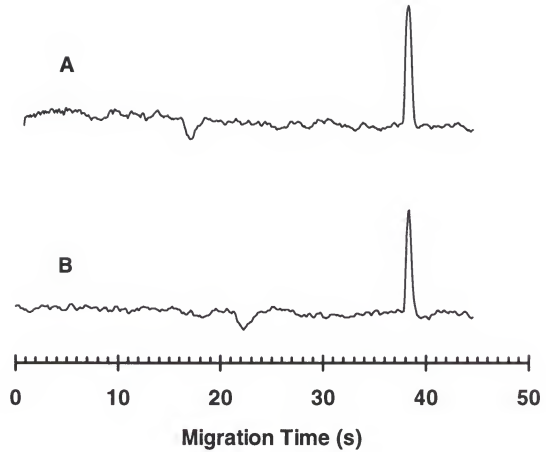

Figure 3-1. Comparison of electropherograms obtained *in vivo* (A) with ascorbate at basal levels and from 250 μM ascorbate standard (B) using the same dialysis probe and column.

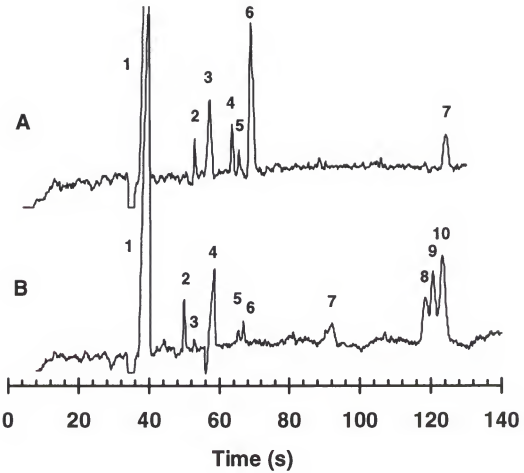

Figure 3-2. Comparison of electropherograms of standards (A) and *in vivo* (B) using the same dialysis probe and column with absorbance detection at 210 nm. Peaks in (A) correspond to: (1) artifact from high salt of dialysate, (2) 1.8 mM pyruvate, (3) 5 mM lactate, (4) 210 mM HIAA, (5) 360 μM uric acid, (6) 300 μM DOPAC, and (7) neutral marker. Peaks in (B) are numbered in order of appearance and are not intended to denote matches with those in (A).

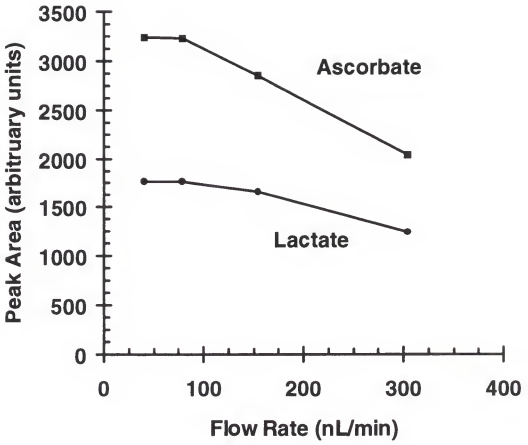

Figure 3-3. Peak areas for ascorbate and lactate as a function of perfusion flow-rate during *in vivo* experiments. Each point is the average of five electropherograms. Error bars of 1 standard deviation are within the size of the points.

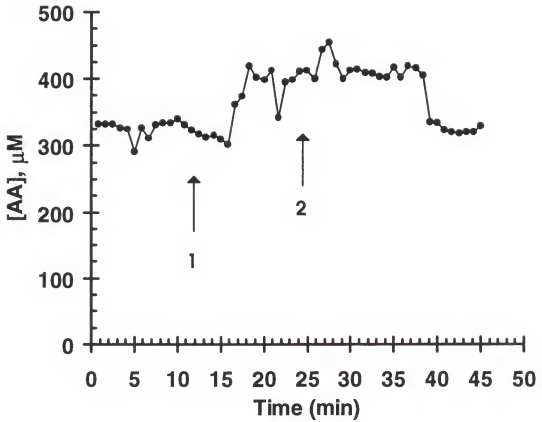

Figure 3-4. Concentration of ascorbate *in vivo* following injections of amphetamine (first arrow) and ketamine/xylazine/acepromazine (second arrow). Each data point was obtained from a single electropherogram. Injections were made every 50 s.

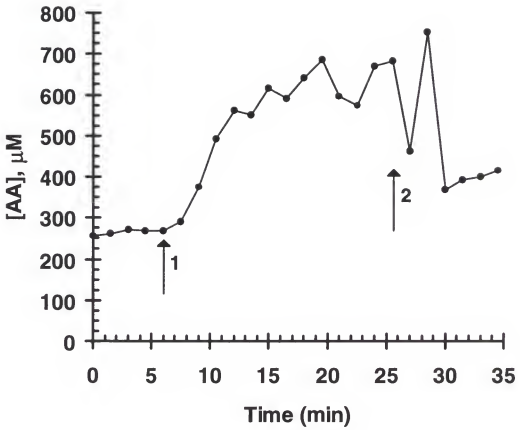

Figure 3-5. Concentration of ascorbate *in vivo* during infusion of the microdialysis probe with 145 mM K^+. Injections were made every 70s. Arrow 1 indicates beginning of K^+ infusion. Arrow 2 indicates injection of ketamine/ xylazine/ acepromazine mixture.

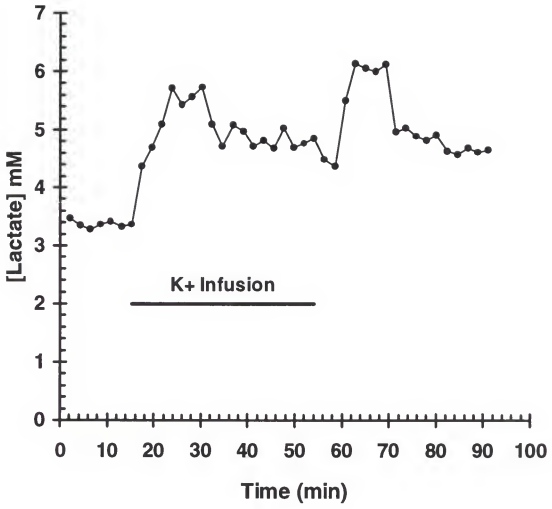

Figure 3-6. Concentration of extracellular lactate *in vivo* during stimulation with elevated K^+. The bar indicates K^+ infusion. Injections were made every 2 min.

CHAPTER 4
QUANTITATIVE IN VIVO MONITORING OF PRIMARY AMINES IN THE RAT STRIATUM USING MICRODIALYSIS COUPLED BY A FLOW-GATED INTERFACE TO CAPILLARY ELECTROPHORESIS WITH LASER-INDUCED FLUORESCENCE DETECTION

Introduction

As mentioned in Chapter 1, a limitation of microdialysis is poor temporal resolution relative to many chemical events. The temporal resolution of microdialysis-based chemical monitoring is typically determined by the mass sensitivity of the analytical method utilized. Better mass detection limits allow more frequent sampling and better temporal resolution. The use of microscale separation techniques such as microbore LC and CZE coupled on-line with microdialysis has significantly improved the temporal resolution compared with off-line methods, allowing sampling rates of 45 to 120 s (Zhou et al., 1995; Chen and Lunte, 1995). The combination of microdialysis with on-line derivatization and fast separation by CZE seems to be an especially powerful approach to *in vivo* monitoring. For example, glutamate and aspartate have been monitored with 120 s temporal resolution by derivatizing dialysates on-line with naphthalene-2,3-dicarboxyaldehyde (NDA) and then automatically assaying the samples by CZE-LIF (Zhou et al., 1995). Many other compounds are potentially amenable to this approach. In the on-line approach, temporal resolution often becomes limited not by mass sensitivity, but by separation time.

In our previous experiments with the flow-gated interface, a UV absorbance detector was used. It was found that poor sensitivity of this detection mode resulted in the method being useful for just a few compounds found in high concentrations. The goal of the present work was to combine the advantages of the flow-gated interface and its low flow rate capability with on-line derivatization in order to expand the applicability of the flow-gated approach. For this initial study, o-phthaldialdehyde/β-mercaptoethanol (OPA/β–ME) was used for on-line derivatization of primary amines in the dialysate. Both CZE and micellar electrokinetic chromatography (MEKC) separation modes were explored. This is the first reported use of on-line derivatization with MEKC and it was found that at least 20 compounds could be detected by this approach. Several amino acids, including the neurotransmitters glutamate, aspartate, and taurine, were identified and monitored with the system. This is the first microdialysis system to generate high relative recoveries and good temporal resolution simultaneously for multiple neurotransmitters.

Experimental

Chemicals

All amino acids, derivatization reagents, and anesthetics were from Sigma (St. Louis, MO) and were used as received. All solutions were prepared with water purified and deionized using a Millipore Milli-Q water purification system (Milford, MA) and filtered through 0.2 μm nylon membrane filters.

Capillary Electrophoresis

All separations were performed in 20 cm lengths of 25 μm inner diameter (i.d.) by 360 μm outer diameter (o.d.) fused silica capillaries coated with polyimide (Polymicro Technologies, Phoenix, AZ). Each day, capillaries were rinsed for 10 minutes with 0.1 M NaOH, deionized water, and electrophoresis buffer. A Spellman 1000R CZE power supply (Plainview, NY) was used to apply voltage.

For *in vivo* measurements by CZE, the inlet to detector length was 15 cm and applied voltage was -15 kV (90 s separation times) or -30 kV (45 s separation times). The migration buffer was 175 mM 2-[N-cyclohexylamino]-ethanesulfonic acid (CHES) adjusted to pH 9.0 with 1 M NaOH. For MEKC separations, the capillary dimensions were the same, but the applied voltage was -10 kV. For faster MEKC separations, the inlet to detector length was reduced to 10 cm and the separation voltage was increased to -12 kV. The migration buffer for MEKC was 175 mM CHES at pH 9 with 100 mM sodium dodecyl sulfate (SDS). To allow the separation capillaries to reach the cathode, a 20 cm piece of 100 μm i.d. by 360 μm o.d. fused silica capillary was connected to the end of the short separation capillary by butting the ends of the capillary inside a Teflon tubing sleeve (1 cm long, 1/16" o.d., 0.01" i.d. from Alltech Associates, Deerfield, IL). This connection allowed the majority of the voltage to be dropped across the short capillary (Monnig and Jorgenson, 1991).

On-line Derivatization and Sample Injection

A diagram of the microdialysis/capillary electrophoresis system with on-line derivatization is shown in Figure 4-1. Microdialysate and the derivatizing agent were

separately pumped into a 0.15 mm bore Teflon tee (Valco, Houston, TX) by a microsyringe pump at 79 nL/min. The tee dead volume was ~50 nL. Unless stated otherwise, the derivatization solution was 110 mM OPA and 220 mM β-ME in 25 mM borate buffer at pH 9.5. The derivatization solution was pumped through a 5.0 cm length of 75 μm i.d. by 360 μm o.d. fused silica tubing to the reaction tee. The dialysis probe was connected to the reaction tee by a 2.5 cm length of 75 μm i.d. by 360 μm o.d. fused silica tubing. The reaction capillary connecting the reaction tee to the interface consisted of 8.0 cm of 75 μm i.d. by 360 μm o.d. fused silica tubing. The dialysis and derivatizing flows combined for a 158 nL/min flow rate through the reaction capillary allowing for a reaction time of 2.2 min. All capillary to capillary connections were made by butting the capillaries together inside a 1 cm long Teflon tubing sleeve.

The separation capillary was coupled to the reaction capillary via a flow-gated interface which allowed dialysate samples to be automatically injected onto the separation capillary. Operation of the interface has been described in detail in Chapter 2. Briefly, the interface consisted of a Lucite block that held the outlet of the reaction capillary and the inlet of the separation capillary aligned with a ~75 μm gap between them. During a separation, a gating flow of electrophoresis buffer was pumped at 0.34 mL/min (Sage 341B syringe pump, Orion Research, Boston MA) through the gap between the capillaries. This flow prevented derivatized dialysate from entering the separation capillary. To perform an injection, the gating flow was stopped by a pneumatically-actuated gating valve. While the gating flow was stopped, the injection voltage was applied. In most cases, a 1 s delay was allowed between the stopping of the gating flow

and application of the injection voltage. Once the injection was complete, gating flow was resumed and the separation voltage applied. For *in vivo* measurements, dialysate injections were typically made with -1 kV for 5 s (CZE) or -100 V for 2 s (MEKC). Smaller injected amounts with MEKC were possible because of the better sensitivity of the lens system (Fluar objective) used for detection during MEKC experiments. The exact injection voltage and time were varied to get consistent performance in terms of theoretical plates and sensitivity. This was necessary because with the flow-gated interface, the injected amount depends not only on the voltage and time, but also the space between reaction capillary and separation capillary which varied from day-to-day.

Detection, Data Collection and Data Reporting

Fluorescence detection was accomplished using an epillumination fluorescence microscope (Axioskop, Carl Zeiss, Hanover, MD) as illustrated in Figures 4-2 and 4-3, and as described in detail elsewhere (Hernandez et al., 1990; Schultz and Kennedy, 1993). The 354 nm line of a 2 mW helium-cadmium laser (Model 4210B, Liconix, Santa Clara, CA) was used as the excitation source. The excitation beam was reflected into the back of a 40x, 0.75 numerical aperture (NA) Neofluar objective (Zeiss) by a dichroic mirror with a 400 nm transition and focused onto the capillary. For MEKC runs, the objective was a 40x, 1.30 NA Zeiss Fluar oil immersion lens. (The Fluar lens became available during the course of the experiments and was therefore used only with MEKC.) The emitted radiation was collected by the objective, passed through the dichroic mirror, and filtered with a 450 nm interference filter with 25 nm bandwidth (Andover Corp., Salem, NH). Light passing through the interference filter was measured using a DCP-2 photometer

system (CRG Electronics, Houston, TX) equipped with a R928 photomultiplier tube (Hamamatsu, Bridgewater, NJ). The output of the current to voltage converter was interfaced to an IBM-compatible computer. Data acquisition and automated control of the flow-gated system was accomplished with a National Instruments AT-MIO-16F-5 multi-function board (Austin, TX). Data collection rate was 10 Hz which was sufficient to give at least 10 points over the narrowest peaks.

All mean values are reported ± standard error of the mean with number of replicates (n) unless stated otherwise.

Microdialysis

Flexible loop (V-shaped) microdialysis probes (ESA, Bedford, MA) made from cellulose fibers (6 kDa cut-off) were used. The flexible loop probes had 450 μm tip diameters and 2 mm tip lengths. The overall length from the tip of the probe to the outlet was 5 cm. Approximately 1 cm of the outlet was sleeved into a fused silica capillary with 150 μm i.d. and 360 μm o.d. and sealed with cyanoacrylate cement. This modification facilitated using a butt connection with Teflon sleeves to the line transferring dialysate to the reaction tee. Dialysis probes were perfused with artificial cerebral spinal fluid (aCSF) consisting of 145 mM NaCl, 2.68 mM KCl , 1.01 mM $MgSO_4$, and 1.22 mM $CaCl_2$. The high K^+ perfusate solutions for stimulation experiments consisted of 2.62 mM NaCl and 145 mM KCl and all other salts were the same. The dialysis flow rate was 79 nL/min unless stated otherwise. *In vitro* relative recovery was determined by comparing peak heights obtained when the dialysis probe was placed in a standards solution (all compounds at known concentrations between 2 and 20 μM) at 37 °C to that obtained

when the probe was removed from the system and the same concentration of standards were pumped directly into the reaction tee.

Surgical Procedures

Male Sprague-Dawley rats weighing 250-350 g were anesthetized with subcutaneous injections of 100 mg/mL of chloral hydrate. The initial injection was 4.0 mL/kg. Booster injections of 2.0 mL/kg were given every 30 min until the animal no longer exhibited limb reflex. After surgery, the rat was kept unconscious with subcutaneous administration of 1.0 mL/kg chloral hydrate as needed. Once the rat was secured in the stereotaxic apparatus, the microdialysis probe was placed in the striatum to the coordinates +0.02 AP, -0.30 ML, -0.65 DV from bregma (Pellegrino et al., 1967). Basal level electropherograms were taken until they were stable, typically 1.5 hours after insertion of the dialysis probe. This time allowed for basal levels to stabilize.

Results and Discussion

On-line Derivatization Conditions

Primary amines react rapidly with OPA in the presence of β-ME to produce fluorescent isoindole products, as illustrated in Figure 4-4 (Chen et al., 1979). In addition, the derivatization agents themselves are not highly fluorescent. These characteristics make OPA an attractive derivatization agent for our on-line assays where minimizing reaction time and interferences are desired. In developing the on-line system, it was important to assess the effect of OPA concentration and reaction time on signals for analytes.

Figure 4-5 demonstrates the effect of OPA concentration on the fluorescence intensity observed for derivatized aspartate and glutamate. For this experiment, a solution of 5 μM aspartate and 4 μM glutamate in aCSF was pumped directly into the reaction tee, which was interfaced with the CZE-LIF, at 79 nL/min. β–ME/OPA at a constant mole ratio of 2:1 dissolved in 25 mM borate buffer (pH 9.5) was also pumped into the reaction tee at 79 nL/min. A 2.2 minute reaction and mixing time was achieved as described in the Experimental section. As shown in the plot, signal intensity for the amino acids peaked at 110 mM OPA. This concentration was used for all further experiments. The decrease in fluorescence intensity at higher OPA concentrations may be related to instability of the isoindole derivative in the presence of large excess of OPA (Stobaugh, et al. 1983).

The effect of reaction time on fluorescence intensity for aspartate and glutamate was also investigated and the results summarized in Figure 4-6. For this experiment, the conditions were similar to those for Figure 4-5 and OPA concentration was 110 mM. The reaction time was varied from 1 to 5 minutes by changing the length of the reaction capillary. As shown in the figure, the fluorescence intensity for both analytes steadily increased from 1 to 5 min reaction time. The long time required is surprising since the expected half-time for the OPA-amine reaction is around 6 s (Chen et al., 1979). Also, if we assume that complete mixing occurs in the average time it takes to diffuse across the diameter of the reaction capillary, then the samples should be mixed in about 5 s. Presumably, faster mixing and reactions could be achieved in smaller bore capillaries.

Detection Limits and Linearity

Detection limits were found to vary significantly with the choice of microscope objective. Some work used a Neofluar objective which gave concentration detection limits for amino acids of about 0.1-0.3 μM in the on-line system. This corresponds to mass detection limits of 6-18 amol. Detection limits were calculated as the concentration or mass that would give a peak height equal to three times the root mean square noise of the electropherogram. Later work used a Fluar objective which had superior UV-transmission characteristics and greater light collection efficiency. This lens resulted in a ~10-fold signal enhancement with no effect on the noise as illustrated in the MEKC data for amino acids in Figure 4-7. Using this detector, the on-line concentration detection limits for the amino acids were approximately 12-24 nM while the mass detection limits were 29-240 zmol. Detection limits were two-fold worse in the on-line system than what could be obtained off-line since the former required that the analyte be diluted by two-fold by the OPA/β–ME stream during derivatization. Calibration curves for all of the identified amino acids were linear up to 50 μM with a linear correlation coefficient of at least 0.999.

Capillary Electrophoresis Conditions

In order to maintain high sampling rates and temporal resolution with the on-line system, it was important that both derivatization and separation be rapid. Maximizing separation speed required high electric field strengths (E). Figure 4-8 illustrates the effect of electric field strength on theoretical plates for 18 μM aspartate in the on-line system using free solution CZE separation conditions similar to those used for *in vivo*

measurements. The plates drop off significantly above -500 V/cm. Heating in the capillary, indicated by positive deviation from linearity in a plot of analyte velocity versus electric field strength, was not apparent until E >-750 (data not shown). Thus, the relatively low plates above -750 V/cm can be attributed mainly to Joule heating while the decline in plates between -500 and -750 V/cm is due to another source.

The lower than expected plates at moderate electric field strength are partially attributed to the fact that the injected sample from the dialysis probe is dissolved in the highly conductive aCSF which creates sample overloading (Luckacs and Jorgenson, 1983). Samples dissolved in water instead of aCSF had slightly higher plates, especially at E < -500 V/cm as shown in Figure 4-8. Another significant source of band broadening was injection volume. Figure 4-8 also shows data from an on-line injection where the injection voltage and time were cut to the smallest values (0 V and 0.25 s) that allowed a peak for the 18 μM aspartate with a signal to noise ratio > 5 when using the Neofluar lens. Under these conditions, sample enters the separation capillary primarily by diffusion and flow from the reaction capillary. With these injection conditions, the plate count is as high as 120,000 at -500 V/cm in a separation that took 2.7 min.

Based on these results, it was possible to choose conditions for *in vivo* experiments that yielded trade-offs that best fit the goals of the experiment. Specifically, injections for *in vivo* measurements were usually at -1 kV for 1-2 s which, as shown above, is too large to give optimum efficiency. However, the larger injections gave better signal-to-noise ratios which was especially important for quantification in experiments that utilized the less sensitive Neofluar lens. Increasing electric field strength decreased

resolution, but gave faster analysis times as illustrated by the *in vivo* electropherograms in Figure 4-9. As discussed below, glutamate and aspartate were the only compounds that were reliably resolved and identified by CZE. The zones due to glutamate and aspartate remain resolved even at E = -1420 V/cm (see Figure 4-9) where Joule heating has a large adverse effect on efficiency. In this case, the separation is over in 35 to 40 s allowing for the best temporal resolution in monitoring. *In vivo*, at E = -825 V/cm, we typically obtained an average of 44,000 plates for glutamate and 68,000 plates for aspartate in separations that required about 90 s.

Calibration of Dialysis Probes

In vitro relative recovery of the dialysis probe is summarized in Table 4-1. As shown, the relative recoveries are within experimental error of 100% when the dialysis flow rate is $\leq$ 79 nL/min. Thus, under these conditions, the concentration inside the probe is approximately that outside the probe which suggests the possibility of quantitative *in vivo* monitoring. To confirm quantitative monitoring *in vivo*, we examined the peak height as a function of flow rate for several identified compounds (compounds measured using MEKC conditions) *in vivo* as shown in Figure 4-10. Since the peak height could vary because of slightly different reaction times at the different flow rates, the peak heights in Figure 4-10 were normalized to those obtained *in vitro* with the probe removed and a given concentration of analyte pumped directly into the tee at the same flow rate. As the flow rate is decreased below 100 nL/min, the normalized peak heights do not increase significantly, which indicates that relative recovery is maximized, that is, near 100% *in vivo*. These results are in agreement with our previous work for other small compounds

(Chapter 2 and 3), and demonstrate that it is possible to quantitatively monitor compounds when using low flow rates without resorting to extensive *in vivo* calibration schemes.

Temporal Resolution

The temporal resolution of the system was evaluated *in vitro* by monitoring step changes in aspartate concentration which were induced by moving the dialysis probe between reservoirs containing different concentrations of aspartate. Figure 4-11 illustrates the changes in aspartate peak height that were observed as the step changes were made while perfusing the probe at both 155 nL/min and 79 nL/min. The aspartate change was observed in the electropherograms 8 min after it was made at the probe when the flow rate was 79 nL/min while the delay was 4 min with a perfusion rate of 155 nL/min. The delay was due to the time required for the analytes to flow through the dead volume from the probe to the interface. In addition to a delay in detecting the concentration changes, there is a broadening of the concentration pulses as shown in Figure 4-11. At 79 nL/min, the step change in aspartate requires about 90 s to develop and at 155 nL/min the time is about 45 s. This effect is attributed to the time required to equilibrate across the probe and band broadening due to flow and diffusion during transfer from probe to interface. Thus, in this case where separations can be accomplished in 45 s, the temporal resolution is limited not by the separation time, but by the sample broadening that occurs in the system. A possible approach to improving temporal resolution would be to decrease dead volume by decreasing the transfer and reaction capillary bore and/or length. With the system as designed; however, temporal resolution of 45 s for glutamate and aspartate can be obtained at the expense of slightly lower relative recovery by operation at 155 nL/min

instead of 79 nL/min. The decrease in recovery is small as seen by comparing peak heights in Figure 4-10.

In Vivo Detection of Glutamate and Aspartate by CZE-LIF

Initial *in vivo* experiments were performed using CZE for separation. Electropherograms obtained from on-line derivatization of dialysate from the rat striatum are compared to amino acid standards in Figure 4-12. The broad bands in the 35 to 50 s time range are associated with excess OPA and unresolved, neutral compounds. The following compounds were tested for matches in the *in vivo* electropherograms: glutamate, glycine, glutamine, aspartate, serine, leucine, isoleucine, taurine, alanine, and lysine. Of these compounds, only glutamate and aspartate were consistently found to be fully resolved and to have matching migration times. In addition to matching migration times, both peaks increased appropriately after spiking the dialysate with glutamate and aspartate. The basal levels of aspartate and glutamate were 1.2 ± 0.1 μM and 5.0 ± 0.4 μM (n=8), respectively. These values and precision are in good agreement with previous reports (Gamache et al., 1993; Obrenovitch et al., 1993; Butcher et al., 1987; Hillered et al., 1989; Anderson and DiMicco, 1992; Tossman et al., 1986a and 1986b).

Infusions of 145 mM K^+ through the dialysis probe caused the expected increase in glutamate and aspartate levels, as illustrated by comparing Figure 4-12A and 4-11B. Results from monitoring the aspartate and glutamate overflow during a K^+ stimulation are illustrated in Figure 4-13. The timing of the increase in aspartate and glutamate concentration shows that they increased immediately after the high K^+ buffer reached the probe. *In vitro* experiments found that the use of high K^+ buffer did not affect the injected

amount of any identified amino acids. The rise time of the increases suggest that they were occurring at least as fast as the system could monitor. The average concentration of aspartate and glutamate during stimulation was 4.8 ± 1.7 μM and 33.8 ± 12.3 μM ($n = 5$), respectively. Although there is considerable variability among different groups, the percent increase and precision are similar to those reported previously using similar stimulations (Anderson and DiMicco, 1992; Tossman et al., 1986a and 1986b). The best previous temporal resolution for glutamate and aspartate by microdialysis was 120 s (Zhou et al., 1995).

In Vivo Detection of other Primary Amines using MEKC-LIF

CZE was well-suited for rapidly resolving glutamate and aspartate in the dialysate samples. By manipulating the migration buffer and other separation conditions, it may be possible to resolve other compounds of interest as well. MEKC is another potentially powerful approach to resolving the OPA-derivatives. This is especially true since many of the compounds that were unresolved by CZE had migration times that were near that expected for neutral compounds. Using MEKC, at least 20 peaks not associated with the reagents were resolved, as illustrated by the typical example in Figure 4-14B. Under conditions used for *in vivo* measurements, we obtained between 140,000 and 270,000 plates for resolved compounds. The results demonstrate the potential for detecting and monitoring a wide variety of compounds using this approach.

By matching migration times to standards (Figure 4-14B and 4-13C), the following compounds were identified in the electropherograms: aspartate, glutamate, isoleucine, leucine, lysine, methionine, phenylalanine, taurine, tyrosine, and valine. The following

compounds were tested but matching peaks could not be reliably found at basal conditions: γ-aminobutyric acid (GABA), tryptophan, cysteine, arginine, asparagine, and glutathione. The basal concentration levels for the identified compounds are shown in Table 4-2.

No attempt was made to vary the MEKC conditions in order to optimize resolution for particular compounds; therefore, it may be possible to develop MEKC conditions for many other compounds. For example, in separations of standards, serine and threonine were not resolved, nor were alanine and glycine (see Figure 4-14C) under the conditions used; however, peaks matching these compound pairs were observed in the *in vivo* electropherograms. Within a given day, the resolution and pattern of peaks observed was stable; however, the retention times and resolution did vary from day-to-day. Especially problematic was variation of the migration times of taurine, valine, glutamate, and methionine. In some cases, taurine was well-resolved from valine and in other cases glutamate could overlap with either valine or methionine. Quantitative data is reported only for cases where resolution was >0.75 for a pair.

As for the CZE case, a number of extraneous background peaks appear in the standards and *in vivo*. For the MEKC separations shown in Figure 4-14B and 4-13C, the background peaks include the broad zone from 80 to 140 s, the peak at 180 s, and several small but perceptible peaks between 215 and 260 s in Figure 4-14B and 4-14C. Most of the peaks appear to be the result of side reactions or minor products and not OPA/β-ME itself since injections of blanks had only a single reagent peak centered at ~120 s. Furthermore, the presence of extraneous peaks tended to be more noticeable with

standards than for *in vivo* data. Compare for example the size of the broad zone in 4-13C with 4-13B. This may be because many more amines were present in the *in vivo* sample and they consumed the OPA preventing it from being involved in side reactions. The presence of extraneous peaks may be a consequence of the large excess of OPA that was used. Reduction of the extraneous peaks, at the expense of sensitivity may be attained by decreasing the OPA concentration (see Figure 4-4). In addition, prior purification of OPA by recrystallization may reduce this effect (Owar et al., 1994). The reagent peaks were problematic in that their magnitude could vary day-to-day. For example, in some cases, the small peaks in the baseline between 210 and 250 s were larger than some of the analyte peaks.

For monitoring the amino acids, the separation time was shortened to ~3 min by decreasing the effective capillary length from 20 cm to 10 cm and by increasing electric field strength from -500 to -600 V/cm. Under these conditions, we obtained between 32,000 and 99,000 theoretical plates depending on the analyte. All of the identified compounds could be at least partially resolved under these conditions as illustrated by the electropherogram in Figure 4-14A. In order to identify peaks and minimize the chance that unknown peaks were contributing to the signals in these electropherograms, data for every animal was always obtained under higher resolution conditions (longer columns) to determine the number of peaks present before utilizing faster, lower resolution runs.

The effect of a 15 min infusion of 145 mM K^+ on the concentration of the analytes is illustrated in Figure 4-15. The average concentration obtained during the K^+ stimulation is summarized in Table 4-2. Some error may be expected in quantification, especially for

valine, glutamate, and methionine since they were not fully resolved under these conditions. It is apparent, especially when the concentration changes are plotted as percent increase from basal level (Figure 4-15B), that the three neurotransmitters (aspartate, glutamate, and taurine) are most affected by the K^+ stimulation as expected. The levels measured during K^+ infusion are in reasonable agreement with previously reported results (Anderson and DiMicco, 1992; Tossman et al., 1986a and 1986b).

Conclusions

We have described a system that couples microdialysis to CZE-LIF with on-line derivatization. While previous publications have reported a similar system using CZE-LIF (Hogan et al., 1994; Zhou et al., 1995) and others have coupled capillary LC on-line with microdialysis (Chen and Lunte, 1995), this system is unique in two respects. First, it is compatible with low perfusion flow rates which results in higher relative recoveries. This results in several advantages including higher concentration of analyte, quantitative monitoring without *in vivo* calibrations, less disturbance to the tissue, and potential compatibility with smaller probes for better spatial resolution. Secondly, the system allows for higher theoretical plates which increase peak capacity in the separation, subsequently allowing more compounds to be monitored simultaneously. The use of MEKC was especially powerful for resolving multiple amino acids in a reasonable time. The results are achieved without sacrifice in temporal resolution. Indeed, the use of CZE for the separation allowed glutamate and aspartate to be quantitatively monitored with the best temporal resolution to date without the need for *in vivo* calibrations. Possible improvements in the system include use of other derivatization reagents which may allow

for improved sensitivity or different selectivity. Further optimization of MEKC or CZE conditions may allow them to be used for more compounds, such as other amino acid neurotransmitters. In addition, use of smaller probes will be explored for better spatial resolution. Finally, improvements in the detection limit and smaller i.d. capillaries may allow faster separations. Faster separations combined with improved engineering of the transfer from dialysis probe to the electrophoresis capillary will allow better temporal resolution.

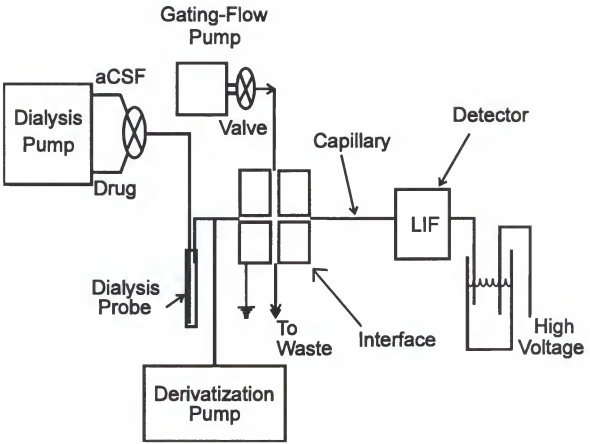

Figure 4-1. Block diagram of microdialysis/CZE-LIF system with on-line derivatization.

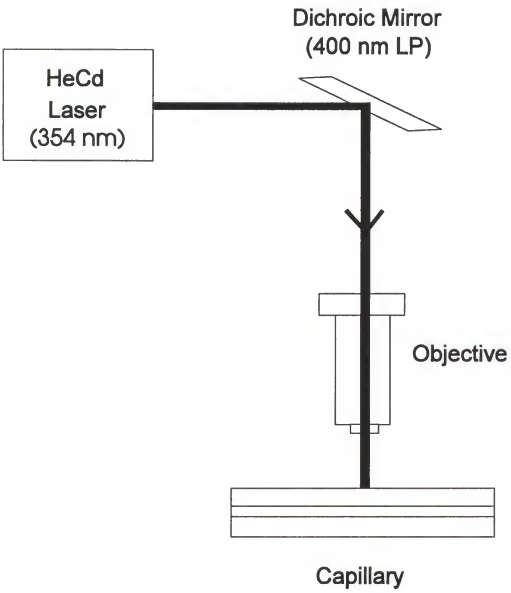

Figure 4-2. Excitation with an epillumination fluorescence microscope. The excitation beam is shown as the black line reflected by the dichroic mirror. Radiation below 400 nm is reflected into the objective.

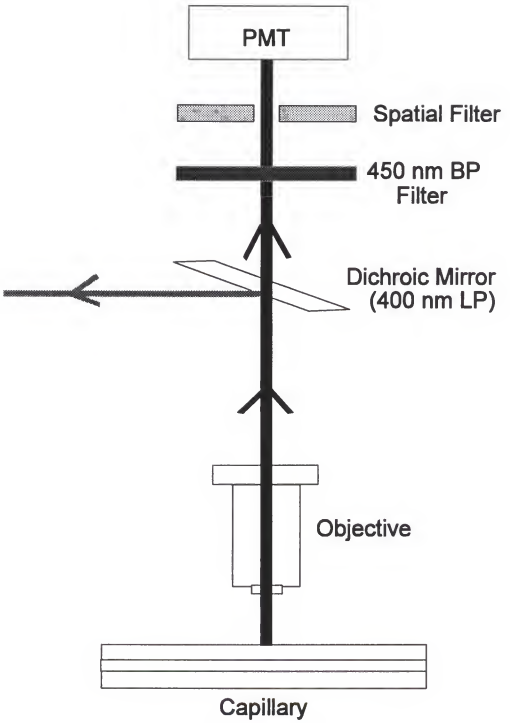

Figure 4-3. Emission with an epillumination fluorescence microscope. The emitted light crosses the objective, dichroic mirror, bandpass filter, and spatial filter. The beam is finally focused on a photodiode that transforms light into an electric signal which is recorded by a computer and a stripchart recorder.

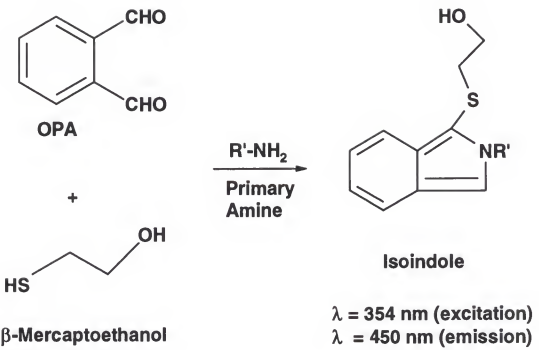

Figure 4-4. Reaction of o-phthaldialdehyde (OPA) with primary amines.

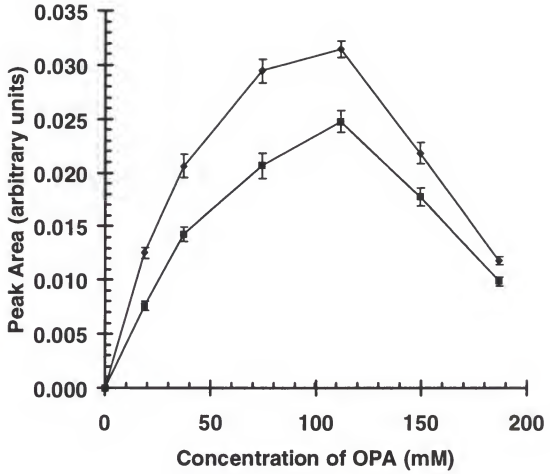

Figure 4-5. The effect of OPA concentration on the fluorescent signal of 5 μM aspartate (◆) and 4 μM glutamate (■) in the on-line assay. Error bars represent ± 1 standard deviation (n=5). Peak areas are in arbitrary fluorescence units.

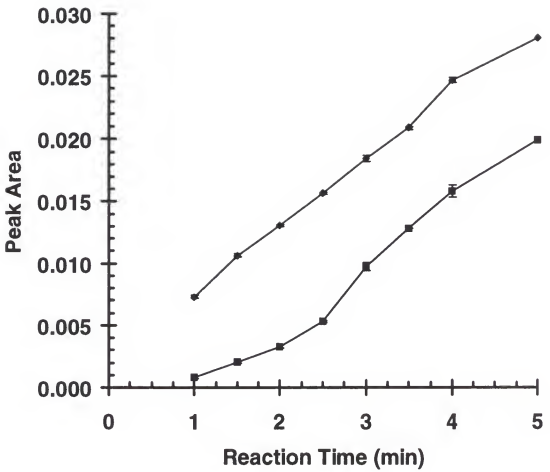

Figure 4-6. The effect of derivatization reaction time on the fluorescent signal of 5 μM aspartate (◆) and 4 μM glutamate (■) standards in the on-line assay. Peak areas are in arbitrary fluorescence units. Error bars represent ± 1 standard deviation.

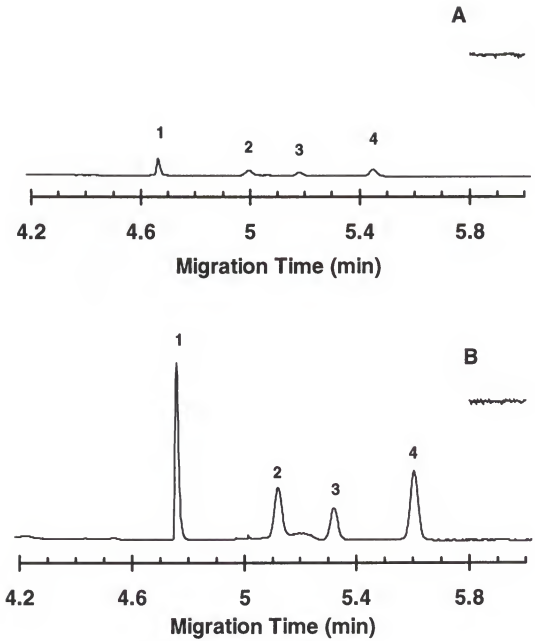

Figure 4-7. Comparison of Fluar (A) and Neofluar (B) objectives for MEKC-LIF. Peaks correspond to OPA derivatives of: aspartate (1), leucine (2), phenylalanine (3), and isoleucine (4). Noise is shown in the inset of each figure at a scale 50x that for the electropherogram. Y-axis is in arbitrary fluorescence units and is the same for both electropherograms.

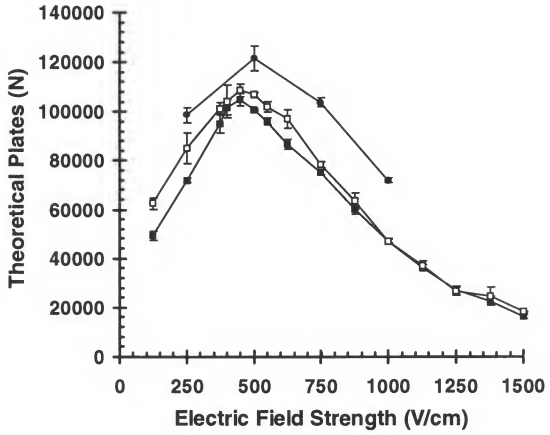

Figure 4-8. Theoretical plates (N) by CZE for aspartate as a function of electric field strength (E) under different experimental conditions: normal injection with sample in H_2O (□), normal injection with sample in aCSF (■), and minimized injection with sample in H_2O (●). Error bars represent ± 1 standard deviation.

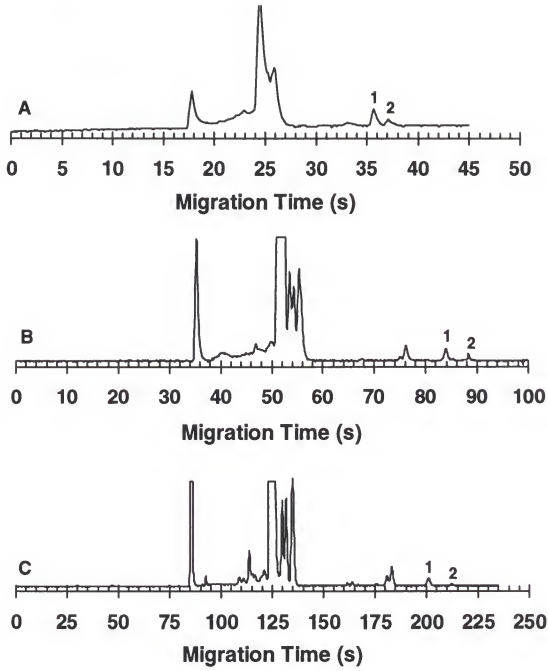

Figure 4-9. The effect of electric field strength on electropherograms obtained *in vivo* with the on-line system. Peaks 1 and 2 correspond to OPA derivatives of glutamate and aspartate, respectively. The electric field strengths were: -1420 V/cm (A), -825 V/cm (B), and -405 V/cm (C). Injection was -1 kV for 3 s. Other conditions are given in Experimental section for CZE. Y-axis is in arbitrary fluorescence units and is the same for all electropherograms.

Table 4-1. *In Vitro* Recovery (%) of Primary Amines using MEKC-LIF (mean ± standard error of the mean, n = 3)

Analyte	57 nL/min	79 nL/min	111 nL/min
Aspartate	98.0 ± 2.1	98.0 ± 3.9	93.3 ± 1.3
Glutamate	98.1 ± 2.2	98.3 ± 2.9	91.2 ± 1.6
Isoleucine	98.2 ± 1.9	98.8 ± 1.6	91.2 ± 1.2
Leucine	98.2 ± 1.9	98.7 ± 1.3	91.7 ± 2.6
Lysine	98.8 + 2.3	98.6 ± 1.9	93.4 ± 1.6
Methionine	97.9 ± 1.9	96.7 ± 3.6	91.1 ± 2.7
Phenylalanine	97.9 ± 2.6	97.3 ± 1.8	92.5 ± 2.8
Taurine	100.2 ± 2.4	99.2 ± 2.1	95.5 ± 1.6
Tyrosine	100.7 ± 1.4	99.9 ± 1.4	89.5 ± 2.1
Valine	99.2 ± 1.9	98.4 ± 3.0	94.3 ± 1.4

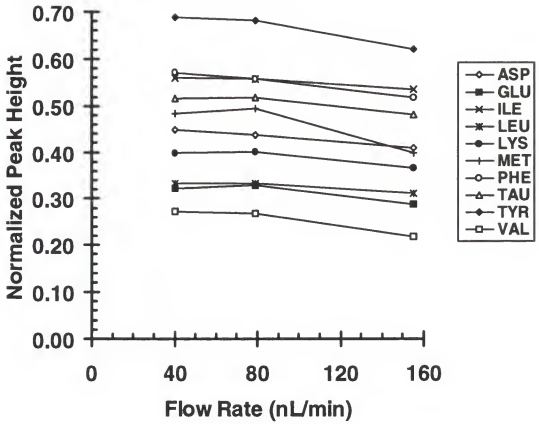

Figure 4-10. The effect of dialysis flow rate on normalized peak heights *in vivo*. Peak heights were normalized as described in the text. MEKC separation conditions as described in the Experimental section were used. Each point is the average of 3 electropherograms. The relative standard deviations were from 1-9%; however, error bars were not included in the figure for figure clarity.

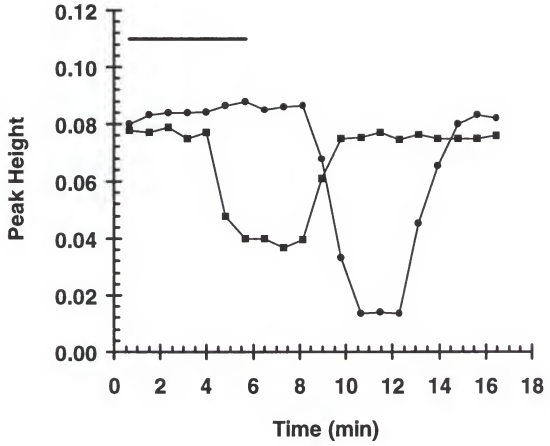

Figure 4-11. Response of the system to step changes in aspartate concentration with 45 s sampling rate. Initially the probe was equilibrated with 10 μM aspartate and was changed to a reservoir containing 5 μM (155 nL/min) or 2.5 μM (79 nL/min) aspartate at t = 0 min. The probe was switched back to the original reservoir at t = 6 min. The overall time the probe was in the 5 μM/2.5 μM solution is indicated by the bar. The delay in response is due to the dead volume of the system. The perfusion rates were ■ = 155 nL/min and ● = 79 nL/min while the temperature of the reservoir was 37 °C. Peak heights are in arbitrary fluorescence units.

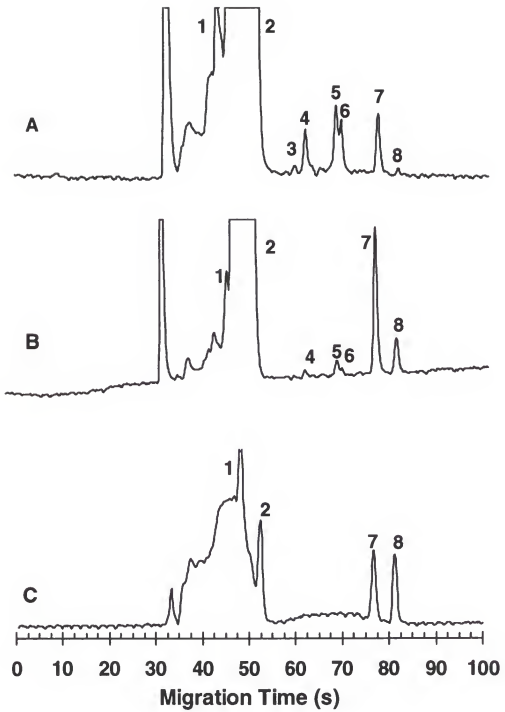

Figure 4-12. Comparison of typical electropherograms obtained *in vivo* before stimulation (A), *in vivo* during stimulation (B), and for 5 μM standards of glutamine (1), glycine (2), glutamate (7), and aspartate (8) (C). Only glutamate and aspartate were consistently identified. E = -825 V/cm and other conditions are given in Experimental section for CZE. Y-axis is in arbitrary fluorescence units and is the same for all electropherograms.

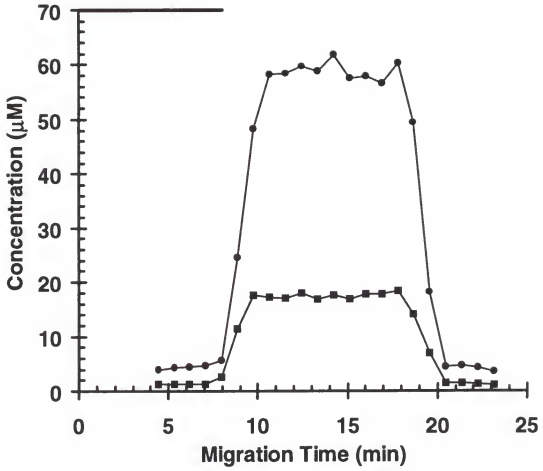

Figure 4-13. Concentration of glutamate (●) and aspartate (■) *in vivo* during K^+ infusion with the microdialysis probe measured by CZE. The bar indicates the time that the probe contains 145 mM K^+. The delay in response is due to the dead volume of the system

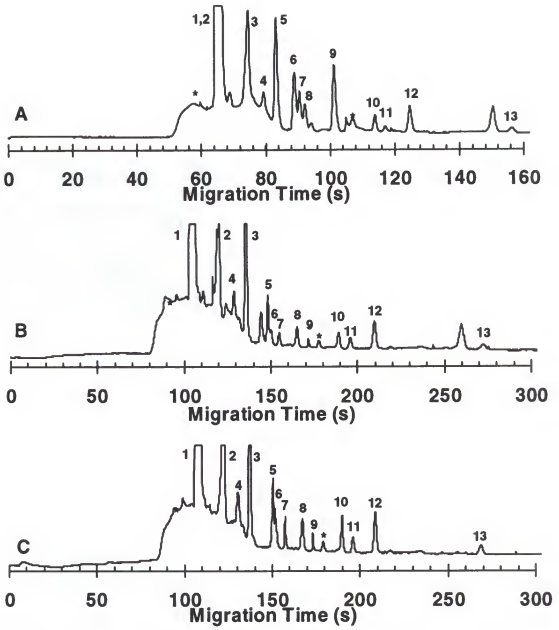

Figure 4-14. Comparison of MEKC electropherograms obtained: *in vivo* with 10 cm effective length (E = -600 V/cm) (A) , *in vivo* with 15 cm effective length and -400 V/cm (B), and for standards (C). Conditions in (C) same as for (B) and other conditions are given in Experimental section. Note the different time scales for (A) and (B,C). Peak identities and concentrations of standards are: 15.2 μM Gln (1), 14.4 μM Ser and 12.1 μM Thr (2), 10.9 μM Ala and 12.2 μM Gly (3), 4.4 μM Tyr (4), 17.0 μM Tau (5), 15.4 μM Val (6), 9.6 μM Glu (7), 3.1 μM Met (8), 4.4 μM Asp (9), 4.1 μM Leu (10), 3.8 μM Phe (11), 6.2 μM Ile (12), and 9.9 μM Lys (13). Impurities and reagent peaks are identified with an asterisk while unidentified peaks are unlabeled. Y-axis is in arbitrary fluorescence units and is the same for all electropherograms.

Table 4-2. Concentration of Primary Amines in Rat Striatum using MEKC-LIF (mean ± standard error of the mean)

Analyte	Basal Concentration (μM)	Stimulated Concentration (μM)
Aspartate	1.9 ± 0.2	4.3 ± 0.9
Glutamate	4.1 ± 0.2	17.6 ± 3.0
Isoleucine	4.6 ± 0.7	5.7 ± 0.8
Leucine	2.6 ± 0.3	3.2 ± 0.4
Lysine	5.4 ± 0.4	6.2 ± 1.0
Methionine	1.8 ± 0.2	3.1 ± 0.4
Phenylalanine	2.0 ± 0.2	2.3 ± 0.2
Taurine	11.3 ± 1.3	60.0 ± 5.4
Tyrosine	3.3 ± 0.9	3.6 ± 0.8
Valine	5.3 ± 0.3	10.6 ± 5.1

Stimulation was achieved by 145 mM K^+ infusion for 15 minutes at 79 nL/min (n = 4 for basal concentrations and n = 3 for stimulated concentrations).

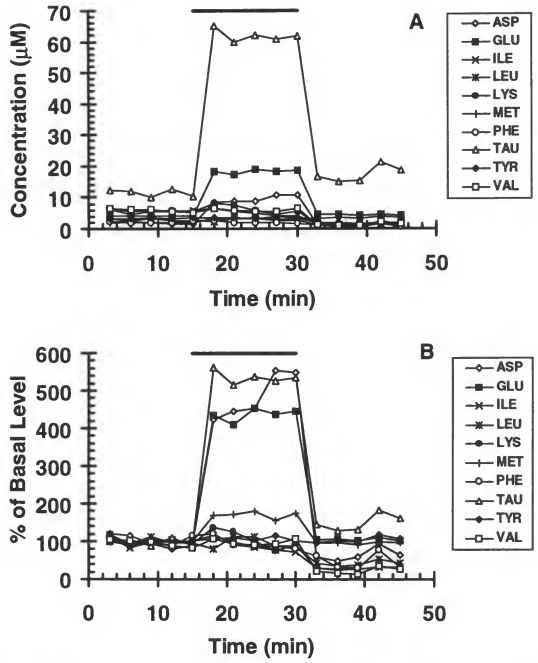

Figure 4-15. *In vivo* (A) concentration and (B) % of basal levels of primary amines during K^+ infusion with the microdialysis probe measured by MEKC. The bar indicates the time the probe contains 145 mM K^+. The delay in response is due to the dead volume of the system.

CHAPTER 5
IN VIVO MONITORING OF GLUTATHIONE AND CYSTEINE IN THE RAT STRIATUM

Introduction

Glutathione and cysteine are two examples of thiols that play significant roles in the brain and brain pathology. The tripeptide glutathione is involved in several important functions including protection of cellular membranes against oxidative damage, maintenance of cellular thiol groups, detoxification of foreign substances, and coenzymatic processes (Orlowsky and Karkowsky, 1976). In addition, inherited disorders of glutathione metabolism such as glutathione synthetase, γ-glutamylcysteine synthetase, serum γ-glutamyl transpeptidase, glutathione reductase, and glutathione peroxidase deficiencies can cause neurological defects such as mental retardation, spinalcerebellar degeneration, and Parkinson's disease (Orlowsky and Karkowsky, 1976). Cysteine, known also as an antioxidant, has possible roles in excitotoxic amino acid tissue damage during stroke (Slivka and Cohen, 1993), neurodegeneration, and brain atrophy (Lund et al., 1981; Olney et al., 1990). Therefore, it is of considerable interest to develop analytical methodology for the *in vivo* study of these neurochemicals in the brain.

Although microdialysis is a widely accepted sampling and infusion technique for neuroscience applications, little work has been reported on its application to the *in vivo* determination and monitoring of glutathione or cysteine in the extracellular space of the brain. In one reported method glutathione, cysteine, and other extracellular antioxidants

were monitored with microdialysis sampling and subsequent off-line analysis using high performance liquid chromatography (HPLC) and electrochemical detection with a gold electrode (Landolt et al., 1992). In another report, glutathione was monitored in the rat brain by microdialysis sampling followed by off-line analysis by HPLC and fluorescence detection with methanolic monobromobimane (mBBr) derivatization (Yang et al., 1994). Although these methods provide adequate monitoring of glutathione and cysteine for some applications, several disadvantages limit their utility. These disadvantages include difficulty in absolute quantification and low analyte concentrations in the dialysate because of the relatively high dialysis perfusion rates that are required, poor temporal resolution, and the requirements for cumbersome off-line sampling and derivatization.

In this chapter, we describe a system for monitoring glutathione and cysteine *in vivo* based on microdialysis coupled on-line with capillary zone electrophoresis with laser-induced fluorescence detection (CZE-LIF). This method improves upon previously reported methods in several respects. Temporal resolution is improved since the high mass sensitivity of CZE-LIF permits frequent sampling. The use of on-line derivatization and automated separations simplifies operation and provides nearly real-time monitoring. Finally, the system is designed to be compatible with perfusion flow rates below 100 nL/min which allows relative recoveries that approach 100% while reducing the absolute recovery. The high relative recovery facilitates quantification and improves detection limits while the low absolute recovery causes less disturbance to the tissue being studied.

Experimental

Chemicals

Glutathione, cysteine, ammonium bicarbonate, N-[2-hydroxyethyl] piperazine-N'-[2-ethanesulfonic acid] (HEPES), and chloral hydrate were from Sigma (St. Louis, MO). Monobromobimane (mBBr) was obtained from Molecular Probes (Eugene, OR) and acetonitrile was obtained from Fisher Scientific (Atlanta, GA). All chemicals were used as received. All solutions were prepared with water purified and deionized using a Millipore Milli-Q water purification system (Milford, MA), filtered through disposable Corning 0.2 μm nylon membrane syringe filters (Corning, NY), and purged for 15 minutes with helium gas.

CZE Conditions

Separations were performed in 19 cm lengths of 25 μm inner diameter (i.d.) by 360 μm outer diameter (o.d.) fused silica capillaries coated with polyimide (Polymicro Technologies, Phoenix, AZ). Each day, capillaries were rinsed for 10-minutes with 0.1 M NaOH, deionized water, and electrophoresis buffer. A Spellman 1000R CZE HV power supply (Plainview, NY) was used for voltage application.

For CZE separations, the inlet to detector length was 15 cm and applied voltage was -10 kV. The electrophoresis buffer was 100 mM (HEPES) adjusted to pH 8.0 with 1 M NaOH. To allow the separation capillaries to reach the cathode, a 20 cm piece of 100 μm i.d. by 360 μm o.d. fused silica capillary was connected to the end of the short separation capillary using a butt-type connection with Teflon tubing sleeve (1 cm long,

1/16" o.d., 0.01" i.d. from Alltech Associates, Deerfield, IL). This connection allowed the majority of the voltage to be dropped across the smaller i.d. capillary.

On-line Derivatization and Sample Injection

The microdialysis/capillary electrophoresis system with on-line derivatization used in this work is similar to the one shown in Chapter 4. Microdialysate and the derivatizing agent were separately pumped into a 0.15 mm bore Teflon tee (Valco Instruments Inc., Houston, TX) by a microsyringe pump at 79 nL/min. The tee dead volume was 53 nL. The capillaries were sleeved into 2 cm lengths of Teflon tubing and held in place inside the tee by 1/16" Teflon ferrules and nuts. The derivatization solution was 2.0 mM mBBr and 1.2 % (v/v) acetonitrile in 10 mM ammonium bicarbonate buffer at pH 8.0. The acetonitrile facilitated solvation of mBBr. Fresh derivatization solution was used for each day of experiments. The derivatization solution was pumped through a 5.0 cm length of 75 μm i.d. by 360 μm o.d. fused silica capillary to the reaction tee. The dialysis probe was connected to the reaction tee by a 2.5 cm length of 75 μm i.d. by 360 μm o.d. fused silica capillary. The reactor capillary connecting the reaction tee to the interface consisted of 11.0 cm of 75 μm i.d. by 360 μm o.d. fused silica capillary. The dialysis and derivatizing flows combined for a 158 nL/min flow rate through the reactor capillary allowing for a reaction time of 3.0 min. All capillary to capillary connections were made by butting the capillaries together inside a 1 cm long Teflon tubing sleeve.

The separation capillary was coupled to the reactor capillary via a flow-gated interface which allowed dialysate samples to be automatically injected onto the separation capillary. Operation and characterization of the interface has been described in Chapter 2.

Briefly, the interface consisted of a Lucite block that held the outlet of the reaction capillary and the inlet of the separation capillary aligned with a ~75 μm gap between them. During a separation, a gating flow of electrophoresis buffer was pumped at 0.34 mL/min by a Sage 341B syringe pump (Orion Research Inc., Boston, MA) through the gap between the capillaries. This flow prevented derivatized dialysate from entering the separation capillary. To inject sample onto the column, the gating flow was stopped by a pneumatically-actuated gating valve. While the gating flow was stopped, the injection voltage was applied. In most cases, no delay was allowed between the stopping of the gating flow and application of the injection voltage. Once the injection was complete, gating flow was resumed and the separation voltage applied. For *in vivo* measurements, dialysate injections were typically made with -100 V for 2 s. The exact injection voltage and time were varied to get consistent performance in terms of theoretical plates and sensitivity. This was necessary because with the flow-gated interface, the injected amount depends not only on the voltage and time, but also the space between reaction capillary and separation capillary which varied slightly from day-to-day.

Detection, Data Collection, and Data Reporting

Fluorescence detection was accomplished using an epillumination fluorescence microscope (Axioskop, Carl Zeiss, Inc., Hanover, MD) described in Chapter 4. The 2 mW, 354 nm line of a He-Cd laser (Model 4210B, Liconix, Santa Clara, CA) was used as the excitation source. The excitation beam was reflected into the back of a 40x, 0.75 numerical aperture (NA) Fluar objective (Zeiss) by a dichroic mirror with a 400 nm transition and focused onto the capillary. The objective was a 40x, 1.30 NA Fluar oil

immersion lens. The emitted radiation was collected by the objective, passed through the dichroic mirror, and filtered with a 450 nm interference filter with 25 nm bandwidth (Andover Corp., Salem, NH). The laser excitation wavelength and emission interference filter wavelength were not optimal for the detection of the mBBr-derivatized thiols since their excitation maximum is 395 nm and their emission maximum is 475 nm. However, they were adequate for physiologically relevant levels of thiols to be measured in this experiment. Light passing through the interference filter was measured using a DCP-2 photometer system (CRG Electronics, Houston, TX) equipped with a photomultiplier tube (R928, Hamamatsu, Bridgewater, NJ). The output of the current to voltage converter was interfaced to an IBM-compatible computer. Data acquisition and automated control of the flow-gated system was accomplished with a National Instruments AT-MIO-16F-5 multi-function board (Austin, TX). Data were collected at 20 Hz and low-pass filtered at 10 Hz.

All mean values are reported ± standard error of the mean (± SEM) with number of replicates (n) unless stated otherwise.

Microdialysis

Flexible loop microdialysis probes (ESA, Bedford, MA) made from cellulose fibers (6 kDa cut-off) were used. The flexible loop probes had 450 µm tip diameters and 2 mm tip lengths. The overall length from the tip of the probe to the outlet was 5 cm. Approximately 1 cm of the outlet was sleeved into a fused silica capillary with 150 µm i.d. and 360 µm o.d. dimensions and sealed with cyanoacrylate cement. This modification facilitated using a butt connection with Teflon sleeves to the line transferring dialysate to

the reaction tee. Dialysis probes were perfused with artificial cerebral spinal fluid (aCSF) consisting of 145 mM NaCl, 2.68 mM KCl , 1.01 mM $MgSO_4$, and 1.22 mM $CaCl_2$. The high K^+ perfusate solutions for stimulation experiments consisted of 2.62 mM NaCl and 145 mM KCl and all other salts were the same. The dialysis flow rate was 79 nL/min.

Surgical Preparations and Procedures

Male Sprague-Dawley rats weighing 250-350 g were anesthetized with subcutaneous injections of 100 mg/mL of chloral hydrate. The initial injection was 4.0 mL/kg. Booster injections of 2.0 mL/kg were given every 30 min until the animal no longer exhibited limb reflex. After surgery, the rat was kept unconscious with subcutaneous administration of 1.0 mL/kg chloral hydrate as needed. Once the rat was secured in the stereotaxic apparatus, the microdialysis probe was placed in the striatum to the coordinates +0.02 AP, -0.30 ML, -0.65 DV from bregma (Pellegrino et al., 1967). Basal level electropherograms were taken until they were stable, typically 1.5 hours after insertion of the dialysis probe.

Results and Discussion

On-Line Derivatization Conditions with mBBr

In order to increase selectivity and make the thiols detectable, we utilized on-line derivatization with mBBr, as illustrated in Figure 5-1. This reagent has been extensively used as a fluorogenic label for the determination of thiols in biological samples (Fahey et al., 1981). It has several attractive features for our application of on-line derivatization including: 1) reasonably fast reaction kinetics with reaction times with thiols at pH 8.0 as

short as 3 minutes, 2) good photostability and chemical stability, and 3) favorable optical properties including emission in visible wavelengths and good quantum yields (Fahey et al., 1981; Kosower and Kosower, 1995).

The initial step in developing an on-line system for thiols was determination of the effect of mBBr concentrations on analyte signal, as demonstrated in Figure 5-2. For this experiment, the microdialysis probe was removed from the system shown in Figure 4-1 and a mixture of 8 μM glutathione and 10 μM cysteine in aCSF was pumped directly into the reaction tee. It was found that for on-line analyses, a large excess of mBBr was necessary to produce detectable amounts of product in the short time required. Glutathione reacted more favorably with mBBr than cysteine as shown by their corresponding peak heights. The concentration of 3 mM mBBr gave the best sensitivity; however, this high of a concentration also caused formation of large reagent peaks that overlapped with the cysteine peak. Therefore, we typically used 2 mM mBBr in the derivatization solution which yielded slightly poorer sensitivity but better resolution.

Calibration of Microdialysis Probes

In vitro calibration of the dialysis probes showed that at 79 nL/min and 37 °C, the relative recovery was 96.6 ± 3.8 % for glutathione and 98.1 ± 3.2 % for cysteine (n=5). These values are within experimental error of 100% indicating quantitative recovery. The high recovery is demonstrated in Figure 5-3 which compares *in vitro* electropherograms obtained with and without the dialysis probe in-line. When the dialysis probe was removed from the system, standard solutions containing 8 μM glutathione and 10 μM cysteine were pumped directly into the reaction tee at 79 nL/min. When the dialysis probe

was in-line, it sampled from a solution of 8 μM glutathione and 10 μM cysteine maintained at 37°C. In this particular example, the peak heights obtained with and without the probe for cysteine were 3.48 and 3.55, respectively, while the peak heights for glutathione were 3.85 and 3.93, respectively (peak heights in arbitrary units). The nearly identical peak heights are obtained are indicative of nearly 100% relative recovery. Once again, we have shown that under these conditions, 100% recovery is achieved *in vivo* as well as allowing the probes to be operated without *in vivo* calibration.

The high recoveries obtained for glutathione and cysteine are not surprising considering its low molecular weight 307 and 121 daltons, respectively, and the 6 kDa molecular weight cut-off of the dialysis membrane. These results are in contrast to the low recoveries of 0.2-21.6 % previously reported for glutathione and cysteine (Landolt et al., 1992; Yang et al., 1994). Part, if not all of the difference may be attributed to the low flow rates used here compared to the more conventional flow rates (0.5-2.0 μl/min) used in the previous work. Low flow rates, unlike conventional flow rates, allow analytes enough time to equilibrate across the dialysis membrane. Another possible difference is that with on-line monitoring, analytes are derivatized and analyzed immediately after being removed from the brain, whereas in the off-line monitoring situation they are stored for some time before analysis. In the latter case, the analytes may have enough time to be oxidized yielding artificially low values.

Besides high recoveries, the other figures of merit of the system were also sufficient for *in vivo* monitoring of glutathione and cysteine. The peak heights for glutathione and cysteine were linear with respect to concentration ($r>0.9998$) in the

physiologically relevant range of 0-20 μM, when the flow rate was 79 nL/min. Over this concentration range, the peak heights had RSD of 2.5-4.9% depending on the concentration and day of experiment. Detection limits for glutathione and cysteine, defined as the concentration or mass that would give a peak height three times the root mean square noise, were between 12-24 nM or 0.3-0.6 attomoles in day-to-day operation.

Temporal Resolution of System

Temporal resolution is an important characteristic when monitoring sudden or rapid concentration changes in the sampling environment. The temporal resolution of our system was evaluated *in vitro* by making step changes in the glutathione and cysteine concentration at the probe while sampling the dialysate with the CZE system. The step changes were performed by moving the probe between reservoirs containing different concentrations of the analytes. Figure 5-4 illustrates the data obtained from one of these experiments where the dialysis flow rate was 79 nL/min and the sampling rate (time to take one electropherogram) was 90 s. Changes in glutathione and cysteine concentration were observed 9 min after it was made at the probe. This delay is the time required to move through the dead volume and derivatization chambers. As shown in the figure, the step change in glutathione and cysteine concentrations is recorded over two electropherograms, thus indicating 180 s temporal resolution. In previous work with off-line systems, the temporal resolution, defined as the time to collect one fraction, for these compounds was about 10-30 min (Landolt et al., 1992; Yang et al., 1994). The improved temporal resolution here is a direct result of improved mass sensitivity of the CZE-LIF method compared to the HPLC methods used previously.

The temporal resolution in an on-line system can be limited by several factors including the separation time and dispersion of concentration zones by flow and diffusion during derivatization and transfer to the interface. Given the time resolution of 180 s, and a separation time of 90 s, it seems likely that flow and diffusion are the dominant factors. A possible approach to improving time resolution would be to decrease dead volume. Unfortunately, this may be a difficult task. Decreasing the length of the capillaries is impractical when working with animals. Decreasing the transfer capillary i.d. would increase the back pressure in the system, which we have found often leads to small, hard to detect leaks in the system.

In Vivo Monitoring of Glutathione and Cysteine

Electropherograms obtained *in vivo* from on-line derivatization of basal and stimulated levels of dialysate from the rat striatum are illustrated in Figure 5-5. As in our *in vitro* tests, the separation was complete in 90 s, allowing for a 90 s sampling rate with 180 s time resolution. The broad band in the 48-54 s range is associated with excess mBBr and unresolved neutral compounds. Although the reagent peak is rather large, the resulting electropherogram is much "cleaner", that is, it exhibits fewer reagent and other interfering peaks, than chromatograms obtained by HPLC with mBBr derivatization (Yang et al., 1994). This fortuitous benefit of CZE is likely related to its separation mechanism. In CZE, samples are resolved based on charge/mass ratios whereas in HPLC the separation is based on hydrophobicity. Apparently, many of the extraneous peaks are not charged or nearly uncharged thus preventing their resolution by CZE. Indeed, when micelles were added to the electrophoresis buffer allowing a chromatographic separation,

that is, micellar electrokinetic capillary chromatography (MEKC), we observed complex chromatograms with many reagent peaks (data not shown). The simple electropherograms shown in Figure 5-5 allow for the resolution of glutathione and cysteine in a short period of time without interferences. The use of different pH buffers, MEKC conditions, or detectors optimized for mBBr derivatives may allow other thiols to be monitored by this approach.

Basal levels of glutathione and cysteine measured using this system were 2.0 ± 0.1 μM and 2.3 ± 0.3 μM ($n = 5$), respectively. We were unable to find literature estimates of extracellular glutathione and cysteine in the rat striatum; however, these values and their precisions are in good agreement with previous reports of approximately 1.9-3.2 μM glutathione and 2.0-3.2 μM cysteine in the extracellular space of the rat cortex (Landolt et al., 1992; Yang et al., 1994). Thus, this method gives quantitative results similar to those obtained previously using microdialysis sampling, but with better temporal resolution and simpler calibration.

To demonstrate *in vivo* monitoring by the system, glutathione and cysteine were measured in the striatum during infusion of K^+. Infusions of 145 mM K^+ through the dialysis probe caused increases in glutathione and cysteine levels, as illustrated in Figure 5-5. Results from monitoring glutathione and cysteine overflow during a K^+ stimulation are illustrated in Figure 5-6. The average concentration of glutathione and cysteine during stimulation was 3.0 ± 0.9 μM and 3.3 ± 0.5 μM ($n = 3$), respectively. This corresponds to a 1.5 ± 0.4 fold increase for glutathione and a 1.4 ± 0.3 fold increase for cysteine during K^+ stimulation. Although there are no previous reports of detecting these thiols *in vivo*

during K^+ stimulation, these results correlate well with data from rat striatal slices which showed a ~2.7 fold increase for glutathione efflux and ~1.6 fold increase for cysteine efflux during K^+ depolarization (Keller et al., 1989; Zangerle et al., 1992).

Conclusion

This system is the first to simultaneously obtain high relative recoveries and good temporal resolution with microdialysis sampling for brain glutathione and cysteine. Possible improvements in the system include different separation conditions and optimization of the detector, which may allow other brain thiols to be measured. In addition, since the system is compatible with smaller dialysis probes, it should be possible to improve spatial resolution. Finally, improved engineering of the transfer of reagents combined with faster separations, easily achieved by using higher electric fields for the separation, will allow better temporal resolution.

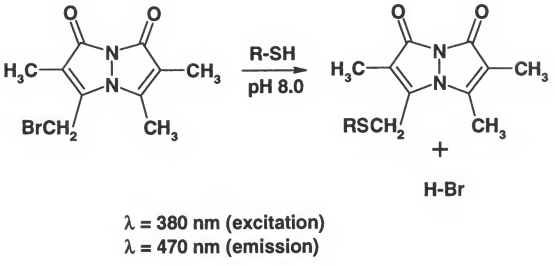

Figure 5-1 . Reaction of the derivatization agent monobromobimane (mBBr) with thiols.

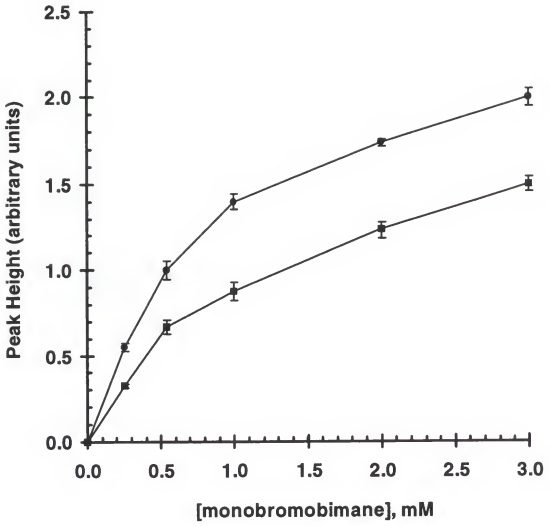

Figure 5-2. The effect of mBBr concentration on the fluorescent signal, measured as the peak height in electropherograms obtained on-line, of 8 μM glutathione(●) and 10 μM cysteine (■) standards in the on-line assay.

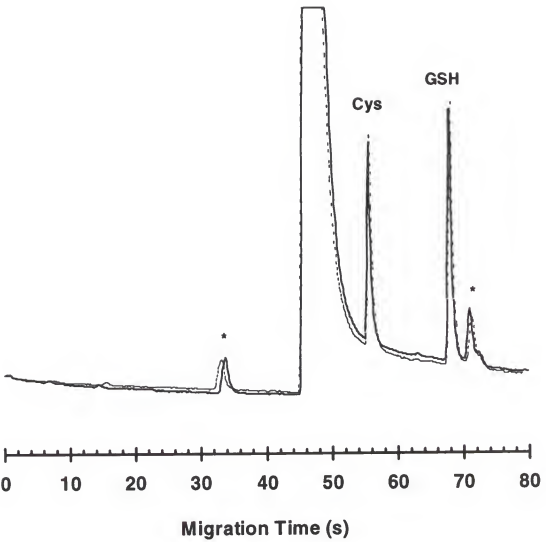

Figure 5-3. Overlay of *in vitro* electropherograms obtained with the dialysis probe (bold line) and without the dialysis probe (dashed line). Glutathione = GSH, cysteine = Cys, and reagent peaks = *. Other conditions given in the text.

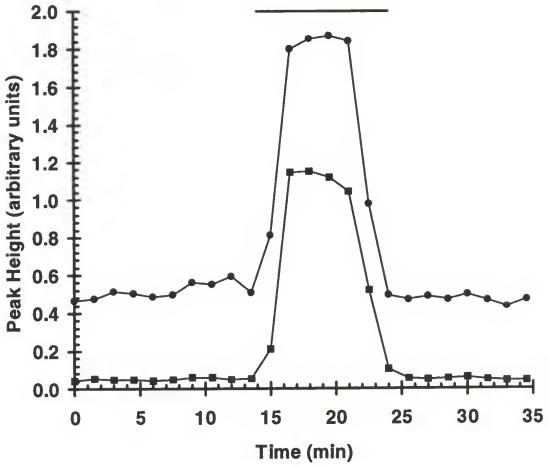

Figure 5-4. Response of the on-line system to step changes in glutathione (●) and cysteine (■) with a 90s sampling rate and a 79 nL/min perfusion rate. The dialysis probe was equilibrated in 2.0 μM glutathione and 2.5 μM cysteine and was then changed to a reservoir containing 8.0 μM glutathione and 10.0 μM cysteine during the time indicated by the bar. The reservoirs were held at 37°C. Each point represents the peak height obtained from one electropherogram.

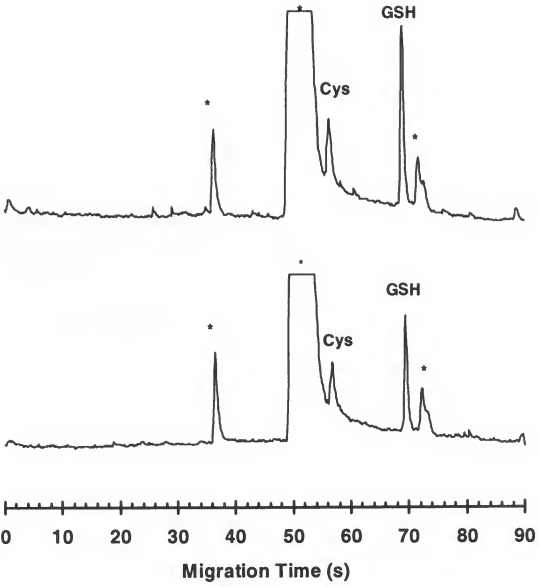

Figure 5-5. Comparison of electropherograms obtained *in vivo* under basal conditions (lower trace) and during stimulation with high K^+ (upper trace). Reagent peaks are identified by asterisks. No other peaks were identified. Separation conditions are found in the Experimental section.

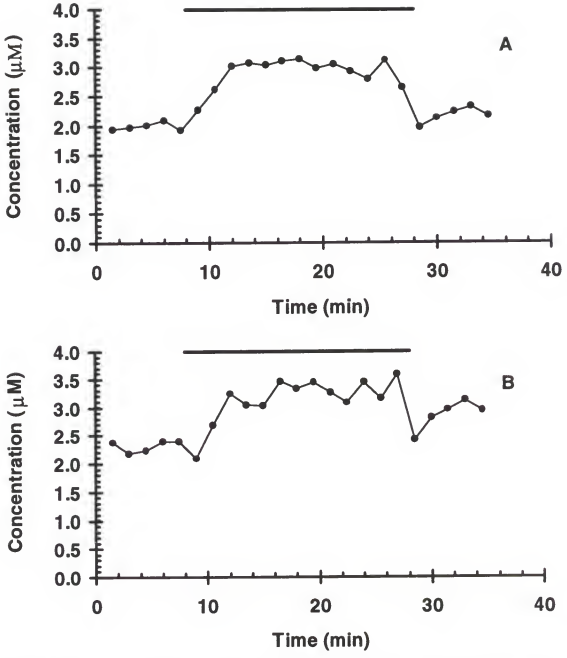

Figure 5-6. *In vivo* concentration of glutathione (A) and cysteine (B) *in vivo* during K^+ infusion with the microdialysis probe implanted in an individual rat. The bars indicate infusion time. Average basal and elevated levels are given in the text.

CHAPTER 6
HIGH TEMPORAL RESOLUTION MONITORING OF GLUTAMATE AND ASPARTATE *IN VIVO*

Introduction

Microdialysis sampling is a frequently used method for monitoring chemical concentrations *in vivo*, especially in the neurosciences (Ungerstedt, 1984). An often quoted disadvantage of microdialysis sampling is poor temporal resolution (Wages et al., 1986; Chen and Lunte, 1995). Insufficient temporal resolution is especially problematic in neurochemical applications where physiological events of interest are often associated with rapid changes in concentration (During, 1991). Temporal resolution in microdialysis is typically limited by the mass detection limit of the analytical method used with the probe. High sensitivity methods utilize smaller samples and therefore allow more frequent sampling of the dialysate. The advent of nanoscale analytical techniques, such as capillary electrophoresis (CE), combined with microdialysis has allowed much faster sampling times and changed the limiting factors in temporal resolution (O'Shea et al., 1992; Hernandez et al., 1993a; Hernandez et al., 1993b; Bert et al., 1996; Robert et al., 1996). With attomole detection limits and nanoliter injection volumes, CE in principle could allow sub-second sampling times; however, the impracticality of collecting nanoliter samples has led to the use of on-line combinations of microdialysis and CE (Hogan et al., 1994; Zhou et al., 1995; Lada et al., 1995; Lada and Kennedy, 1995; Lada and Kennedy, 1996). With on-line analysis, other factors can limit temporal resolution including band broadening during

sampling, transfer to the assay system, derivatization time, and separation time. For example, in an early report using CE with laser-induced fluorescence (LIF) detection on-line with microdialysis, naphthalene-dicarboxyaldehyde (NDA)-derivatized glutamate and aspartate were monitored with 120 s temporal resolution with the limiting factors being a combination of reaction time and separation time (Zhou et al., 1995). In Chapter 4, the separation time was reduced to 45 s; however, temporal resolution was limited to 90 s by band broadening that occurred during sampling and derivatization. In that work, the dialysis flow rate was much lower than typically used in order to improve the quantification of *in vivo* concentration.

The goal of this study was to explore the upper limit to temporal resolution for *in vivo* monitoring that is possible with a microdialysis/on-line CE-LIF combination. The initial part of the work was devoted to exploring and minimizing, where possible, the effect of sampling, derivatization, and separation on temporal resolution. As a result of this study, we demonstrate the highest temporal resolution monitoring reported by a microdialysis sampling method.

The latter part of the work involved using *in vivo* measurements to demonstrate the utility of rapid sampling. For these experiments, our target analytes were the excitatory neurotransmitters glutamate and aspartate. It has been well documented that these amino acids play significant roles in many important physiological processes including synaptic transmission, aging, learning, memory, synaptic plasticity, neuronal survival, and dendritic outgrowth and regression (Jahr and Lester, 1992; Lynch et al., 1990; Dagani and D'Angelo, 1992; D'Angelo and Rossi, 1992). Dysfunction of the

excitatory amino acid system may be responsible for many neurodebilitating diseases, such as Alzheimer's disease and epilepsy (Greenmyre and Young, 1989; Maragos et al., 1987). Progress in a greater understanding of the role of these neurotransmitters and treatments for diseases associated with them will benefit from analytical methodology that allows high temporal resolution monitoring. The high resolution possible with this method allows the first demonstration of monitoring overflow of glutamate and aspartate simultaneously during acute electrical stimulation in the rat brain.

Experimental

Chemicals

Glutamate, aspartate, OPA, β-mercaptoethanol, ascorbate, and chloral hydrate were from Sigma (St. Louis, MO). All chemicals were used as received. All solutions were prepared with water purified and deionized using a Millipore Milli-Q water purification system (Milford, MA), filtered through disposable Corning 0.2 μm nylon membrane syringe filters (Corning, NY), and purged for 15 min with He before use.

Capillary Zone Electrophoresis Conditions

Separations were performed in 6.5 cm lengths of 11 μm inner diameter (i.d.) by 360 μm outer diameter (o.d.) fused silica capillaries coated with polyimide (Polymicro Technologies, Phoenix, AZ). Each day, capillaries were rinsed for 10 min each with 0.1 M NaOH, deionized water, and electrophoresis buffer. A Spellman 1000R CZE HV power supply (Plainview, NY) was used for voltage application.

For CE separations, the inlet to detector length was 4.5 cm and applied voltage was between -24.0 and -27.5 kV. The electrophoresis buffer was 40 mM carbonate buffer adjusted to pH 9.5 with 1 M NaOH. To allow the separation capillaries to reach the cathode, a 20 cm piece of 150 μM i.d. by 360 μm o.d. fused silica capillary was connected to the cathode end of the separation capillary using a butt-type connection with Teflon tubing sleeve (1 cm long, 1/16" o.d., 0.01" i.d. from Alltech Associates, Deerfield, IL). This connection allowed the majority of voltage to be dropped across the separation capillary (Lada and Kennedy, 1996; Monnig and Jorgenson, 1991).

To perform the Ohmic Law experiment, the separation capillary was filled with electrophoresis buffer (40 mM carbonate, pH 9.5) and the voltage was applied for short intervals (1 minute). Current was recorded at each voltage and no injections were made. Current measurements were taken while microdialyisis was on-line with CZE..

Fluorescence detection was accomplished using an epillumination fluorescence microscope (Axioskop, Carl Zeiss, Hanover, MD) described in Chapter 4. The 354 nm line of a 7 mW helium-cadmium laser (Model 4210B, Liconix, Santa Clara, CA) was used for excitation. The objective for excitation and emission collection was a 40x, 1.30 numerical aperture Zeiss Fluar oil immersion lens. Data acquisition and automated control of the system was accomplished with a National Instruments AT-MIO-16F-5 multi-function board (Austin, TX). Data were collected at 2000 Hz and low-pass filtered at 1000 Hz using an RC filter available on the photometer system (DCP-2, CRG Electronics, Houston, TX).

On-line Derivatization and Sample Injection

A detailed description of the system used for on-line derivatization and coupling of microdialysis and CE can be found in Chapter 4. Dialysate and derivatizing solution (75 mM OPA, 150 mM β-ME, and 2 % (v/v) methanol in 35 mM borate buffer at pH 11.5) were separately pumped into a 0.15 mm bore Teflon tee (Valco Instruments Inc., Houston, TX) by a microsyringe pump at 1.2 μL/min. The outlet of the tee was connected to a flow-gated interface which allowed the sample stream to be periodically injected onto the CE column. The tubing joining the tee and flow-gated interface consisted of 16 cm of 75 μm i.d. by 360 μm o.d. fused silica capillary. This capillary served as the reactor capillary. The dialysis and derivatizing flows combined for a 2.4 μL/min flow rate through the reactor capillary allowing for a reaction time of 18 seconds. In some cases, the length of the capillary was varied to test different reaction times.

Injections of derivatized dialysate were performed using a flow-gated interface as described in Chapter 2. Briefly, the interface consisted of a Lucite block that secured and aligned the outlet of the reaction capillary and the inlet of the separation capillary with a 10-25 μm gap between them. High voltage was constantly applied to the separation capillary throughout the experiments. During a separation, a gating flow of electrophoresis buffer was pumped at 0.34 mL/min by a Sage 341B syringe pump (Orion Research Inc., Boston, MA) through the gap between the capillaries. This flow prevented derivatized dialysate from entering the separation capillary and provided fresh buffer for electrophoresis. To inject sample onto the column, the gating flow was stopped by a pneumatically-actuated gating valve equipped with a high speed switching assembly

(#HSSA, Valco). The injection time was determined by the valve close time, typically 60 ms, and injection voltage was the same as separation voltage.

Microdialysis

Flexible loop microdialysis probes (ESA, Bedford, MA) made from cellulose fibers (6 kDa cut-off) with 450 μm o.d. tip diameters and 2 mm tip lengths were used for all sampling experiments. The dialysis membranes had an i.d. of 210 μm for an internal volume of 0.12 μL. Probes come from the manufacturer with 75 μm i.d. tubing on the outlet end. This tubing was trimmed to 5 cm, the minimum workable length, for a volume of 0.22 μL. A microsyringe selector (BAS, West Lafayette, IN) was used for changing perfusion fluids during *in vivo* dialysis experiments. Dialysis probes were perfused with artificial cerebral spinal fluid (aCSF) consisting of 145 mM NaCl, 2.68 mM KCl , 1.01 mM $MgSO_4$, and 1.22 mM $CaCl_2$ at 1.2 μL/min. *In vitro* relative recoveries at 37 °C for glutamate and aspartate were 30.6 and 34.3% respectively.

Surgical Preparations and Procedures

`Male Sprague-Dawley rats weighing 250-350 g were anesthetized with subcutaneous injections of 100 mg/mL of chloral hydrate. The initial injection was 4.0 mL/kg. Booster injections of 1.0 mL/kg were given every 30 min until the animal no longer exhibited limb reflex. After surgery, the rat was kept unconscious with subcutaneous administration of 1.0 mL/kg chloral hydrate as needed. Once the rat was secured in the stereotaxic apparatus, a stimulating electrode was placed in the prefrontal cortex at the coordinates +0.35 AP, +0.15 ML, and -0.02 cm DV from bregma and the microdialysis probe was placed in the striatum to the coordinates +0.02 AP, -0.30 ML, -

0.65 cm DV from bregma (Pellegrino et al., 1967). Basal level electropherograms were taken until they were stable, typically 1.5 hours after insertion of the dialysis probe. Electrical stimulations consisted of 0.5 ms, 80 V square wave pulses applied at 80 Hz for 10 s using a S5 Stimulator (Grass Medical Instruments, Quincy, MA). A mineral oil droplet was placed on the stimulating electrode to ensure electrical connection with the rat.

Testing of Temporal Resolution of Probe. In experiments designed to test limitations imposed by the probe on temporal resolution, the dialysis probe was connected directly to a UV-detector (Spectra-Physics) equipped with capillary flow cell which allowed on-line monitoring. The probe outlet was connected to the detector by a 25 or 75 μm i.d. by 7.5 cm long piece of fused silica tubing which added 0.037 or 0.33 μL respectively to the total internal volume of the probe and connection tubing. This tubing was connected to the 5 cm length of 75 μm i.d. tubing that was part of the probe by butting the capillaries together inside a Teflon sleeve. The dialysis probe was placed in a reservoir containing ascorbate in aCSF at 37 °C. Step changes in concentration at the probe were made by using pipettes to rapidly change the concentration of analyte in the reservoir while stirring the reservoir solution. Alternatively, the probe was placed in the flow stream of a flow injection apparatus (FIA) and step changes in concentration made by injecting ascorbate of different concentrations into the FIA.

Results and Discussion

On-Line Derivatization with OPA

As mentioned in the introduction, with on-line coupling of microdialysis and CE-LIF, any step in the assay can limit temporal resolution. For this work, as in previous studies, we used OPA/β-ME as the derivatization reagent because of its rapid product formation and relatively low level of interferences (Chen et al., 1979). While minimizing reaction times is important to achieving the best possible temporal resolution, it is necessary to allow time for sufficient product formation. Therefore, we investigated the reaction time and its effect on fluorescent signal yield as measured by CE-LIF. For this experiment, the reaction time was varied from 5 to 50 s by changing the length of reaction capillary. As shown in figure 6-1, the fluorescence intensity began to level off at 18 s; therefore, 18 s reaction times were used for all future work since it provided adequate fluorescent signal in a relatively short reaction time. In Chapter 4, where much lower dialysis flow rates were used (79 nL/min), we reported reaction times of a few minutes. The longer time was in part due to less optimal conditions for the on-line reaction in the previous study (lower pH) and possible artifacts associated with the low flow rate system. The time for complete reaction seen here is in better agreement with prior work with OPA derivatization (Chen et al., 1979).

With 60 ms injections and 1.2 μL/min dialysis flow rates, the concentration detection limit for glutamate and aspartate was 0.2 μM and the mass detection limit was 10 attomoles at the dialysis probe. Detection limits were determined as the concentration

or mass that would yield peak heights three times the root mean square noise. Detection limits could possibly be improved by using a derivatization flow system that does not dilute the sample stream by two-fold during derivatization; however, better detection limits were not needed for *in vivo* determination of glutamate and aspartate. Calibration curves were linear up to 50 μM, with linear correlation coefficients of at least 0.999.

Capillary Zone Electrophoresis

In order to minimize the chance that the separation step will limit temporal resolution, we investigated the speed with which the OPA-derivatives could be separated. As has been previously demonstrated, high speed and high efficiency separations are possible in CE by increasing the electric field and decreasing the separation distance (Monnig and Jorgenson, 1991; Moore and Jorgenson, 1993; Jacobson et al., 1994). To be successful; however, the capillary i.d. must be decreased to prevent excessive Joule heating. In addition, extra-column band broadening due to injection and detection must be controlled. In the present study, it was also necessary to take into account practical considerations associated with the need for long term monitoring applications. Thus, a microscope was used for detection optics because of its ease of use and reliability; however, the minimum injection to detection length that could be practically used was 4.5 cm because of the configuration of the microscope stage. With these conditions, electric field strengths as high as -4.2 kV/cm could be used before efficiencies began to decrease.

This upper electrical field strength limit is demonstrated in the ohmic plot of Figure 6-2. An Ohm's Law plot allows for the simple determination of buffer concentration and maximum voltage that can be utilized with the particular buffer system. Linearity in the

plot is usually an indication that the capillary temperature is being adequately maintained, that is, the generated Joule heat is being effectively dissipated. At the point where linearity is lost, the thermostatic capacity of the system is exceeded and band broadening in the separation results. As shown in Figure 6-2, the current linearly increased as the electric field strength was increased from -2.6 to -4.2 kV/cm. Above -4.2 kV/cm, the current increased in an exponential manner. Thus, the upper electrical field strength boundry where Joule heat was still effectively dissipated was -4.2 kV/cm. A possible solution to avoiding excessive Joule heating would be to use separation capillaries with smaller inner diameters.

Our next experiments were directed at characterizing the injection of glutamate and aspartate under conditions of high electric field and short column distances. For this experiment, the electric field strength was held constant at -4.2 kV/cm while the injection time was varied from 20 to 100 ms. As shown in Figure 6-3, the efficiency peaked at 60 ms injection times resulting in an average maximum of 270,000 and 220,000 theoretical plates for glutamate and aspartate (n = 3), respectively. This corresponds to an average of 87,000 and 69,000 plates per second, respectively. The value of plates per second achieved here are among the highest reported and are comparable to those previously reported with optically-gated injection systems (Moore and Jorgenson, 1993).

The signal-to-noise ratio dependency on injection time was also studied. As with the previous experiment, the electric field strength was held constant at -4.2 kV/cm while the injection time was varied from 20 to 100 ms. As shown in figure 6-4, the signal-to-noise ratio peaked at 60 ms injection times. At injection times longer than 60 ms, the

separation efficiency began to deteriorate, leading to a reduction in peak heights and signal-to-noise ratios. Thus, it was found that 60 ms injections provided for both a maximum in efficiency and signal magnitude.

A typical electropherogram obtained with 60 ms injections is shown in Figure 6-5. The glutamate and aspartate peaks under these conditions are about 25 ms wide at the base which is narrower than the injection time. The narrowness of the zone may be due to bias against negatively charged analytes during injection. In addition, it may be due to the fact that during injection a finite time is required for analyte to cross the gap between reaction capillary and CE inlet so that analyte is at the CE inlet for only part of the 60 ms injection. The decrease in theoretical plates at longer injections may be attributed to overinjection; however, the decrease in efficiency with shorter injections is difficult to explain and suggests the possibility of a more complex phenomenon, possibly stacking, occurring during injection in the flow-gated interface.

This perplexing occurrence is further demonstrated by the atypical electropherograms shown in Figure 6-6. With an injection time of 20 ms and an electric field strength of -4.4 kV/cm, it was sometimes possible to separate both glutamate and aspartate standards (4 μM) in under 3 s with 1,930,000 and 1,920,000 theoretical plates, respectively. This corresponds to 694,000 and 688,000 plates/s, respectively, and is approximately a 7-8 fold improvement over this work and previously reports (Moore and Jorgenson, 1993). The glutamate and aspartate peaks under these conditions are about 8 ms wide at the base, which is once again narrower than the injection time. It is difficult to

repeat and explain such atypical results, and as a result, further work will be necessary to explain this phenomena.

Figure 6-7 illustrates typical electropherograms obtained at -3.7 and -4.2 kV/cm during *in vivo* sampling. Under *in vivo* conditions, these compounds could be routinely resolved from each other and other peaks in the sample in 3 to 5 s with between 160,000 and 240,000 theoretical plates. Although slightly better separations were obtained at -4.2 kV/cm (higher plates and shorter times), -3.7 kV/cm was utilized for all *in vivo* work because of better peak height reproducibility. At -4.2 kV/cm peak heights had an RSD of 15-20% while at -3.7 kV/cm the RSD was 1-6%.

The broad bands in Figure 6-7 are due to positive and neutral species present in dialysate. If injection time is reduced, these bands are narrowed, suggesting that at least part of the zone breadth is due to broadening during injection at 60 ms. It is not surprising that positively charged compounds would require shorter injection times than negatively charged compounds for optimal results during electrokinetic injection because of bias; however, the large difference in zone width is a further indication of a complex injection mechanism in the flow-gated interface as discussed above. Further optimization would be required to obtain high efficiency injection for cations and anions simultaneously.

Temporal Resolution with Microdialysis Sampling

In order to determine the effect of the dialysis probe and sampling on temporal resolution, experiments were performed in which step changes in concentration were made at the probe surface. The resulting changes in concentration were monitored by UV-absorbance detection as described in the Experimental section. Figure 6-8 illustrates

traces recorded for two different dialysis flow rates for monitoring ascorbate changes from 300 to 600 μM. The traces show that the step change is broadened during the sampling process to an extent that depends on the flow rate with higher flow rates giving sharper responses. The difference in plateau levels is indicative of the difference in recovery at the different flow rates.

The broadening observed in Figure 6-8 could be due to the time required to equilibrate the concentration in the probe or to band broadening that occurs by flow and diffusion as the concentration step moves from the probe to the detector. In order to further clarify the limiting factors, the temporal response (defined as the time for the signal to change from 10% to 90% of its maximum value) was plotted as a function of flow rate in Figure 6-9. In the figure, the data are compared to experiments where the tubing connecting the probe to the detector was reduced to 25 μm i.d. Therefore, in the former case the total dead volume is 0.77 μL (0.12 μL probe, 0.22 μL probe tubing, and 0.33 μL connection to the detector) and in the latter it is 0.38 μL (same as before but 0.037 μL for connection). Similar curves were obtained for both flow injection and manual step changes in concentrations. As shown, at lower flow rates the smaller dead volume gives a faster temporal response suggesting that broadening in the tubing contributes to the sluggish response. Above 1 μL, the curves converge suggesting that the dialysis probe and/or the minimal tubing associated with it are determining the temporal resolution at these flow rates.

The *in vitro* temporal resolution reaches a limiting value of about 10 s for a response time. This limiting value is set by the time required to equilibrate the dialysis

tubing with the extra-probe concentration and/or broadening that occurs in the tubing exiting the probe. Decreasing the size of the dialysis tubing or the connection tubing could improve temporal resolution. Decreasing probe size would result in lower recovery and compromise detection limits. These experiments do not account for possible detrimental effects on temporal resolution of the tissue, but rather illustrate the limit imposed by the probe itself.

The limitation in the response of the dialysis probe can be seen when monitoring glutamate and aspartate be CE-LIF as shown in Figure 6-10. In this experiment, the dialysate was sampled every 7 seconds and the dialysis probe was initially exposed to a solution of 5 μM glutamate and 2.5 μM aspartate in aCSF. At the first arrow, the concentrations of glutamate and aspartate were doubled as described in the Experimental section and at the second arrow concentration was returned to the original level. As shown in the figure, the step change in glutamate and aspartate is recorded over two electropherograms, thus indicating temporal resolution between 7 and 14 s, which is in good agreement with the results shown in Figure 6-9.

To summarize, when analyzing the sample stream with CE-LIF every 5 to 7 s, the temporal response will be 10 to 14 s representing a 7.5-fold improvement over previous work which used lower dialysis flow rates (Chapter 4). The best temporal resolution possible with this system at 1.2 μl/min is approximately 10 s. Since it is possible to achieve even faster separations, temporal resolution is ultimately limited by the sampling process, not the assay rate possible by CE-LIF with on-line derivatization.

In Vivo Monitoring of Glutamate and Aspartate with High Temporal Resolution

To demonstrate high temporal resolution *in vivo* monitoring by microdialysis/CE, glutamate and aspartate were measured in the rat striatum during electrical stimulation of the prefrontal cortex. Basal dialysate levels of glutamate and aspartate were 1.15 ± 0.27 and 0.30 ± 0.03 μM ($n = 5$), respectively. These values are in agreement with previously published reports (Gamache et al., 1993; Obrenovitch et al., 1993; Butcher et al., 1987; Hillered et al., 1989; Anderson and DiMicco, 1992; Tossman et al., 1986a and 1986b). Ten-second electrical stimulations of the prefrontal cortex caused a rapid and brief increase in both glutamate and aspartate as shown in Figure 8. The peak increase was 4.5 $\pm$ 1.4 and 4.9 ± 1.1 ($n = 5$) times the basal level for glutamate and aspartate, respectively. The timing of the increase in glutamate and aspartate suggests that their rise was at least as fast as could be monitored by the system and occurred immediately after stimulation. Elevated levels of glutamate and aspartate returned to basal levels within 35 s of the initial rise from basal levels. As a result, a 6-s sampling rate allowed for 7 measurements of elevated level of glutamate and aspartate, an observation impossible with preexisting microdialysis systems. In previous experiments using an enzyme electrode to monitor electrically stimulated glutamate overflow in the hippocampus, similar times to basal levels were seen (Hu et al., 1994). The high rate of removal is due to active uptake of the amino acids (Fonnum, 1984).

When the glutamate uptake inhibitor L-trans-pyrrolidine-2,4-dicarboxylic acid (PDC) was perfused into the striatum, basal levels of glutamate and aspartate increased 5.0 ± 1.4 and 8.9 ± 2.6 fold ($n = 5$), respectively indicating the basal level is controlled, at

least in part, by the uptake transporters. PDC also affected the time course of elevated glutamate and aspartate following electrical stimulation as seen in Figure 6-11. Specifically, PDC increased the half-life of glutamate and aspartate by over 3-fold. The maximal increase over basal level during electrical stimulation during PDC treatment was 1.7 (glutamate) and 2.1 (aspartate) fold which is significantly lower than the maximal increases elicited by electrical stimulation without PDC. Preliminary experiments suggest that this decrease in stimulated overflow is due to autoinhibition of amino acid release caused by the higher extracellular levels in the presence of an uptake inhibitor (see next chapter). While it is clear that more work is required to carefully characterize the neurotransmitter dynamics that are measured with this technique, the data presented here demonstrate the potential utility of high temporal resolution monitoring. Indeed, these results are the first report of simultaneous recording of glutamate and aspartate overflow *in vivo* during acute electrical stimulation.

Conclusions

The system described here is the first to simultaneously obtain high temporal resolution and multi-analyte capabilities. The temporal resolution of this system allows measurements not previously possible by microdialysis, such as time-resolved observation of concentration changes in neurotransmitters during brief electrical stimulations. It should be noted that it would be possible to use CE at even higher sampling rates; however, band broadening within the dialysis probe prevents the microdialysis/capillary zone electrophoresis system from achieving better than 10 s temporal responses. Thus, although many new measurements are possible with this system, the distortions caused by

microdialysis sampling is a limiting factor in accurately recording fast concentration changes. Despite this disadvantage, separation-based biosensors will continue to approach the temporal resolution of electrochemically-based biosensors. The future of separation-based biosensors; however, remains in its ability to concurrently measure multiple analytes without chemical interferences.

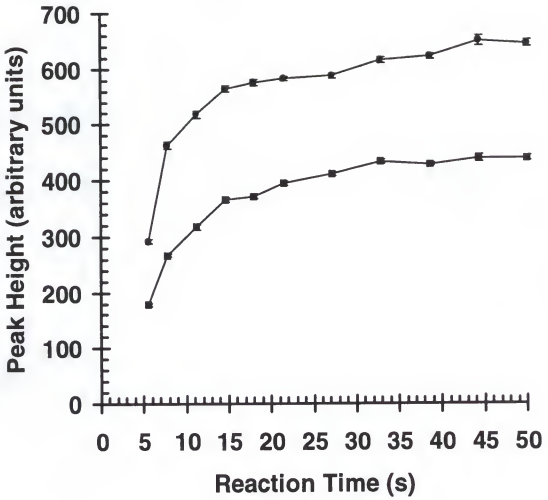

Figure 6-1. The effect of derivatization reaction time on the fluorescent signal of 4 μM glutamate (●) and aspartate (■). Peak heights are in arbitrary fluorescent units. A reaction time of 18 s was used for all remaining experiments.

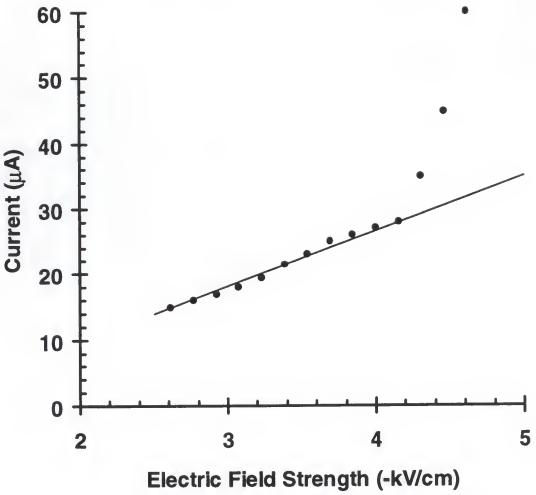

Figure 6-2. Effect of electric field strength on current (Ohm's Law Plot). The straight solid line is used as a linear reference while the points indicate each current measurement.

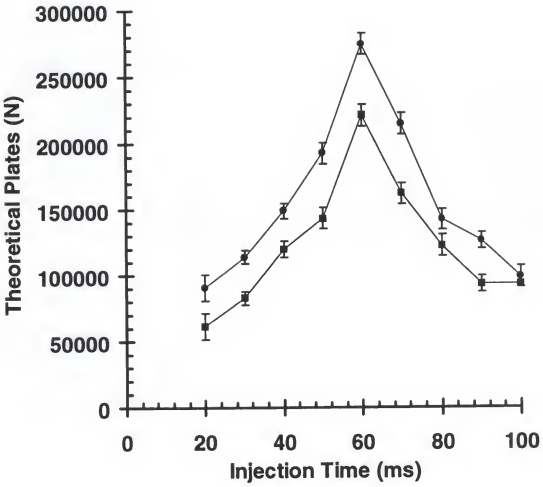

Figure 6-3. Effect of injection time on theoretical plates for 4 μM glutamate (●) and 2 μm aspartate (■). For the separations E = -4.2 kV/cm. All other conditions are given in the Experimental section.

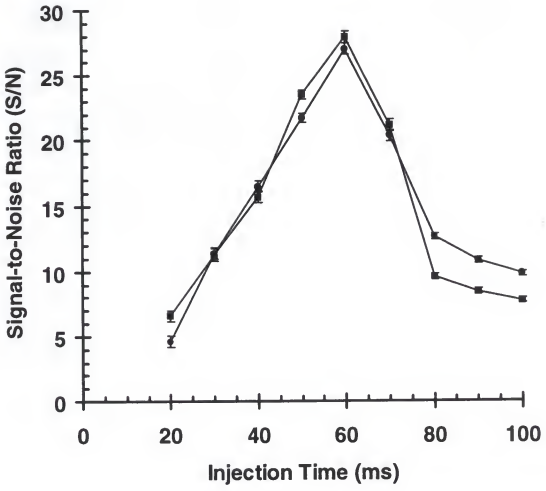

Figure 6-4. Effect of injection time on signal-to-noise ratio for 4 μM glutamate (●) and 2 μm aspartate (■). For the separations E = -4.2 kV/cm. All other conditions are given in the Experimental section.

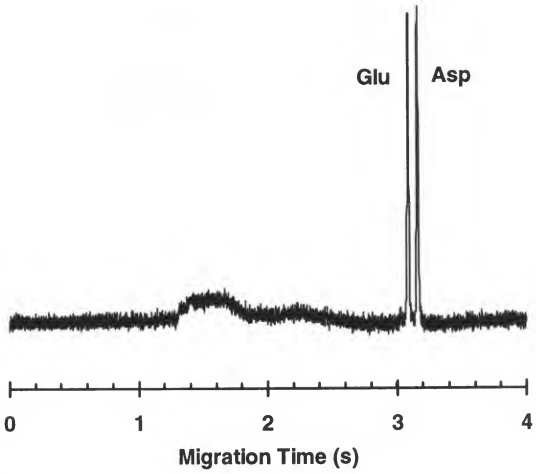

Figure 6-5. Typical electropherogram of 4 μM glutamate and aspartate standards sampled by microdialysis from a vial, derivatized on-line, and injected using the flow-gated interface.

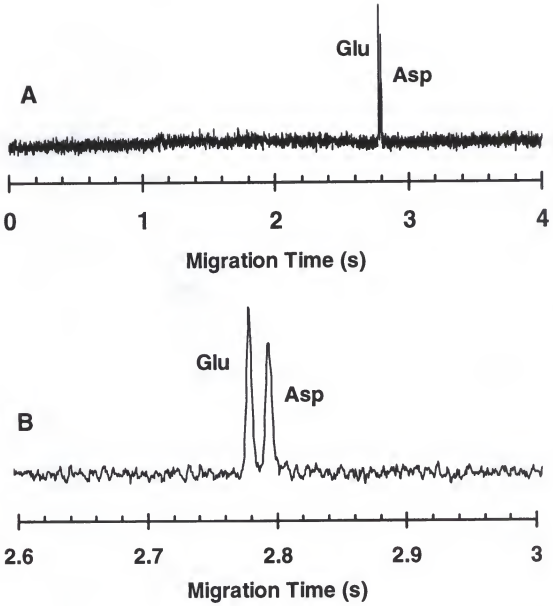

Figure 6-6. An atypical electropherogram of 4 μM glutamate and aspartate standards (A) and expanded view (B) sampled by microdialysis from a vial, derivatized on-line, and injected using the flow-gated interface. The electric field strength was -4.4 kV/cm and the injection time was 20 ms.

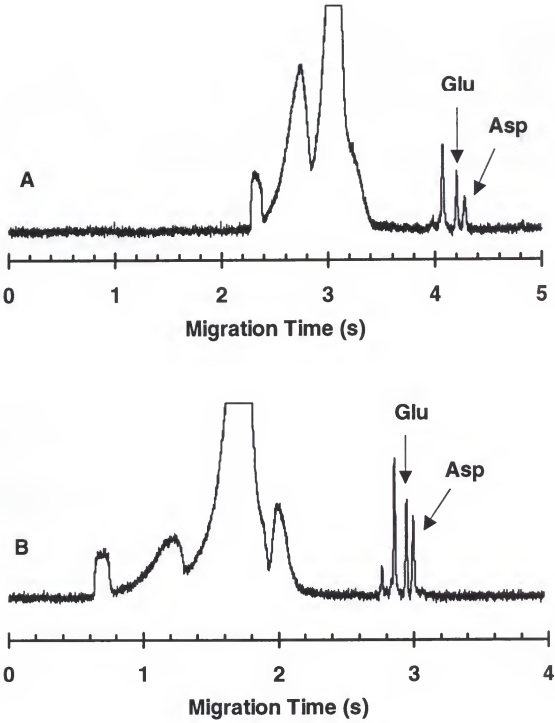

Figure 6-7. Comparison of *in vivo* basal electropherograms using -3.7 kV/cm (A) and -4.2 kV/cm (B) field strengths.

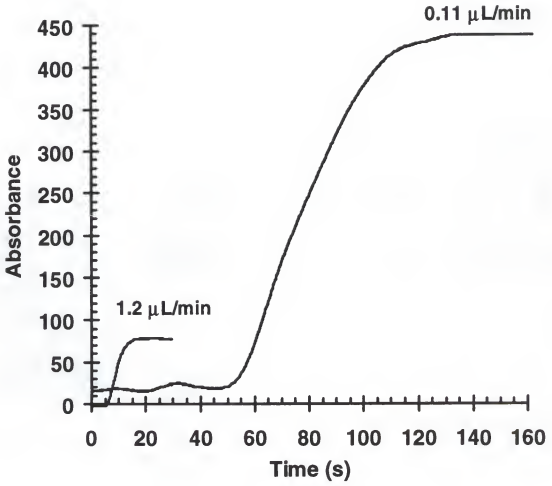

Figure 6-8. Traces recorded by UV absorbance during step changes from 300 μM to 600 μM ascorbate at the dialysis probe surface. Absorbance was measured in the capillary exiting the dialysis probe as described in the Experimental section. The tubing from the probe outlet to the detector was 0.65 μL.

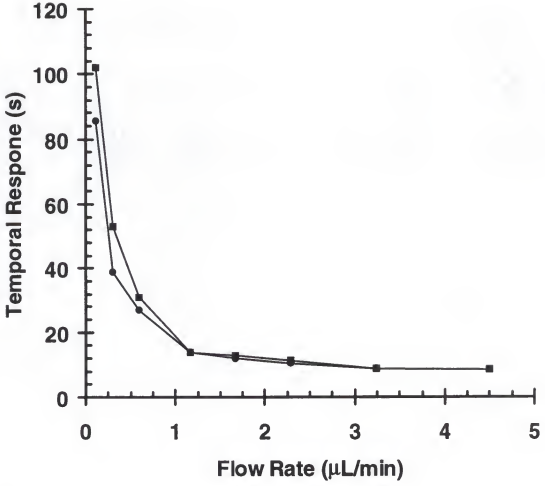

Figure 6-9. Effect of dialysis flow rate on response time for step changes in ascorbate concentration at the microdialysis probe surface recorded by UV absorbance as described in the text. Probe to detector volume was 0.65 µL (■) and 0.26 µL (●). In both cases the dialysis probe volume was 0.12 µL.

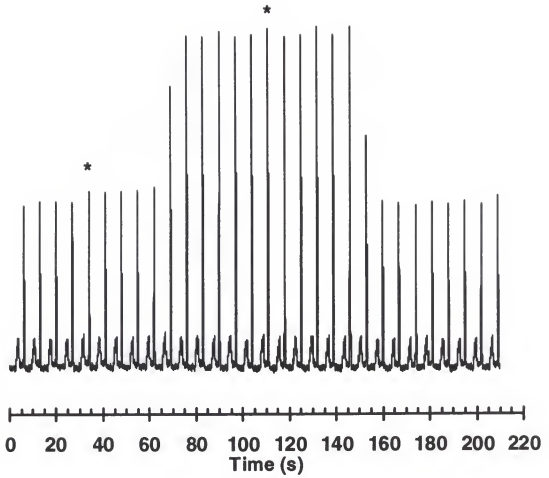

Figure 6-10. Test of response time of the system during in vitro step changes in glutamate and aspartate with 7 s sampling rate by CE-LIF. Thirty individual electropherograms were obtained. Initially the probe was equilibrated with 5 μM glutamate and 2.5 μM aspartate. At the first asterisk, the concentration was changed to 10 μM glutamate and 5 μM aspartate. The second asterisk indicates a change back to the original concentrations. The delay in response is due to the dead volume of the system. The perfusion rate was 1.2 μl/min.

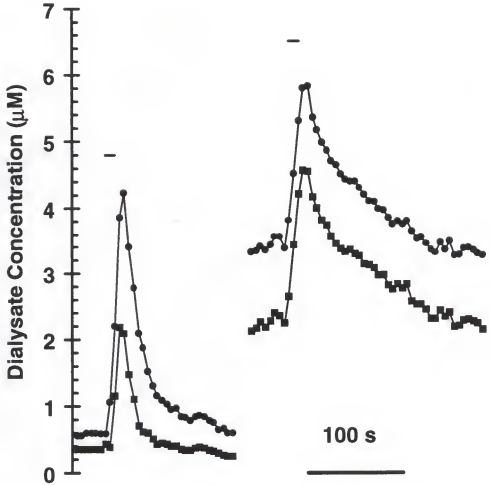

Figure 6-11. Effect of electrical stimulation on glutamate and aspartate *in vivo*. Each data point for glutamate (●) and aspartate (■) is from one electropherogram. The bar indicates electrical stimulation and it was corrected for the dead volume of the system. The stimulation on the left was during basal conditions and on the right in the presence of PDC. The second stimulation was obtained 60 min after the first and 20 min after addition of PDC to the perfusate.

CHAPTER 7
IN VIVO EVIDENCE FOR NEURONAL ORIGIN AND METABOTROPIC RECEPTOR-MEDIATED REGULATION OF EXTRACELLULAR GLUTAMATE AND ASPARTATE IN RAT STRIATUM

Introduction

The basic unit of communication in all nervous systems is the neuron, or nerve cell. Neurons collectively sense environmental change, swiftly integrate sensory inputs, and then activate effectors, such as muscle cells or gland cells, that carry out responses (Smith, 1996). The neuron consists of a cell body, dendrites, an axon, and axon terminals. The cell body contains the nucleus and the necessary components for protein synthesis while the dendrites of the neuron are viewed as the input zone, where the neuron receives and integrates excitatory and inhibitory information. The input may cause an electrical signal to be produced at an adjacent, specialized area of plasma membrane called the trigger zone. The signal rapidly propogates itself along the conducting zone, which extends from the start of the axon to its terminals. It is in the axon terminals where signaling molecules are sent to other cells.

Like all cells, neurons show polarity of charge across its plasma membrane, the inside being more negative than the outside. This polarity, which is regulated by sodium-potassium pumps located along the axon, results from differences in the concentration of potassium ions, sodium ions, and other charged substance present in the cytoplasm and extracellular fluid. When a neuron is stimulated, ions move across its plasma membrane

via the sodium-potassium pump, and in doing so, create a flow of electric charge called an action potential. When an action potential arrives at a neuron, the resulting voltage depolarization causes gated calcium channels to open. Calcium entry into presynaptic terminals leads to the fusion of neurotransmitter-containing vesicles to the plasma membrane and the subsequent release of chemical messengers to the extracellular space (Jessel and Kandel, 1993). The neurotransmitter-releasing neuron is known as the presynaptic cell while the extracellular space between two neurons is called the synaptic cleft. Once in the synaptic cleft, diffusion carries the transmitters to the postsynaptic or target cell. The transmitter molecules then bind briefly to receptors that are coupled to ion channels. With this binding, the channels open and give rise to a synaptic potential leading to either an excitatory or inhibitory response. The size of this potential depends on the receptors that are activated and the electrical state of the membrane.

The amino acid glutamate has been demonstrated to be a primary neurotransmitter for rapid synaptic transmission in the corticostriatal pathways of the rat brain (see critical review by Orrego and Villanueva, 1993). Aspartate, also present in the same corticostriatal pathway, may exert similar excitatory actions (Orrego and Villanueva, 1993; Maura et al., 1989; Palmer et al., 1989). Once released into the synaptic cleft by some form of excitatory action potential, both glutamate and aspartate are rapidly uptaken by a sodium-dependent, high-affinity transport system in the glutamatergic and aspartatergic nerve endings and also by adjacent glial cells. Glial cells provide physical support, metabolic assistance, and protection for the neurons. Within these glial cells, glutamate is transformed into glutamine by glutamine synthetase and then transferred back

into the glutamatergic nerve ending, where it is deaminated once more to glutamate. This pathway is shown in Figure 7-1. A similiar biochemistry exists for aspartate and appears to share the same uptake system with glutamate.

While evidence for the excitatory neurotransmitter role of glutamate appears definitive, previous attempts to characterize glutamatergic transmission *in vivo* through direct measurement of extracellular glutamate concentrations have fostered the view that glutamate levels are not regulated in the same manner as other chemical neurotransmitters. The atypical regulation of extracellular glutamate has been attributed to the diverse cellular sources and complex interaction among processes which ultimately control extracellular central nervous system (CNS) levels of this amino acid (Nicholls and Attwell, 1990) and has led investigators to conclude that, unlike other CNS transmitters, measurement of extracellular glutamate concentration does not provide a useful index of synaptic release (Herrera-Marschitz et al., 1996).

In the measurement of extracellular concentrations of neurotransmitters, two criteria, namely calcium-dependency and sensitivity to the sodium channel blocker tetrodotoxin (TTX), are frequently used to differentiate between contributions from neuronal release and other processes which may influence the extracellular pool of transmitter. Calcium-dependency, as mentioned earlier, refers to the requirement of calcium influx into presynaptic terminals for subsequent neurotransmitter release. Hence, calcium depletion should inhibit neurotransmitter release. TTX, on the other hand, inhibits sodium influx into nerve terminals, blocking action potential discharges and ensuing neurotransmitter release. Since both of these criteria are considered as minimal evidence

for neuronal release, failure to satisfy either requirement is usually regarded as an indication that processes other than neuronal release are contributing to the extracellular pool. The calcium-dependency and TTX-sensitivity requirements can be applied to both basal levels and to levels achieved in the presence of stimuli which promote neuronal release of the transmitter. Using this approach, investigators have concluded that glutamate levels measured by *in vivo* microdialysis are unrelated to synaptic release of the neurotransmitter. In contrast to the near complete reduction in levels of most classical transmitters following depletion of extracellular calcium, basal glutamate levels in the striatum of rats have been reported to decrease slightly (Morari et al., 1993; Semba et al., 1995; Xue et al., 1996), remain unchanged (Westerink et al., 1988; Yamamoto and Cooperman, 1994) or increase substantially (Herrera-Marschitz et al., 1996). Similar inconsistent results have been reported for glutamate following TTX treatment insofar as levels are unaffected (Westerink et al., 1987; Moghaddam, 1993; Hashimoto et al., 1995) or increased (Morari et al., 1993; Abarca et al., 1995; Herrera-Marschitz et al., 1996) by TTX treatments which cause near-complete reductions in the levels of other transmitters. Similar albeit more variable results have been reported for studies in which chemical stimuli have been used to facilitate neuronal glutamate release *in vivo*. While chemical agents such as veratridine and potassium chloride significantly increase extracellular glutamate concentration, the stimulated rise in glutamate levels is only partially reduced by local calcium depletion or TTX treatment (Young et al., 1990; Yamamoto and Cooperman, 1994; Hashimoto et al., 1995; Semba et al., 1995) and the effectiveness of such treatments vary considerably among different investigators (see Herrera-Marschitz et

al., 1996). Measurements of aspartate have had similar inconsistent results (Herrera-Marschitz et al., 1996).

In addition to the inconsistent dependencies of glutamate levels on calcium and neuronal action potentials, recent evidence has provided further support for the view that glutamate levels fail to accurately reflect glutamatergic synaptic activity *in vivo*. Previous reports based on studies *in vitro* have demonstrated the presence of presynaptic nerve terminal metabotropic glutamate receptors (mGluR) on glutamatergic neurons in the corticostriatal pathway (Lovinger et al., 1993 and 1994; Tyler and Lovinger, 1995), hippocampal mossy fibers (Forsythe and Clements, 1990; Baskys and Malenka, 1991; Maki et al., 1994; Manzoni et al., 1995) as well as other forebrain pathways (Glaum and Miller, 1993; Nakanishi, 1994). Within striatal synaptosomes, activation of mGluRs inhibits stimulus-dependent transmitter release and thereby decreases synaptic transmission (East et al., 1995). However, despite *in vitro* evidence for the existence of release-inhibiting mGluRs on corticostriatal terminals, recent investigations using *in vivo* measurements have failed to provide confirmatory evidence. To the contrary, striatal levels of glutamate have been reported to increase following mGluR activation in freely-moving awake rats (Liu and Moghaddam, 1995) as well as chloral hydrate-anesthetized rats (Samuel et al., 1996). While it may be true that previous *in vivo* methods have failed to provide confirmatory evidence of mGluRs inhibiting striatal glutamate release, there has been *in vivo* evidence for such inhibitory regulation by mGluRs with respect to stimulated dopamine release in the ventral striatum (Taber and Fibiger, 1995 and 1997).

In view of evidence for the inhibitory effect by mGluR on glutamate release *in vitro*, these observations appear to provide additional indication that conventional approaches for measuring glutamate *in vivo* do not provide an index of synaptic glutamate release. Therefore, we have undertaken the task of applying the novel method described in the previous chapter for measuring extracellular glutamate and aspartate with 5 s sampling as an approach for solving this dilemma. In this present study, the high temporal resolution afforded by this technque has enabled the detection of transient increases in striatal concentration resulting from brief, high-frequency electrical stimulation of the prefrontal cortex (PFC) in chloral hydrate-anesthetized rats. Use of electrical stimulation to selectively initiate neuronal release rather than the use of chemical stimulation was considered important in view of the protracted temporal effects caused by chemical stimuli as well as the potential impact of such manipulations on multiple cellular processes which could affect glutamate levels (Robinson et al., 1993). Furthermore, the present results demonstrate that stimulus-dependent changes in extracellular EAA levels under these conditions derive almost exclusively from neurogenic release of these substances and that release is under inhibitory control by mGluRs.

Experimental

Drugs and Reagents

Glutamtate, aspartate, o-phthaldialdehyde (OPA), β-mercaptoethanol (β-ME), bis-(aminoethyl)glycoether-N,N,N',N'-tetraacetic acid (EGTA), tetrodotoxin (TTX), L-trans-pyrrolidine-2,4-dicarboxylic acid (PDC), and chloral hydrate were from Sigma (St. Louis,

MO). (RS)-α-methyl-4-carboxyphenylglyine (MCPG) and (1S,3R)-1-aminocyclopentane-trans-1,3-dicarboxylic acid (trans-ACPD) were purchased from Tocris Cookson (St. Louis, MO).

Capillary Electrophoresis/Laser Induced Fluorescence Detection

A detailed description of the system used for on-line derivatization and coupling of microdialysis and CE has been given in the previous chapter. Separations were performed in 6.5 cm lengths of 11 μm inner diameter (i.d.) by 360 μm outer diameter (o.d.) fused silica capillaries coated with polyimide (Polymicro Technologies, Phoenix, AZ). The inlet to detector length of the separation capillary was 4.5 cm and applied voltage was -27.5 kV. The electrophoresis buffer was 40 mM carbonate buffer adjusted to pH 9.5 with 1 M NaOH. Fluorescence detection was accomplished using an epillumination fluorescence microscope (Axioskop, Carl Zeiss, Hanover, MD) described in Chapter 4. Data acquisition and automated control of the system was accomplished with a National Instruments AT-MIO-16F-5 multi-function board (Austin, TX). Data were collected at 2000 Hz and low-pass filtered at 1000 Hz using an RC filter available on the photometer system (DCP-2, CRG Electronics, Houston, TX).

For on-line derivatization, dialysate and derivatizing solution (75 mM OPA, 150 mM β-ME, and 2 % (v/v) methanol in 35 mM borate buffer at pH 11.5) were pumped separately into a 0.15 mm bore Teflon tee (Valco Instruments Inc., Houston, TX) by a microsyringe pump at 1.2 μl/min. The outlet of the tee was connected to a flow-gated interface which allowed the sample stream to be periodically injected onto the CE column. Electrokinetic injections of derivatized sample were made every 5 seconds.

Microdialysis

Flexible loop microdialysis probes (ESA, Bedford, MA) made from cellulose fibers (6 kDa cut-off) with 450 μm o.d. tip diameters and 2 mm tip lengths were used for all experiments. A microsyringe selector (BAS, West Lafayette, IN) was used for changing infusion fluids during *in vivo* dialysis experiments. Dialysis probes were perfused with artificial cerebral spinal fluid (aCSF) consisting of 145 mM NaCl, 2.68 mM KCl , 1.01 mM $MgSO_4$, and 1.22 mM $CaCl_2$ at 1.2 μl/min. When indicated, 2 μM TTX, 200 μM PDC, 200 μM MCPG, or 200 μM trans-ACPD were added to the dialysis medium. Unless stated otherwise, the calcium-free solution contained 2 mM EGTA. All drugs, except chloral hydrate, were administered by reverse microdialysis infusion into the striatum (1.2 μL/min). Measurements of glutamate and aspartate were taken thirty minutes after infusion with the indicated chemical treatment. *In vitro* relative recoveries at 37 °C for glutamate and aspartate were 30.6 and 34.3% respectively.

Surgical Preparations and Pharmacological Treatments

Male Sprague-Dawley rats weighing 250-350 g were anesthetized by subcutaneous injections of 100 mg/mL of chloral hydrate. The initial dose of 4.0 mL/kg was followed by booster injections of 1.0 mL/kg at 30 min intervals until the animal no longer exhibited a reflex to limb pinch. After surgery, the rat was kept unconscious with subcutaneous administration of 1.0 mL/kg chloral hydrate as needed. Once the rat was secured in the stereotaxic apparatus, a stimulating electrode (1 mm in length and diameter) was placed in the prefrontal cortex at the coordinates +0.35 AP, +0.15 ML, and -0.02 cm DV from bregma and the microdialysis probe was placed in the striatum to the coordinates +0.02

AP, -0.30 ML, -0.65 cm DV from bregma (Pellegrino, et al. 1967). These coordinates were chosen because the prefrontal cortex projects heavily to the dorsal and ventral striatum in a topographically organized manner (Sesack et al., 1989; Berendse et al., 1993). This projection has been found to use glutamate and aspartate as neurotransmitters, since lesions in the prefrontal cortex have been shown to reduce glutamate uptake in the dorsal striatum (Divac et al., 1977; McGreer et al., 1977). *In vivo* studies have demonstrated that electrical or chemical stimulation of the prefrontal cortex increases the release of both glutamate and apartate in the dorsal striatum (Godikhin, et al., 1980; Young and Bradford, 1986; Palmer et al., 1989; Perschak and Cuenod, 1990).

After insertion of the microdialysis probe into the rat striatum, basal level electropherograms were taken until baseline readings were stable, typically 1.5 hours after insertion of the dialysis probe. The stimulation period started 30 minutes after drug administration. Electrical stimulations consisted of 0.5 ms, square wave pulses (80 μA) applied at 20 Hz for 10 s using a S5 Stimulator (Grass Medical Instruments, Quincy, MA). For multiple stimulations on one animal, 30 min was allowed between stimulations. Also, mineral oil droplets were placed on the stimulating electrode to provide thorough electrical connection with the rat. Preliminary studies showed that this time allowed reproducible evoked responses to be obtained without apparent fatigue.

Data Reporting and Analysis

All basal levels are reported as concentrations in the dialysate (1.2 μl/min). Peak areas for glutamate and aspartate in the electropherograms were compared to calibration curves obtained after the *in vivo* experiment to determine concentrations. All calibration

curves had correlation coefficients >0.999. Plots of glutamate and aspartate concentration changes were prepared by comparison of the concentration of glutamate and aspartate determined from each electropherogram to the basal level prior to the electrical stimulation and/or drug application. Each plot is the average of at least 4 animals and at least 2 stimulations per animal. Amounts of increased glutamate and aspartate collected shown in Table 7-2 were determined by integrating the area under peaks induced by electrical stimulation. Statistical comparisons were made by a two-tailed Student's t-test. Unless stated otherwise, all values are reported as mean ± one standard error of the mean (SEM) with the number of experiments given as n.

Results

CE Measurement of Extracellular Glutamate and Aspartate Levels

Figure 7-2 illustrates a typical electropherogram obtained *in vivo* using the on-line system described in the Experimental section. The identity of the glutamate and aspartate peaks has been well-established in previous work based on migration times, spiking of samples with authentic glutamate and aspartate, and the expected migration order based on the separation mechanism (Chapters 4 and 6). Basal extracellular levels of glutamate and aspartate in dialysates obtained from the striatum were 0.92 ± 0.08 μM and 0.24 ± 0.04 μM (n = 21), respectively. These values and their ratio are in good agreement with previous measurements in this brain region in anesthetized rats (Tossman and Ungerstedt, 1986; Butcher et al., 1987; Butcher and Hamberger, 1987; Hillered et al., 1989).

As shown in Figure 7-2, the separation system developed for this work allowed the two amino acids to be separated rapidly following their collection and on-line

derivatization. The speed and sensitivity of the separation allowed the dialysate stream to be assayed every 5 s. The high temporal resolution in turn allowed us to observe the concentration changes of glutamate and aspartate during brief electrical stimulations of the PFC. As shown in Figure 7-3, we observed that with the onset of electrical pulses, both glutamate and aspartate levels rose instantaneously within the limits of our temporal resolution, and continued to increase during the entire stimulation. As soon as the stimulus was terminated, glutamate and aspartate levels began to decline and returned to pre-stimulus basal levels within 60 s. Also, the time given between electrical stimulations allowed for reproducible evoked responses without apparent fatigue. The amount of glutamate and aspartate collected by the dialysis probe over basal level as a result of the stimulation averaged 891 ± 70 and 284 ± 25 fmol (n = 52 stimulations in total of 20 rats), respectively. It is likely that inter-subject variability in stimulated responses was due in part to the strong dependence on electrode placement.

Effect of Calcium Depletion

Removal of calcium from the dialysis medium, with or without the addition of the calcium-chelating agent EGTA (2 mM), resulted in no change in the basal level for glutamate or aspartate, as shown in Table 7-1. Simply removing calcium from the dialysis medium did not affect the electrically stimulated concentration changes of glutamate and aspartate; however, when EGTA (2 mM) was added to calcium-free aCSF, the electrically stimulated release of glutamate and aspartate was diminished by 94% and 98% respectively as shown in Table 7-2 and Figure 7-4. Upon re-infusion with normal aCSF,

the electrically stimulated concentration changes of glutamate and aspartate recovered to previous control levels (see Figure 7-4 and Table 7-2).

Effect of Sodium-Channel Blockade with TTX

Infusion of the sodium channel blocker TTX (2 μM) into the striatum did not significantly affect basal glutamate levels, but did increase aspartate levels by 86.8 % ($p < 0.025$) as summarized in Table 7-1. TTX infusion completely eliminated electrically stimulated increases in glutamate and aspartate concentration, as seen in Figure 7-5 and Table 7-2. After 60-90 minutes of infusion with normal aCSF, electrically stimulated increases in glutamate and aspartate level only partially recovered to previous control values (see Figure 7-5).

Effect of Metabotropic Receptor Activation and Blockade

It was found that infusion with either the mGluR antagonist MCPG (200 μM) or agonist trans-ACPD (200 μM) alone did not significantly affect basal levels of glutamate and aspartate (Table 7-1). As shown in Figure 7-6 and quantified in Table 7-2, MCPG infusion did not significantly affect electrically stimulated concentration changes of glutamate and aspartate. In contrast, the agonist trans-ACPD decreased electrically stimulated concentration changes of glutamate and aspartate by 91% and 72%, respectively. This is illustrated by the plots in Figure 7-7 and the quantitative data in Table 7-2. Although MCPG had no effect by itself, it strongly antagonized the effect of trans-ACPD on glutamate and aspartate stimulated concentration increases as shown in Figure 7-7 and summarized in Table 7-2. The simultaneous infusion of MCPG and trans-ACPD had the unexpected effect of increasing the basal level of aspartate by 71%

(significant with $p < 0.025$) and a small, but not statistically significant effect on basal glutamate level as shown in Table 7-1.

Effect of Uptake Inhibition by L-trans-PDC

Infusion of the highly potent and competitive glutamate uptake inhibitor PDC (200 μM) into the striatum caused a dramatic increase in both glutamate (250%) and aspartate (380%) basal levels. This result is in agreement with previous studies on the effect of PDC on basal glutamate level in the striatum (Herrera-Marshitz et al., 1996; Rawls and McGinty, 1997; Massieu et al., 1995) and other brain regions (Zuiderwijk et al., 1996; Obrenovitch et al., 1996). PDC had no consistently observable effect on the electrically stimulated concentration changes of glutamate and aspartate, as illustrated in Figure 7-8 and quantified in Table 7-2. Since PDC did raise basal levels, the effect of MCPG was re-tested under these elevated basal conditions. Simultaneous infusion of PDC and MCPG (both at 200 μM) did not affect the basal level relative to PDC alone (see Table 7-1). Electrically stimulated rises in glutamate and aspartate concentration were dramatically increased, 600 and 585% respectively, as illustrated in Figure 7-7 and Table 7-2.

Discussion

Basal Levels of Glutamate and Aspartate Are Not Consistent with Neuronal Control

Concentrations of analytes measured by microdialysis are indicative of the actual extracellular concentrations which are ultimately determined by the rates of efflux from intracellular compartments and their ensuing removal from extracellular space (Herrera-Marschitz et al., 1996). Since glutamate and aspartate are involved in many different

physiological roles, their efflux may be caused by a variety of processes including release from synaptic vesicles, neuronal cytoplasmic pools, and glial cells. Moreover, removal of glutamate and aspartate from the synapse is thought to be dominated by amino acid transporters on both glia and neurons (Nicholls and Atwell, 1990). Under basal conditions, efflux and uptake remain in balance and a steady state level is achieved. The steady state level for glutamate was unaffected by addition of TTX and depletion of extracellular calcium. Aspartate concentration was unaffected by calcium removal, but actually increased by addition of TTX. While it is unclear what causes these effects, the results demonstrate that the efflux of glutamate and aspartate that generates the basal levels of these compounds is not exocytosis from neurons, but most likely from metabolic pools (Nicholls and Atwell, 1990). These data are illustrative of the dilemma of using basal levels of glutamate and aspartate as a measure of their neurotransmitter activity, as concluded previously (Orrego and Villanueva, 1993; Herrera-Marschitz et al., 1996). It should be noted; however, that basal glutamate levels measured 24 hours after probe implantation in awake rats quite possibly may be more related to neuronal activity. For instance, several studies using awake rats have found decreased basal glutamate levels after calcium removal (Semba et al., 1995; Morari et al., 1996; Xue et al., 1996) as well as altered basal glutamate levels following various physiological and pharmacological manipulations (Yamamoto and Cooperman, 1994; Moghaddam, 1993; Kalivas and Duffy, 1995; Xue et al., 1996; Liu and Moghaddam, 1995; Smolders et al., 1996). Differences between awake and anesthetized rats may reflect the ability of chloral hydrate anesthesia

to produce significant decreases in extracellular glutamate levels (Moghaddam and Bolinao, 1994).

Detection of Electrically Stimulated Neuronal Release of Glutamate and Aspartate

During electrical stimulation of the prefrontal cortex, the concentration of glutamate and aspartate detected by microdialysis sampling increases, indicating an increase in the rate of efflux in the striatum. Efflux was found to be clearly dependent on stimulation as the concentration increase began immediately with stimulation, continued for the entire stimulation, and decreased promptly with removal of stimulus (see Figure 7-4). Thus, unlike the efflux that occurs under basal conditions, the increased efflux of glutamate and aspartate during electrical stimulation satisfies the conventional criteria for neuronal release. Evidence for neuronal release is further confirmed in this study, since electrically stimulated release of glutamate and aspartate is strongly TTX-sensitive and completely calcium-dependent (see Table 7-2 and Figures 7-3 and 7-4). While not impervious, these results are consistent with the conclusion that increased efflux of glutamate and aspartate during electrical stimulation is a reflection of neuronal exocytosis associated with membrane depolarization. Thus, these results demonstrate, for the first time, direct measurement of changes in both glutamate and aspartate extracellular concentration *in vivo* that clearly exhibit the suitable characteristics expected for a neuronal source of neurotransmitters.

The only other previous report of detecting electrically stimulated changes in glutamate and aspartate striatal concentration following electrical stimulation of the PFC utilized 4-min of stimulation and 1-min sampling intervals (Perschak and Cuenod, 1990).

A clear neuronal origin for EAA release was not apparent from that study as the EAA concentrations were elevated for only the first minute of stimulation and no attempt was made to establish TTX-sensitivity and calcium-dependency. This present study demonstrates that measurement of neuronally derived glutamate and aspartate release is facilitated by the use of brief electrical stimulations in combination with a technique that allows high temporal resolution in monitoring concentration changes. This combination avoids the complications associated with non-specific chemical stimuli or prolonged electrical stimulations by allowing detection of short-lived concentration changes that occur during brief electrical stimulations. The only technique that offers temporal resolution comparable to this microdialysis-CE-LIF method is an electrochemical glutamate sensor based on L-glutamate oxidase (Hu et al., 1994). This device however will not allow simultaneous measurement of aspartate with glutamate, which may be of significance given the apparent neuronal origin of aspartate found in the present study.

If the detected glutamate and aspartate are released from neurons, then our results suggest that glutamate and aspartate can overflow from synapses and gather in the extracellular fluid for several seconds. Such a result may be unexpected since the common view of EAA-mediated neurotransmission suggests that once transmitters are released into the synaptic cleft, their actions are quickly terminated by uptake to ensure that communication occurs in a rapid, point-to-point fashion at synapses (Hille, 1992). It is possible that overflow does not occur under normal neuronal activity, but that the duration and intensity of the electrical stimulation evoked the substantial overflow detected. However, the possibility of overflow, under normal electrical activity, should not be

discounted since a recent study demonstrated that EAAs in hippocampal mossy fiber synapses may overflow and elicit more diffuse pre-synaptic and/or post-synaptic actions (Scanziani, et al., 1997). Such a result is consistent with our findings of overflow and persistence of elevated glutamate and aspartate concentrations after stimulation. Even if glutamate and aspartate synaptic overflow does not occur under normal physiological activity, the ability to evoke and detect overflow with temporal resolution is still of interest because it offers the opportunity to study, by direct chemical measurement, the regulation of release and uptake, as well as their interactions.

Regulation of Glutamate and Aspartate by Metabotropic Glutamate Receptors and Uptake

There are several types of glutamate receptors that mediate neurotransmission in the corticostriatal pathway, including the ionotropic N-methyl-D-asparate (NMDA), α-amino-3-hydroxy-5-methylisoxazole-4-propionate (AMPA), and kainate (KA) subtypes, and the mGluR subtype (Orrego and Villanueva, 1993). The three former subtypes are considered to be ionotropic receptors since they can be found coupled to ion channels along synaptic membranes. Furthermore, fast synaptic excitation in the striatum caused by glutamate release from corticofugal fibers occurs largely through the kainate or AMPA subtypes, whereas the NMDA receptor seems to be involved in more sustained responses (Calabresi et al., 1991; Herrling, 1985; Greenmyre et al., 1995; Cotman and Iversen, 1987). Although the ionotropic recepters have been extensively characterized in the striatum, the specific role of mGluRs in neurotransmission is still unknown, and this uncertainty has been mainly attributable to conflicting *in vivo* (Liu and Moghaddam, 1995;

Samuel et al., 1996) and *in vitro* (East et al., 1995; Lovinger et al., 1993 and 1994; Tyler and Lovinger, 1995) data from the corticostriatal pathway in the rat brain.

The ability of this methodology to measure glutamate and aspartate overflow that is apparently neuronal in origin has allowed further characterization of the metabotropic regulation of these compounds. Moreover, the emergence of phenylglycine derivatives as selective antagonists and cyclic glutamate analogues as specific agonists of mGluRs has enabled this receptor to be distinguished physiologically and pathologically.

The basal levels of glutamate and aspartate were not affected by the mGluR agonist trans-ACPD or antagonist MCPG, once again supporting the notion that basal levels in anesthetized rats are not determined by neuronal release (see Table 7-1). Trans-ACPD strongly suppressed electrically stimulated overflow (Table 7-2, Figure 7-7), in a fashion antagonized by MCPG, indicating that inhibition of neurotransmitter release is possible by activation of presynaptic mGluRs. MCPG alone did not effect electrically stimulated overflow, demonstrating that the tonic and stimulated levels of glutamate and aspartate are too low in the anesthetized rat to initiate inhibitory effects.

When the uptake inhibitor PDC is introduced into the striatum via reverse dialysis, the basal levels of glutamate and aspartate are greatly increased; however, the amount of glutamate and aspartate overflow observed during electrical stimulation is not significantly different than overflow obtained during control. This is somewhat surprising since it is expected that uptake impedence should increase the overal amount of released EAA that reaches the dialysis probe. This lack of an effect is clarified by considering that: 1) overflow is a balance between release and uptake and 2) PDC can indirectly affect the

amount of release by increasing the glutamate and aspartate levels such that mGluRs are activated. The latter is demonstrated by the strong effect of MCPG (Table 7-2 and Figure 7-8) when extracellular levels are increased by PDC. Thus, during infusion with PDC alone, electrically stimulated overflow is unaffected relative to control because the diminished uptake is apparently offset by an autoreceptor-mediated reduction in release. Also, PDC is a transportable competitive inhibitor and thus can increase glutamate efflux via reversal of glutamate transport. Therefore, under basal contitions, some of the PDC-stimulated glutamate efflux may reflect PDC uptake coupled to reverse transport of glutamate. During electrical stimulation, it is expected that glutamate transport would be inhibited. Under these conditions, PDC would not be transported and would therefore be unable to promote reverse transport of glutamate. Perhaps this accounts for the failure of PDC to augment electrically-induced glutamate efflux.

With MCPG present, autoinhibition of release is blocked allowing massive electrically stimulated overflow to be observed due to the lack of strong uptake combined with relatively unrestrained release. Comparison of results with PDC alone and PDC plus MCPG (Figure 7-8) illustrates the strength of autoinhibition. With PDC and MCPG present, the expected increase in the time required to clear glutamate and aspartate overflow caused by uptake inhibition is seen in a prolonged decay back to basal concentrations relative to control (Figure 7-8). In summation, these results demonstrate the potential for a synergistic relationship between uptake, tonic glutamate and aspartate level, and autoinhibition in regulating extracellular glutamate and aspartate concentrations.

Potential Functional Role of Autoreceptors

In the anesthetized rat, it is apparent that glutamate and aspartate release can be strongly inhibited by activation of mGluR; however, the basal and electrically stimulated concentrations appear too low to activate autoinhibition as indicated by the lack of effect of antagonist alone. These results call into question the possible physiological relevance of mGluR-mediated regulation of neuronal release; however, it is reasonable to speculate that mGluR in the striatum are activated in an awake animal since basal glutamate and aspartate levels in awake animals are comparable to what we have observed with PDC in an anesthetized animal (Hernandez et al., 1993; Young and Bradford, 1986). With the higher extracellular levels caused by PDC, electrically stimulated release was strongly inhibited by MCPG, suggestive of tonic mGluR activation.

It is interesting to note; however, that NMDA receptor stimulation activates a positive feedback loop within the basal ganglia, leading to further glutamate release from corticostriatal afferents (Rawls and McGinty, 1997). It should be then plausible to suggest the existence of inhibitory receptors, quite possibly mGluRs, to compliment the excitatory actions of such NMDA receptors. Clarification of the possible role of autoinhibition by mGluR under normal physiological conditions, such as an awake animal, requires further study.

Conclusion

The electrically stimulated changes in extracellular concentration of glutamate and aspartate observed by this methodology is apparently a measure of neuronal release and high-affinity uptake by amino acid transporters. Thus, this system provides a potentially

useful model for monitoring excitatory neurotransmission in the corticostriatal pathway of the rat brain. In addition, it seems likely that similar measurements could be used for other EAA pathways. The fact that electrically stimulated overflow could be regulated by metabotropic autoreceptors and amino acid transporters illustrates potentially important routes to manipulate the synaptic release of EAAs and to better understand their roles in numerous processes including learning, memory, and excitotoxicity.

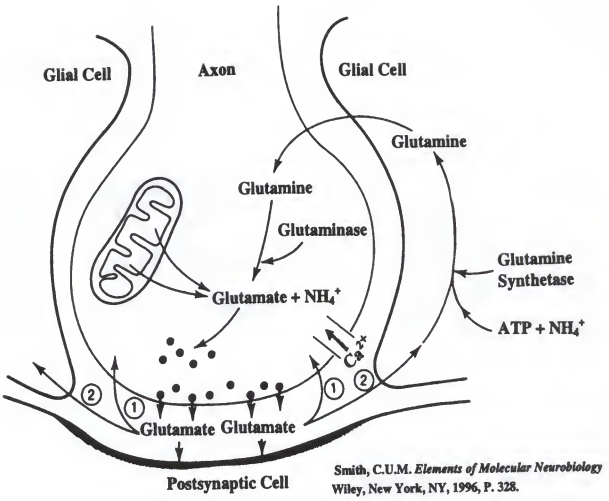

Figure 7-1. Schematic of a glutamatergic synapse. Glutamate, once released from synaptic vesicles into the synaptic cleft after some action potential, can be uptaken along two pathways: (1) reentry into the synaptic terminal or (2) into neighboring glial cells. In glial cells, glutamine synthetase forms glutamine from glutamate and is then passed back into the synaptic terminal. Here glutaminase reforms glutamate and subsequently forms pools of glutamate with fresh glutamate derived from Krebs cycle activity in mitochondria. The free glutamate is sequestered into synaptic vesicles to await the arrival of the next action potential.

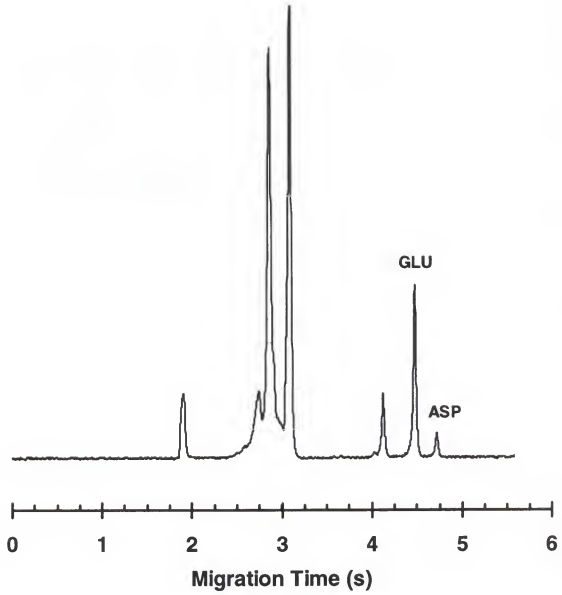

Figure 7-2. Typical electropherogram obtained in vivo with on-line derivation by CE-LIF.

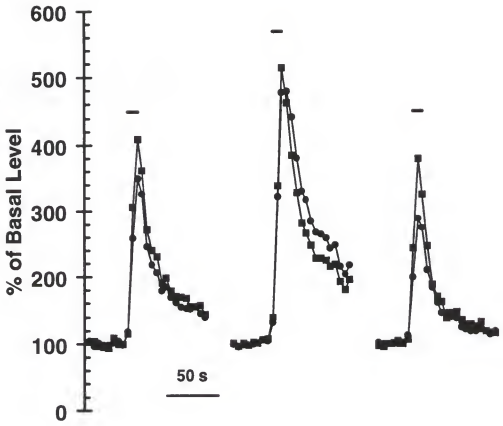

Figure 7-3 . Glutamate (squares) and aspartate (circles) striatal dialysate concentration changes elicited by three successive electrical stimulations of the prefrontal cortex in a single anesthetized rat. Bar indicates the stimulation. The stimulations were 30 minutes apart.

Table 7-1. Effect of Chemical Additives in Microdialysis Medium on Basal Levels of Glutamate and Aspartate.

Treatment	GLU (% of Control)	ASP (% of Control)
Control	100 ± 9	100 ± 17
2 μM TTX	101 ± 9	187 ± 15 *
2 mM EGTA/Ca^{2+}-free	99 ± 17	101 ± 20
200 μM PDC	250 ± 9 *	380 ± 15 *
200 μM PDC/ 200 μM MCPG	252 ± 24	365 ± 81
200 μM MCPG	107 ± 9	128 ± 20
200 μM ACPD	98 ± 14	101 ± 17
200 μM ACPD/ 200 μM MCPG	114 ± 11	171 ± 8 *

Basal levels of glutamate and aspartate in dialysate from untreated rats were 0.92 ± 0.08 and 0.24 ± 0.04 μM (n = 21) respectively. Values in the table are expressed as percent of control levels (mean ± SEM) for a given animal following a 30 min infusion of the indicated drugs. For each treatment, 4 subjects were used. Significant differences ($p < 0.025$) from control values are indicated by an asterisk (*).

Table 7-2. Effect of Chemical Additives in Microdialysis Medium on Electrically Stimulated Overflow of Glutamate and Aspartate (Mean ± SEM)

Treatment (Concentration in μM)	N	GLU (%)	ASP (%)
Control	52	100 ± 8	100 ± 9
EGTA (2000)	8	6.2 ± 0.2*	2.4 ± 0.1*
Post EGTA	10	104 ± 15**	129 ± 32**
TTX (2)	9	5.1 ± 0.1*	0.7 ± 0.003*
Post-TTX	8	33 ± 2**	104 ± 5**
MCPG (200)	8	93 ± 7	92 ± 6
ACPD	9	9.3 ± 1.8*	27 ± 5*
ACPD (200) + MCPG (200)	9	62 ± 14**	89 ± 8**
PDC (200)	12	96 ± 7	97 ± 8
PDC (200) + MCPG (200)	12	597 ± 109**	568 ± 78**

Data for electrically stimulated increases in glutamate and aspartate levels were determined as net changes (measured in fmol) over baseline values. Control evoked responses for glutamate and aspartate for all subjects were 891 ± 70 and 284 ± 25 fmol (n = 52 total stimulations in a total of 20 rats), respectively. Values in the table are expressed as percentages of control responses (mean ± SEM) in rats subjected to each particular treatment. N indicates the total number of stimulations recorded in 4 rats for each treatment. At least two stimulations were performed in each subject for both control and treatment(s). Experiments with trans-ACPD plus MCPG and PDC plus MCPG were performed on the same rats as the trans-ACPD and PDC treatments respectively. Likewise, the post-EGTA and post-TTX treatments were performed on the same rats as the EGTA and TTX treatments, respectively. Asterisk (*) indicates a statistically significant difference from control ($p < 0.01$) and double asterisk (**) indicates a statistically significant difference from previous treatment ($p < 0.01$) on same animal. Statistical differences were determined as described in the text.

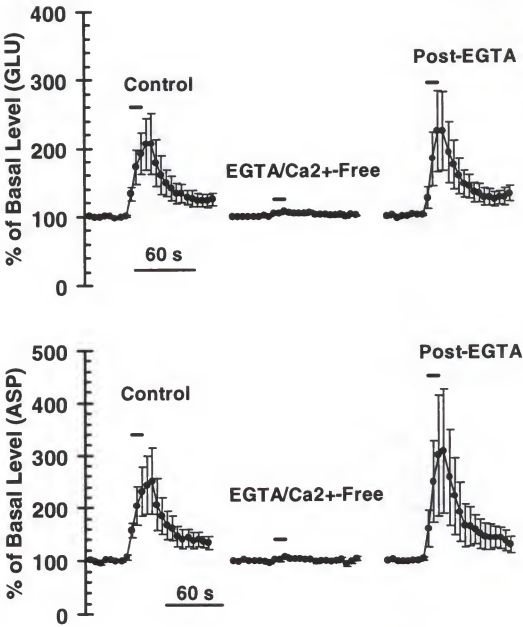

Figure 7-4. Effects of calcium-depletion (calcium-free aCSF with 2 mM EGTA) on basal and electrically stimulated glutamate (top) and aspartate (bottom) dialysate levels in rat striatum. Bar indicates 10-s of electrical stimulation of PFC. Data are presented as means ± SEM (n = 4) and are expressed as the percentages of the mean baseline of dialysate concentrations of glutamate and aspartate in the same animals.

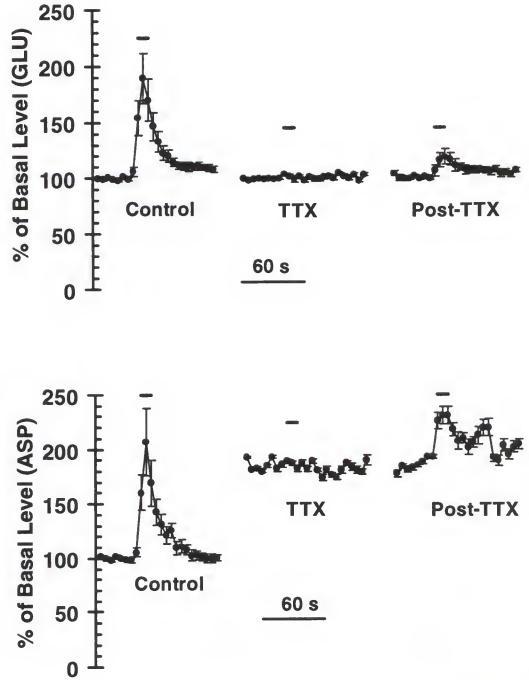

Figure 7-5. Effects of 2 μM tetrodotoxin (TTX) infusion on basal and electrically stimulated glutamate (top) and aspartate (bottom) dialysate levels in the striatum of anesthetized rats. Bar indicates 10-s of electrical stimulation of PFC. Data are presented as means ± SEM (n = 4) and are expressed as the percentages of the mean baseline of dialysate concentrations of glutamate and aspartate in the same animals.

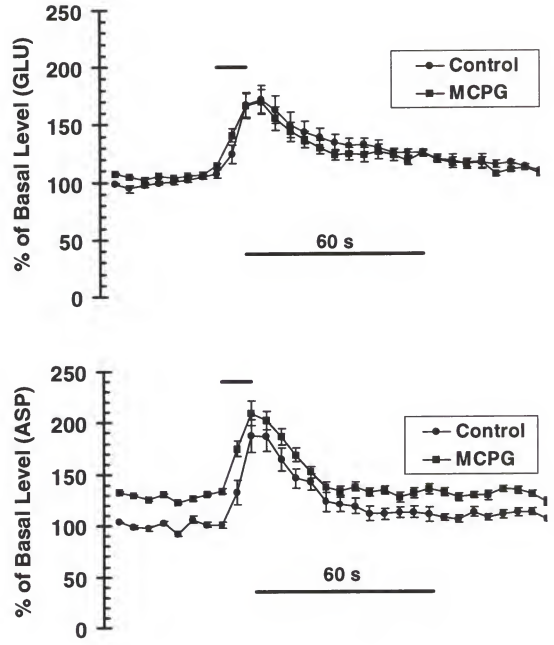

Figure 7-6. The effect of 200 μM MCPG infusion on basal and electrically stimulated glutamate (top) and aspartate (bottom) levels in the striatum of anesthetized rats. Bar indicates 10-s of electrical stimulation of the PFC. Data are presented as means ± SEM (n = 4) and are expressed as the percentages of the mean baseline of dialysate concentrations of glutamate and aspartate in the same animals.

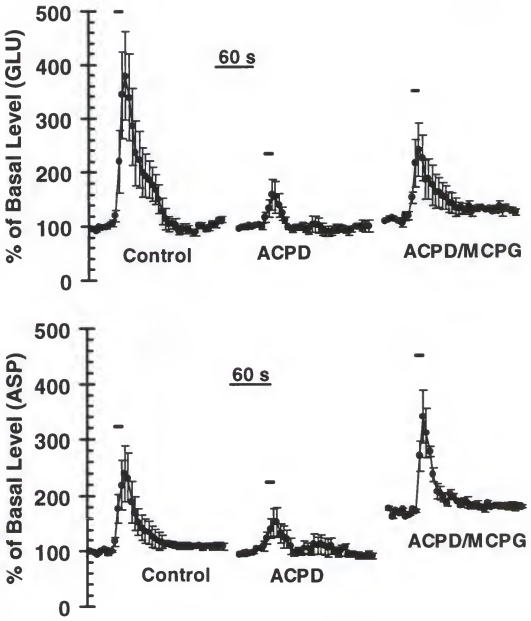

Figure 7-7. Effects of 200 μM trans-ACPD in the presence and absence of 200 μM MCPG on basal and electrically stimulated glutamate (top) and aspartate (bottom) levels in the striatum of anesthetized rats. Bar indicates 10-s of electrical stimulation of the PFC. Data are presented as means ± SEM (n = 4) and are expressed as the percentages of the mean baseline of dialysate concentrations of glutamate and aspartate in the same animals.

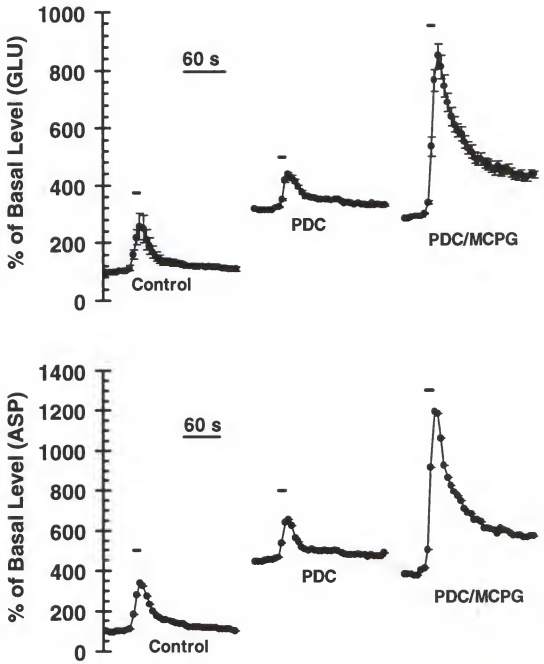

Figure 7-8. Effects of 200 μM PDC in the presence of 200 μM MCPG on basal and electrically stimulated glutamate (top) and aspartate (bottom) levels in the striatum of anesthetized rats. Bar indicates 10-s of electrical stimulation of the PFC. Data are presented as means ± SEM (n = 4) and are expressed as the percentages of the mean baseline of dialysate concentrations of glutamate and aspartate.

CHAPTER 8
CONCLUSIONS AND FUTURE DIRECTIONS

Summary

Microdialysis is a universal technique for monitoring relative changes in the chemical composition of living tissue without altering the fluid balance. Automated, continuous measurements are possible by coupling microdialysis on-line with a high mass sensitive technique such as capillary electrophoresis. As a result, we have developed and demonstrated separation-based monitoring with sensor-like temporal characteristics. With such temporal characteristics, it is now possible to use microdialysis sampling in neurochemical applications not previously possible.

Table 8-1 is a partial list of contemporary monitoring systems, both separation and biosensor-based, for the fast analysis of the neurotransmitter glutamate. The enzyme-based amperometric glutamate sensor was found to possess the best temporal characteristics (2 s); however, chemical interferences typically limited its reliability, since H_2O_2 usually reacted with many reducing agents (Hu et al., 1994). So from a practical point of view, the researcher is never quite sure what is measured, especially in an *in vivo* environment where many compounds are present. For separation-based systems, chemical interferences are often separated away from analytes of interest, thus improving reliability of the measurement. Capillary zone electrophoresis seemed to be the popular separation choice with either LIF or electrochemical detection. In each case, separations allowed for

multi-analyte capabilities; however, temporal resolution was poor except in those cases where on-line systems were developed or when special sample collection methods (for the off-line case) were used. Unfortunately for off-line methods, improving temporal resolution involved the handling of nanoliter volumes, a task not easily performed. So once again from a practical point of view, performing microdialysis analyses with superior temporal characteristics requires the use of advanced on-line methods, where small sample volumes are easily handled.

Besides producing more reliable chemical information, separation-based on-line analyses provide substantially more data about the extracellular region of the brain, and as a result, gives researchers a more comprehensive profile of the region compared with information obtained from tissue cultures, homogenates, and implanted biosensors. Unlike biosensors, microdialysis can simultaneously sample multiple analytes. All molecules below the molecular weight cutoff diffuse across the membrane and the analytical method determines what is seen in the dialysate. In contrast, biosensors typically target one analyte and are susceptible to electrode contamination and fouling, not to mention non-specific analyte interferences. Furthermore, the linearity of the analytical method is usually better than linearity of an implanted sensor.

In comparison to *in vitro* tissue cultures and homogenates, microdialysis provides a sample which is more representative of the normal physiological functions of the brain, with all metabolic and neural pathways intact. Furthermore, there is no loss of analyte due to sample preparations and the samples are protein-free, ready for analysis without further

cleanup. No further metabolism of analyte by enzymes in the sample occurs, especially important when dealing with peptides and proteins.

Future Directions

Separation-based chemical monitoring involves a relatively new technology with many hopeful prospects. However, its future utility involves applications requiring fast analyses and multi-analyte capabilities, not to mention microscale sampling. Below are listed possible ways in which chemical monitoring with this system can be improved, including the areas of sampling, separation, and detection.

Sampling

The on-line microdialysis/capillary electrophoresis system is now at a point where the membrane of the microdialysis probe is limiting further improvements in temporal resolution. As a consequence, it is imperative that future development be taken to eliminate the disadvantages associated with the membrane. One manner in which this can be accomplished is to completely remove the membrane from the dialysis probe, hence developing a membrane-less probe. Also, by miniaturizing the capillaries and reducing flow rates, a less obtrusive *in vivo* sampling technique can be created yielding minimal tissue damage and concentration gradients, yet improving spatial and temporal resolution. Finally, a membrane-less sampling probe would eliminate many of the problems associated with non-specific binding to the semipermeable membrane, which is especially characteristic of peptides, thus providing for an efficient means for sampling, that is, 100 % relative recovery of these compounds.

We have recently initiated feasibility studies on the prospects of such a membrane-less probe system, and the design is illustrated in Figure 8-1. A bare fused silica capillary, which is connected to an on-line membrane reactor, is implanted into the rat brain. A second piece of capillary, also attached to the reactor and opposite the sampling capillary, is connected to a vacuum chamber. This second capillary allows for separations to be performed. When the vacuum is applied (20 psi), the extracellular fluid of the rat brain is drawn into the sampling capillary at flow rates as low as 1-3 nL/min. Once the sample is drawn into the sampling capillary, it is derivatized on-line within the semipermeable membrane reactor and subsequently separated by CE with fluorescence detection. The electrophoretic separation is facilitated by applying an electric field across the separation capillary. As a result, both vacuum and electroosmotic pumping contribute to the volumetric flow.

The reactor, which is simple to construct and allows for adequate mixing of the derivatizing reagent with the analyte of interest, is an integral part of the membrane-less probe system, and is illustrated in Figure 8-2. It was based on a semipermeable membrane reactor that was previously used for post-column derivatization with CE and on-line pH adjustments (Kostel and Lunte, 1997; Zhou and Lunte, 1995). Briefly, a 50 cm piece of fused silica capillary (10 μm i.d. and 150 μm o.d.) was scored at the 15 cm mark and sleeved into a 1 cm section of a hollow cellulose fiber (200 μm i.d. and 360 μm o.d.). The capillary was then carefully pulled apart inside the fiber to a nominal distance of 20-75 μm and placed onto a glass microscope slide. Cyanoacrylate was used to secure the capillaries within the fiber and also onto the microscope slide. The gap distance was confirmed

under a microscope. A reagent reservoir was then constructed by cutting the top 0.5 cm section of a 3 mL Eppendorf vial (with cap) and then gluing the bottom of it onto the microscope slide. As a result, the membrane was centered directly on the bottom of the reservoir. The derivatization reagent, OPA/β-ME in 30 mM borate buffer (pH 10.5), was then placed into the reservoir and allowed to diffuse through the semipermeable membrane and into the reactor. Upon diffusion into the reactor, the OPA/β-ME reacted with primary amines, flowing through the sampling capillary, to form fluorescent isoindole products. Finally, a 0.5 cm section of the polyimide coating on the capillary was removed at the 45 cm mark for an optical window for detection. The same fluorescence detector that was used in Chapters 4, 6 and 7 was also used in this preliminary work.

The initial step in characterizing this new system was to determine the temporal resolution, and in particular, evaluate the effect of reactor volume on temporal resolution. Experiments were performed in which step changes in glutamate concentration were made at the sampling capillary. The resulting changes in concentration were monitored by frontal zone analysis with fluorescence detection. Separations were not performed. Figure 8-3 illustrates the traces recorded when reactor volumes of 0.3 and 1 nL were used. As seen in the figure, the step changes were broadened during the sampling process to an extent that directly depended on the reactor volume, with the smaller volume giving the sharper response of 18 s. Although the smaller volume provided for higher temporal resolution, it was necessary to double the OPA/β-ME concentration, since less derivatizing agent was able to enter the reactor. When the larger reactor volume was used, more membrane surface area was available for reagent diffusion, but the resulting

void volume was too large and caused excess band broadening. The temporal resolution was 60 s. Further work will be required to determine the optimal conditions for providing high temporal resolution while simultaneously affording low detection limits.

Other preliminary work included the evaluation of the membrane-less probe as an *in vivo* sampling technique. For this experiment, the sampling capillary was implanted into the rat striatum and the extracellular fluid sampled. As shown in Figure 8-4, a 30 s electrical stimulation of the prefrontal cortex caused an immediate rise in the concentration of primary amines in the striatum, resulting in a temporal resolution of 100 s. This data is promising for many reasons, but most importantly, it showed that it was possible to sample extracellular fluid from such a tortuous environment like the rat brain without capillary clogging. If clogging ever becomes an issue, the capillary tip could be casted with an ultrafiltration or size exclusion membrane, thus allowing for unobstructed transfer of filtered extracellular fluid. Future work will also include the implementation of an optically-gated capillary electrophoresis system for the separation of our isoindole products (Monnig and Jorgenson, 1991; Moore and Jorgenson, 1993; Tao et al., 1997).

Although this preliminary data suggests that it may be possible to sample from the brain, much work is still necessary to make this system a reliable and efficient sampling technique. If the membrane-less probe fails to meet our temporal and spatial expectations; however, then miniaturization of conventional microdialysis probes would be necessary to improve spatial and temporal resolution. With small dialysis membranes; however, less analyte would diffuse into the probe, resulting in lower recoveries and analyte signal. Consequently, improvements in detection limits would be required. Nonetheless,

miniaturization is the key to improving spatial and temporal resolution, whether using a microdialysis probe or a membrane-less probe.

Faster Separations

Although the separation step in the on-line microdialysis/capillary electrophoresis assay in no longer a limiting factor for temporal resolution, it is still prudent to continue with technical advancements. Technical advancements, such as faster separations with varying modes of separation, can increase the number of possible analytes resolved and eventually detected. Possible strategies for faster analyses include increasing detector sensitivity while simultaneously decreasing the separation capillary inner diameter, capillary length, and injection time. If all of the analytical complications associated with these adjustments are overcome, it is not unreasonable to expect sub-second separation times. Besides using fast capillary electrophoresis as mode of separation, fast capillary electrochromatography can also be utilized, where analytes are separated by their hydrophobicities in addition to their electrophoretic mobilities.

Improved Detection

Although microdialysis has become the method of choice for monitoring neurotransmitters in the extracellular space of the rat brain, it has received less attention with respect to monitoring neuropeptides. This can be easily explained by the fact that the currently available analytical techniques do not possess the sufficient detection limits to detect the femtomole quantities of endogenous peptides recovered by the microdialysis probe. Obviously, detection limits of this system must be improved in order to monitor these types of compounds. A possible solution may involve the use of other fluorogenic

derivatization agents such as 3-(p-carboxybenzoyl) quinoline-2-carboxaldehyde (CBQ) or 3-(2-furoyl)quinoline-2-carboxaldhyde (FQ), where they have shown promise in biological assays (Arriaga et al., 1995; Beale et al., 1990). Different modes of detection, such as nanoelectrospray or picoelectrospray mass spectrometry, are possible alternatives which may improve detector sensitivity and/or specificity.

Applications

Microdialysis has been used most frequently for quantifying the concentration of a variety of brain neurotransmitters and their metabolites in extracellular fluid, including amino acids, acetylcholine, norepinephrine, serotonin, and dopamine, but not all at the same time due analytical constraints. It now may be possible to simultaneously monitor dopamine with glutamate and aspartate using this system simply by implanting a microelectrode bilateral with a microdialysis probe. This would be of interest and significance, especially since the neurotransmitter glutamate has been implicated in the mechanism and/or modulation underlying dopamine release evoked by the stimulation of the prefrontal cortex. Many questions associated with the dopamine-glutamate relationship not previously answerable would then be realized.

By using fast capillary electrochromatography with LIF or ED, it may be possible to monitor as many as five amino acid neurotransmitters including glutamate, aspartate, taurine, glycine, and GABA with sensor-like temporal characteristics. By increasing CZE separation speed and detector sensitivity of the assay in Chapter 5, it may be also be possible to monitor glutathione and cysteine in the brain with impressive temporal characteristics, possibly allowing for biological studies in the confirmation of cysteine as a

neurotransmitter. Also, similar studies to those found in Chapter 7 may be performed for glutathione and cysteine, if angonists or antagonists can be found for these compounds. Future applications may also include monitoring neuropeptides such as vasopressin, oxytocin, enkephalins, substance P, cholecystokinin, luteinizing hormone, and neuropeptide Y, to name a few. Temporally inadequate monitoring systems currently exist for the analysis of these peptides *in vivo*, such as immunoassays which are tedious to perform and are subject to numerous specificity issues, so further work in the separation-based biosensor field is very promising and exciting. Numerous applications are plentiful for separation-based biosensors; however, analytical advancements must continue, whether through sampling, separation, or detection, in order for many of these desires to be realized.

Table 8-1. Comparison of Glutamate Sensors.

Investigators	MD	Sep'n	On-Line	Multi-Analyte	Detect'n	LOD (μM)	Temporal Resolution	*In Vivo*
Lada et al. ('97)	Y	CZE	Y	Y	LIF	0.2	12-14 s	Y
Lada et al. ('96)	Y	CZE	Y	Y	LIF	0.1	90 s	Y
Zhou et al. ('95)	Y	CZE	Y	Y	LIF	0.1	120 s	Y
Robert el. ('96)	Y	CZE	N	Y	LIF	0.2	2 min	Y
Hernandez et al. ('93)	Y	CZE	N	Y	LIF	0.1	10 min	Y
O'Shea et al. ('92)	Y	CZE	N	Y	ED*	0.1	3 min	Y
Bert et al. ('96)	Y	CZE	N	Y	LIF	0.1	30 s	N
Hu et al. ('94)	N	No	N/A	N	ED**	0.2	< 2 s	Y
Zilkha et al. ('94)	N	No	N/A	N	ED**	2.0	< 1min	Y
Obrenovitch ('93)	N	No	N/A	N	ED**	0.5	< 1 min	Y

MD = microdialysis, ED = electrochemical detection, LIF = laser induced fluorescence detection.

* Carbon fiber microelectrode

** L-glutamate oxidase based amperometric biosensors

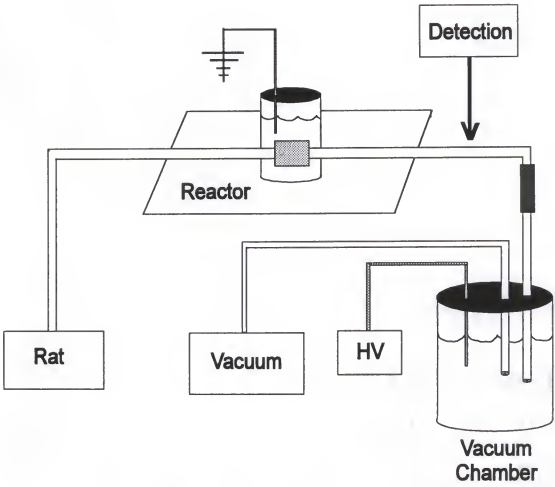

Figure 8-1. Block diagram of the membrane-less probe/capillary electrophoresis system. Description of operation is given in the text.

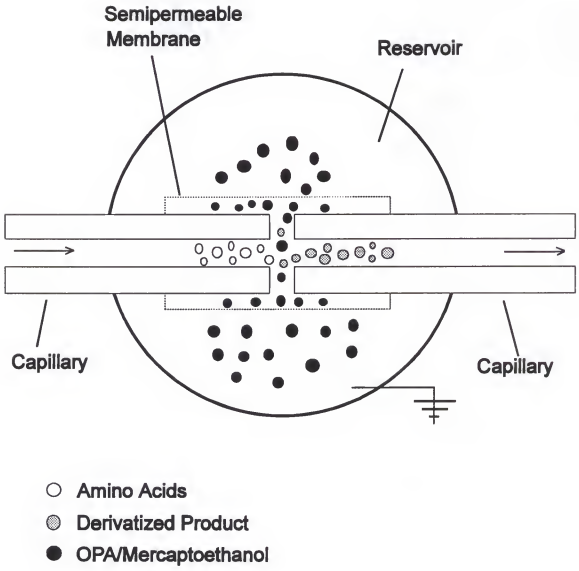

Figure 8-2. Schematic of the on-line semipermeable membrane reactor. Description of operation is given in the text.

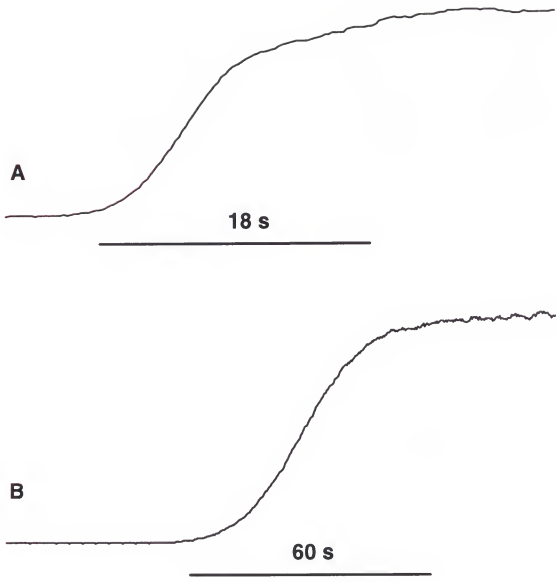

Figure 8-3. Comparison of traces recorded by fluorescence detection during *in vitro* step changes in glutamate concentration at the sampling capillary (0 to 1 mM). The volume of reactor A was 0.3 nL while the volume of reactor B was 1 nL. Bars indicate time scale.

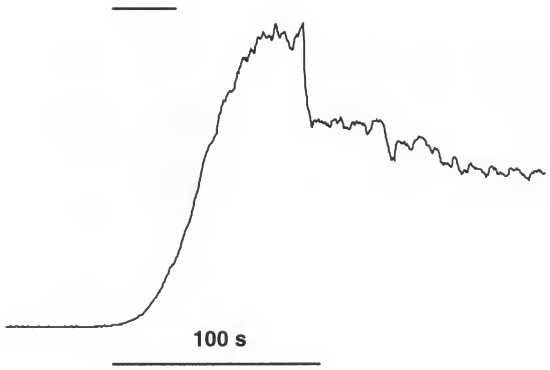

Figure 8-4. Fluorescence trace of striatal primary amines *in vivo* elicited by an electrical stimulation of the prefrontal cortex in a single anesthetized rat. Electrical stimulation consisted of 0.5 ms, square wave pulses (320 μA) applied at 20 Hz for 30 seconds. The top bar indicates stimulation time while the bottom bar indicates experiment time scale.

APPENDIX A
TROUBLESHOOTING THE ON-LINE MD/CE SYSTEM

PROBLEM	CAUSE	SOLUTION TO PROBLEM
No current	plugged sep'n capillary	rinse or replace capillary
	broken sep'n capillary	replace capillary
	microbubbles	rinse capillary, degas buffers
	safety interlock off	close interlock box
Fluctuating current	arcing	replace teflon connector
	microbubbles	rinse capillary
	contaminants in buffer	filter buffer
Current too high	ionic strength of buffer too high	reduce voltage dilute buffer smaller i.d. sep'n capillary try new buffer
	gating breakthrough	increase interface gap increase gating flow
Irreproducible migration times	gating breakthrough of salt	increase interface gap increase gating flow
	dirty capillary	rinse or replace capillary
No signal or poor signal	shutter closed	open shutter
	microdialysis membrane leak	replace the probe
	leak in transfer or reaction capillaries	replace teflon connectors
	plugged transfer or reaction capillaries	replace capillaries
	gating flow too high	reduce gating flow
	interface gap b/w sep'n and reaction capillary too large	reduce the interface gap
	laser not aligned	align laser with optical mirrors
	capillary out of focus	focus laser spot on the i.d. of sep'n capillary
	old reagents	make a fresh batch

PROBLEM	CAUSE	SOLUTION TO PROBLEM
	anodic sample	reverse polarity change pH
Fluctuating signal	microdialysis membrane leak	replace probe
	interface gap too small or large	increase gating flow decrease interface gap
	leak in transfer capillaries	replace teflon connectors
	inconsistent flow rates by microsyringe pump	call manufacturer
Baseline drifts	detector instability	allow detector to warm up
	gating breakthrough	increase gating flow or interface gap
	capillary vibration	tighten capillary onto holder reduce voltage
	oil heating (for fluar lens)	allow some time for temperature equilibration, then refocus objective onto capillary
	contaminated capillary	rinse or replace capillary
	loose microscope stage	tighten or replace
	dirty detector cell (UV)	clean with methanol
Poor efficiency	overinjection	increase interface gap decrease injection voltage decrease injection time
	Joule heating	increase gating flow decrease voltage dilute buffer use smaller i.d. capillaries
Too many peaks	microbubbles	rinse separation capillary
	sample or derivatization agent degradation	make fresh batch
	solid particle contamination	filter all buffers
Too few peaks	not injecting enough	increase injection voltage decrease interface gap increase injection time
	analytes have similar charge/mass	alter buffer pH reduce EOF try new buffer try alternative sep'n mode

separation time too short	decrease EOF increase sep'n capillary length

APPENDIX B
LASER BEAM ALIGNMENT

It is crucial to be sure that the PMT shutter is closed during laser beam alignment with the fluorescence microscope since the PMT can be easily damaged by excess light. The microscope shutter, located directly above the lens holder, should also be closed. The alignment of the laser with the fluorescent microscope is accomplished by directing the laser beam path with optical mirrors into the back of the microscope chamber with the lens holder removed. The beam can be viewed on the inner wall of the microscope; it is more easily seen if a white business card is placed along the back wall. Both the optical mirrors and microscope position can be manipulated to position the beam onto the card. When the laser beam is centered on the front inner wall, the white business card is removed and the optics holder is placed back to its original position. The laser beam will now pass through the interference filter and dichroic mirror, and directly focus down onto the microscope stage. Place the yellow fluorescent card onto the stage for easy viewing of the laser spot. Next, begin to move the stage towards the objective such that a small, bright blue spot appears on the fluorescence card. This spot should also be visible when viewing through the optical eyepieces. The distance between the fluorescence card and the objective will be approximately 1 mm.

At this point, both a blue laser beam spot and a black bullseye should be visible if viewed through the eyepiece. The next step is to place the bullseye directly over the laser

beam spot. This is the most difficult part of alignment since it can be frustrating to simultaneously position the laser spot onto the bullseye *and* have the spot in a circular geometry. Either one by itself is very easy to accomplish, but both are difficult at the same time. Fortunately, with a few helpful hints alignment can become a trivial task. Alignment of the bullseye with the laser spot is also accomplished with minor manipulation of the optical mirrors and slight movement of the microscope. It was found helpful to direct the laser spot past the fixed bullseye with one mirror and then bring the laser spot back onto the bullseye with the other mirror. For example, if the laser spot is left of the bullseye, use one of the mirrors to direct the spot just right of the bullseye. This will result in a half-moon laser spot. Then use the other mirror to move the laser spot back in the left direction until the laser spot is directly over the bullseye. As a result, the laser will be circular in shape, not a half-moon, and be in perfect alignment. This hint is not only applicable to horizontal directions, but also vertical directions. Repeat this procedure until perfect alignment is achieved.

When this initial alignment is complete, the yellow fluorescence card is replaced with the separation capillary in its holder. The capillary is brought into view using the XYZ positioner of the microscope and focused. The bullseye should be placed directly within the inner diameter of the capillary. This will not only perfectly align the laser within the capillary, but will also reduce light scattering. In addition, the microscope spatial filter, which is located directly in front of the PMT opening, should also have its spatial dimensions set within the inner diameter of the capillary. Once this alignment is complete, the system is ready for fluorescence measurements.

APPENDIX C
ANESTHETIC AND SURGICAL PROTOCOL

All experimental uses of laboratory rats in this work were reviewed and approved by the University of Florida Institutional Animal Care and Use Committee (IACUC) and conform with policies and procedures set forth by U.S. Public Health Service Policy on Humane Care and Use of Laboratory Animals.

Male Sprague-Dawley rats weighing 250-350 grams were anesthetized with subcutaneous injections of 100 mg/ml of chloral hydrate that was dissolved in artificial cerebral spinal fluid (aCSF). The initial injection was 4.0 ml/kg. The second injection of 2.0 ml/kg of chloral hydrate was given thirty minutes after the initial injection. Booster injections of 1.0 ml/kg were given every thirty minutes until the rat no longer exhibited limb reflex. If it was difficult to make the initial injection due to rat uncooperation, the rat was placed into a dessicator containing 1 ml of metofane. After the rat has fallen asleep (approximately 30-90 seconds), the rat was removed from the dessicator and the initial injection with chloral hydrate was made. The rat was then placed into its storage container.

After the rat was anesthetized, the fur from the top of the head was shaven. The rat was then placed on a thermostatically controlled heating pad on the stereotaxic frame. After incising the scalp, the skin and debris was scraped from the skull so that the bone suture lines were clearly visible and the skull could dry. Washing the skull with water can help clean the debris and clearly expose bregma. Four retractors (paper clips and weights)

were placed in such a way as to keep the skin flaps from interfering in the area of interest. Bleeding was controlled by applying light pressure with cotton swabs.

When the skull was dry, bregma should be evident at the intersection of the coronal and sagittal sutures (tee-like structure). Bregma was used as an indicator of the stereotaxic "zero" reference point. Using the micromanipulators and the microdialysis probe, the zero reference point was determined by moving the probe to bregma. These stereotaxic zero coordinates were marked into the lab notebook. The relative coordinates of the intended microdialysis target structure were then determined. The coordinates for the striatum were +0.02 AP, -0.30 ML, and -0.65 cm DV from bregma and the coordinates for the prefrontal cortex were +0.35 AP, +0.15 ML, and -0.02 cm DV from bregma. If you are interested in other brain structures, you will need to consult a stereotaxic atlas and/or relative journal publications. The probe was then positioned above the target and lowered until it just touched the bone. Using a felt tip marker, this position was marked on the skull. The probe was moved away from the skull to prevent accidental membrane breakage. Also, the dialysis probe was placed into a vial containing aCSF in order to prevent the membrane from drying out and becoming brittle.

Using a high speed drill (Dremel tool), a hole was drilled at the microdialysis target position. Using a light touch, be careful not to drill past the cranium bone because major tissue damage and bleeding will result. Replacing the drill bit (1/16") after five rats allowed for easier drilling. If excess bleeding began, firm and direct pressure was applied onto the freshly drilled hole with a cotton swab. Hold for several minutes until the bleeding stops. The next step involved the careful removal of the dural membrane using

forceps, if necessary. Then, by using the micromanipulators located on the stereotaxis, the microdialysis probe was slowly lowered into the hole to the required depth. While lowering the probe into the brain, be certain that aCSF fluid is perfusing through the probe at 1.2 µl/min. After surgery, the rat was kept unconscious with subcutaneous injections of 1.0 ml/kg of chloral hydrate as needed. Urination is a dependable sign that anesthesia is necessary. After the experiments were complete, the animal was properly euthanized by interperionately injection of 2 ml of the anesthesia into the rat. The animal was then properly disposed at Shands.

LIST OF REFERENCES

Abarca, J.; Gysling, K.; Roth, R.; Bustos, G. *Neurochem. Res.* **1995,** 2: 159-169.

Anderson, J.J.; DiMicco, J.A. *Life Sci.* **1992,** 51: 623-630.

Arriaga, E.A.; Zhang, Y.; Dovichi, N.J. *Anal. Chim. Acta* **1995**, 299: 319-326.

Baskys, A.; Malenka, R.C. *J. Physiol.* **1991**, 444: 687-701.

Basse-Tomusk, A.; Rebec, C. *Pharmacol. Biochem. Behav.* **1990**, 35: 55-60.

Basse-Tomusk, A.; Rebec, G.V. *Brain Res.* **1991**, 538: 29-35.

Beale, S.C.; Hsieh, Y.; Weisler, D.; Novotny, M. *J. Chromatogr.* **1990**, 499: 579-587.

Benveniste, H.; Hansen, A.J.; Ottosen, N.S. *J. Neurochem.* **1989**, 52: 1741-1750.

Berendse, H.W.; Galis-De-Graaf, Y.; Groenewegen, H.J. *J. Comp. Neurol.* **1992**, 316: 314-347.

Bert, L.; Robert, F.; Denoroy, L.; Stoppini, L; Renaud, B. *J. Chromatogr. A* **1996**, 755: 99-111.

Boutelle, M.G.; Zetterstrom, T.; Pei, Q.; Svensson, L.; Fillenz, M. *J. Neurosci. Methods.* **1990**, 34: 151-158.

Brazell, M.P.; Mitchell, S.N.; Joseph, M.H.; Gray, J.A. *Neuropharmacology.* **1990**, 29: 1177-1185.

Bungay, P.M.; Morrison, P.F.; Dedrick, R.L. *Life Sci.* **1990**, 46: 105-119.

Butcher, S.P.; Hamberger, A. *J. Neurochem.* **1987**, 48: 713-721.

Butcher, S.P.; Sandberg, M.; Hagberg, H.; Hamberger, A. *J. Neurochem.* **1987**, 48: 722-728.

Caprioli, R.M.; Lin, S. *Proc. Natl. Acad. Sci.* **1990**, 87: 240-243.

Chen, A.; Lunte, C.E. *J. Chromatogr. A.* **1995**, 69: 29-35.

Chen, R.F.; Scott, C.; Trepman, E. *Biochim. Biophys. Acta.* **1979**, 576: 440-455.

Church, W.H.; Justice, J.B. *Anal. Chem.* **1987**, 59: 712-716.

Clemens, J.A.; Phebus, L.A. *Life Sci.* **1984**, 35: 671-677.

Crespi, F.; Mobius, C.; Keane, P. *Pharmacol. Res.* **1992**, 26: 55-66.

Dagani, F.; D'Angelo, E. *Funct. Neurol.* **1992**, 7(4): 315-336.

D'Angelo, E.; Rossi, P. *Funct. Neurol.* **1992**, 7(2): 145-161.

Delgado, J.M.R.; DeFeudis, F.V.; Roth, R.H.; Ryugo, D.K.; Mitruka, B.M. *Arch. Int. Pharmacodyn.* **1972**, 198: 9-21.

Divac, I; Fonnum, F.; Storm-Mathisen, A.C. *Nature* **1977**, 24: 377-378.

During, M.J. *Microdialysis in the Neurosciences*; Elsevier Science Pubishers BV: New York, **1991.**

East, S.J.; Hill, M.P.; Brotchie, J.M. *Eur. J. Pharmacol.* **1995**, 277: 117-121.

Ewing, A.G.; Wightman, R.M.; Dayton, M.A., *Brain Res.* **1982**, 249: 361-370.

Fahey, R.C.; Newton, G.L.; Dorian, R.; Kosower, E.M. *Anal. Biochem.* **1981**, 111: 357-365.

Fonnum, F. *J. Neurochem.* **1984**, 42(1): 1-11.

Forsythe, I.D.; Clements, J.D. *J. Physiol.* **1990**, 429: 1-16.

Gaddam, J.H., *J. Physiol.* **1961,** 155: 1-2.

Gamache, P.; Ryan, E.; Svendsen, C.; Murayama, K.; Acworth, I.N. *J. Chromatogr. Biomed. Appl.* **1993**, 614: 213-220.

Glaum, S.R.; Miller, R.J. *J. Neurophysiol.* **1993**, 70:2669-2672.

Godukhin, O.V.; Zharikova, A.D.; Novoselov, V.I. *Neuroscience* **1980**, 5: 2151-2154.

Gonon, F.; Buda, M.; Cespuglio, R.; Jouvet, M.; Pujol, J.F., *Brain Research.* **1981**, 223: 69-80.

Greenamyre, J.T.; Young, A.B. *Neurobiol. of Aging*. **1989**, 10: 593-602.

Grunewald, R.A., *Brain Res. Rev*. **1993**, 18: 123-133.

Grunewald, R.A.; O'Neill, R.D.; Fillenz M.; Albery, W.J. *Neurochem. Int*. **1983**, 5: 773-778.

Hashimoto, A.; Oka, T.; Nishikawa, T. *Neuroscience* **1995**, 66: 635-643.

Hernandez, L.; Escalona, J.; Joshi, N.; Guzman, N. *J Chromatogr*. **1991**, 559:183-191.

Hernandez, L.; Escalona, J.; Verdeguer, P.; Guzman, N.A. *J. Liq. Chromatogr*. **1993a**, 16: 2149-2160.

Hernandez, L.; Marquina, R.; Escalona, J.; Guzman, N. *J. Chromatogr*. **1990**, 502: 247-255.

Hernandez, L.; Tucci, S.; Guzman, N.; Paez, X. *J. Chromatogr. A*. **1993b**, 652: 393-398.

Herrera-Marschitz, M.; You, Z.; Goiny, M.; Meana, J.J.; Silveira, R.; Godukhin, O.V.; Chen, Y.; Espinoza, S.; Petterson, E.; Loidl, C.F.; Lubec, G.; Andersson, K.; Nylander, I.; Terenius, L.; Ungersted, U. *J. Neurochem*. **1996**, 66:1726-1735.

Hille, B. *Neuron* **1992**, 9: 182-195.

Hillered, L.; Hallstrom, A.; Segersvard, S.; Persson, L.; Ungerstedt, U. *J. Cereb. Blood Flow and Metab*. **1989**, 9: 607-616.

Hillered, L.; Persson, L.; Bolander, H.G.; Hallstrom, A.; Ungerstedt, U. *Neurosci. Lett*. **1988**, 95: 286-290.

Hogan, B.L.; Lunte, S.M.; Stobaugh, J.F.; Lunte, C.E. *Anal. Chem*. **1994**, 66: 596-602.

Hu, Y.; Mitchell, K.M.; Albahadily, F.N.; Michaelis, E.K.; Wilson, G.S. *Brain Research* **1994**, 659: 117-125.

Jacobson, I.; Sandberg, M.; Hamberger, A. *J. Neurosci. Meth*. **1985**, 15: 263-268.

Jacobson, S.C.; Hergenroder, R.; Koutny, L.B.; Ramsey, J.M. *Anal. Chem*. **1994**, 66: 1114-1118.

Jahr, C.E.; Lester, R.A. *Curr. Opin. Neurobiol*. **1992**, 2: 270-274.

Jessell, A.M.; Kandel, E.R. *Neuron* **1993**, 10: 1-30.

Kalivas, P.W.; Duffy, P. *J. Neuroscience* **1995**, 15: 5379-5388.

Keller, H.J., Do, K.Q., Zollinger, M., Winterhalter, K.H., and Cuenod, M. *J. Neurochem.* **1989**, 52:1801-1806.

Kosower, E.M. and Kosower, N.S., *Methods in Enzymol.* **1995**, 251: 133-166.

Kostel, K.L.; Lunte, S.M. *J. Chromatogr. B.* **1997**, 695: 27-38.

Kuhr, W.G.; Korf, J. *J. Cerebr. Blood Flow Metab.* **1988**, 8:130-137.

Lada, M.W.; Kennedy, R.T. *J. Neurosci. Methods.* **1995**, 63: 147-152.

Lada, M.W.; Kennedy, R.T. *Anal. Chem.* **1996**, 68: 2790-2797.

Lada, M.W.; Schaller, G.;Carriger, M.H.; Vickroy, T.W.; Kennedy, R.T. *Anal. Chim. Acta* **1995**, 307: 217-225.

Landolt, H.; Lutz, T.W.; Langemann, H.; Stauble, D.; Mendelowitsch, A.; Gratzl, O.; Honneger, C.G., *J. Cerebr. Blood Flow and Metab.* **1992**, 12: 96-102.

Laroche, S. *Prog. Brain Res.* **1990**, 83:251-256.

Lemmo, A.V.; Jorgenson, J.W. *Anal. Chem.* **1993**, 65: 1576-1581.

Liu, J.; Moghaddam, B. *J. Pharmacol. Exp. Ther.* **1995**, 274:1209-1215.

Lonnroth, P.; Jannson, P.A.; Smith, U. *Am. J. Physiol.* **1987**, 256: E250-E255.

Lovinger, D.M.; Meritt, A.; Reyes, D. *Neuroscience* **1994**, 62:31-40.

Lovinger, D.M.; Tyler, E.; Fidler, S.; Meritt, A. *Neuroscience* **1993**, 69: 1236-1244.

Luckacs, K.D.; Jorgenson, J.W. *Science* **1983**, 222: 266-272.

Lund Karlson, R.; Grofova, I.; Malthe-Sorenssen, D.; Fonnum, F. *Brain Research* **1981**, 208: 167-180.

Lunte, C.E.; Scott, D.O.; Kissenger, P.T. *Anal. Chem.* **1991**, 63: 773A-780A.

Lynch, M.A.; Errington, M.L.; Clements, M.P.; Bliss, T.V.; Redini-Del-Negro, C.; Laroche, S. Prog. *Brain Research.* **1990**, 83: 251-256.

Lyrer, P.; Landolt, H.; Kabiersch, A.; Langemann, H.; Kaeser, H. *Brain Research.*, **1991**, 567: 317-320.

Maidment, N.T.; Brumbaugh, D.R.; Rudolph, V.D.; Erdelyi, E.; Evans, C.J. *Neuroscience.* **1989**, 33: 549-557.

Maki, R.; Robinson, M.B.; Dichter, M.A. *J. Neuroscience* **1994**, 14: 6754-6762.

Manzoni, O.J.; Castillo, P.E.; Nicoll, R.A. *Neuropharmacol.* **1995**, 34: 965-971.

Maragos, N.F.; Greenmyre, J.T.; Penney, J.B.; Young, A.B. *TINS* **1987**, 10: 65-68.

Massieu, L.; Morales-Villagran, A.; Tapia, R. *J. Neurochem.* **1995**, 64: 2262-2272.

McGreer, P.L.; McGreer, E.G.; Scherer, U.; Singh, K. *Brain Research* **1977**, 128: 369-373.

Menacherry, S.D.; Hubert, W.; Justice, J.B. *Anal. Chem.* **1992**, 64: 577-583.

Menacherry, S.D.; Justice, J.B. *Anal. Chem.* **1990**, 62: 597-601.

Moghaddam, B. *J. Neurochem.* **1993**, 60: 1650-1657.

Moghaddam, G.; Boliano, M.L. *Synapse* **1994**, 18: 337-342.

Monnig, C.A.; Jorgenson, J.W. *Anal. Chem.* **1991**, 63: 802-807.

Moore, A.W. Jr.; Jorgenson, J.W. Anal. Chem. **1993**, 65: 3550-3560.

Morari, M.; O'Connor, W.T.; Ungerstedt, U.; Fuxe, K. *J. Neurochem.* **1993**, 60:1884-1893.

Morrison, P.F.; Bungay, P.M.; Hsiao, J.K.; Ball, B.A.; Mefford, I.N.; Dykstra, R.L.; Dedrick R.L. in T.E. Robinson and J.B. Justice (eds.) *Microdialysis in the Neurosciences*; Elsevier: New York, **1991**.

Mueller, K.; Kunko, P.M. *Pharmacol. Biochem. Behav.*, **1990**, 35: 871-876.

Myers, R.D. *Methods in Psycobiology*, Academic Press: New York, **1972**.

Nakanishi, S. *Neuron* **1994**, 13:1031-1037.

Nicholls, D.; Atwell, D. *Trends Pharmacol. Sci.* **1990**, 11:462-468.

Nelson, R.J.; Paulus, A.; Cohen, A.S.; Guttman, A.; Karger, B.L. *J. Chromatogr.* **1989**, 480:111-117.

Newton A.P.; Justice, J.B., *Anal. Chem.* **1994**, 66: 1468-1472.

Obrenovitch; T.P.; Urenjak, J.; Zilkha, E. *J. Neurochem.* **1996**, 66:2246-2254.

Obrenovitch; T.P.; Urenjak, J.; Richards, D.A.; Ueda, Y.; Curzon, G.; Symon. *J. Neurochem.* **1993**, 61: 178-186.

Olney, J.W.; Zorumski, C.; Price, H.T.; Labruyere, J. *Science.* **1990** , 248: 596-599.

O'Neill, R.D.; Grunewald, R.A.; Fillenz, M.; Albery, W.J. *Neuroscience.* **1982**, 7: 1945-1954.

Orlowski, M.; Karkowsky, A. *Int. Rev. Neurobiol.* **1976**, 19: 75-121.

Orrego, F.; Villanueva, S. *Neuroscience* **1993**, 56: 539-555.

O'Shea, T.J.; Weber, P.L.; Bammel, B.P.; Lunte, C.E.; Lunte, S.M.; Smyth, M.R. *J. Chromatogr.* **1992**, 608: 189-195.

Owar, O.; Sandberg, M.; Jacobson, I.; Sundahl, M.; Folestad, S. *Anal. Chem.* **1994**, 66: 4471-4482.

Palmer, A.M.; Hutson, P.H.; Lowe, S.L.; Bowen, D.M. *Exp. Brain Res.* **1989**, 75: 659-663.

Parsons, L.H.; Justice, J.B. *J. Neurochem.* **1992**, 58: 212-218.

Pellegrino, L., Pellegrino, A. and Cushman, A. *A Stereotaxic Atlas of the Rat Brain*; Century Crofts: New York, **1967**.

Perschak, H.; Cuenod, M. *Neuroscience* **1990**, 35: 283-287.

Rawls, S.M.; McGinty, J.F. *J. Neurochem.* **1997**, 68: 1553-1563.

Robert, F; Bert, L.; Lambas-Senas, L.; Denoroy, L.; Renaud, B. 1996, *J. Neurosci. Methods* **1996**, 70: 153-162.

Robinson, M.B.; Sinor, J.D.; Dowd, L.A.; Kerwin, J.F. *J Neurochem.* **1993**, 60: 167-179.

Samuel, D.; Pisano, P.; Forni, C.; Nieoullon, A.; Kerkerian-Le Goff, L *Brain Research* **1996**, 739: 156-162.

Scanziani, M.; Salin, P.A.; Vogt, K.E.; Malenka, R.C.; Nicoll, R.A. *Nature* **1997**, 385: 630-634.

Schultz, N.M.; Kennedy, R.T. *Anal. Chem.* **1993**, 65: 3161-3165.

Schenk, J.O.; Miller, E.; Gaddis, R.; Adams, R.N. *Brain Res.* **1982**, 353-356.

Semba, J.; Kito, S.; Toru, M. *J. Neural Transm.* **1995**, 100:39-52.

Sesack, S.R.; Deutch, A.Y.; Roth, R.H.; Bunney, B.S. *J. Comp. Neurol.* **1989**, 290:213-242.

Slivka, A.; Cohen, G. *Brain Res.* **1993**, 608: 33-37.

Smith, C.U.M. *Elements of Molecular Biology*; Wiley: New York, **1996**.

Smolders, I.; Sarre, S.; Vanhaesendonck, C.; Ebinger, G.; Michotte, Y. *J. Neurochem.* **1996**, 66:2373-2380.

Stobaugh, J.F.; Repta, A.J.; Sternson, L.A.; Garren, K.W. *Anal. Biochem.* **1983**, 135, 495-504.

Svensson, L.; Wu, C.; Hulthe, P.; Johannessen, K.; Engel, J.A. *Brain Res.* **1993**, 609: 36-45.

Taber, M.T.; Fibiger, H.C. *Neuroscience* **1997**, 76:1105-1112.

Taber, M.T.; Fibiger, H.C. *J. Neuroscience* **1995**, 15(5): 3896-3904.

Tao, L.; Thompson, J.E.; Kennedy, R.T. *Anal. Chem.* **1997**, submitted.

Taylor, D.L.; Richards, D.A.; Obrenovitch, T.P.; Symon, L. *J. Neurochem.* **1994**, 62: 2368-2374.

Tossman, U.; Jonsson, G.; Ungerstedt, U. *Acta Physiol. Scand.* **1986a**, 127: 533-545.

Tossman, U.; Segovia, J.; Ungerstedt, U. *Acta Physiol. Scand.* **1986b**, 127: 547-551.

Tossman, U.; Ungerstedt, U. *Acta Physiol. Scand.* **1986**, 128: 9-14.

Tyler, E.C.; Lovinger, D.M. *Neuropharmacol.* **1995**, 34:939-952.

Ungerstedt, U. *Measurement of Neurotransmitter Release in vivo*; John Wiley and Sons: New York, **1984**.

Wages, S.A.; Church, W.H.; Justice J.B. *Anal. Chem.* **1986**, 58: 1649-1656.

Westerink, B.H.C.; Damsma, G.; Rollema, H.; DeVries, J.B.; Horn, A.S. *Life Sci.* **1987**, 41:1763-1776.

Westerink, B.H.C.; Hofsteede, H.M.; Damsma, G.; DeVries, J.B. *Naunyn Schmledebergs Arch. Pharmacol.* **1988**, 337:373-378.

Wilson, R.L.; Wightman, R.M. *Brain Res.* **1985**, 384: 342-347.

Xue, C-J.; Ng, J.P.; Li, Y; Wolf, M.E. *J. Neurochem.* **1996**, 67:352-363.

Yamamoto, B.K.; Cooperman, M.A. *J. Neuroscience* **1994**, 14: 4159-4166.

Yang, C.S.; Chou, S.T.; Lin, N.N.; Liu, L.; Tsai, P.J.; Kuo, J.S.; Lai, J.S. *J. Chromatogr. B.* **1994**, 661:231-235.

Young, A.M..; Bradford, H.F. *J. Neurochem.* **1986**, 47: 1399-1404.

Young, A.M..; Foley, P.M.; Bradford, H.F. .*J. Neurochem.* **1990**, 55: 1060-1063.

Zangerle, L.; Cuenod, M.; Winterhalter, K.H.; Do, K,Q. *J. Neurochem.* **1992**, 59: 181-189.

Zhou, S.Y.; Lunte, S.M. *Anal. Chem.* **1995**, 67: 13-18.

Zhou, S.Y.; Zuo, H.; Stobaugh, J.F.; Lunte, C.E.; Lunte, S.E. *Anal.Chem.* **1995**, 67: 594-599.

Zilkha, E.; Koshy, A.; Obrenovitch, T.P. Bennetto, H.P.; Symon, L. *Anal Lett.* **1994**, 27:453.

Zuiderwijk, M.; Veenstra, E.; Lopes da Silva, F.H.; Ghijsen, W.E.J.M. *Eur. J. Pharmacol.* **1996**, 307:275-282.

BIOGRAPHICAL SKETCH

Mark Witold Lada was born June 29, 1971, in Cleveland, Ohio. After receiving a Bachelor of Science in chemistry (cum laude) from the Ohio State University in June 1993, he worked at Lubrizol Corporation (Cleveland, Ohio) as a summer intern. Responsibilities as an analytical chemist included methods development and validation of polymers and paint additives using various chromatographic techniques. Following the internship, he began graduate school at the University of Florida in August 1993 and joined the research group of Dr. Robert T. Kennedy. He soon became interested in bioanalytical methods using capillary electrophoresis (CE), in particular, coupling microdialysis to CE for *in vivo* monitoring. In December of 1997, Mark Witold Lada received his Doctor of Philosophy in analytical chemistry from the University of Florida.

I certify that I have read this study and that in my opinion it conforms to acceptable standards of scholarly presentation and is fully adequate, in scope and quality, as a dissertation for the degree of Doctor of Philosophy.

Robert T. Kennedy, Chairman
Associate Professor of Chemistry

I certify that I have read this study and that in my opinion it conforms to acceptable standards of scholarly presentation and is fully adequate, in scope and quality, as a dissertation for the degree of Doctor of Philosophy.

Richard A. Yost
Professor of Chemistry

I certify that I have read this study and that in my opinion it conforms to acceptable standards of scholarly presentation and is fully adequate, in scope and quality, as a dissertation for the degree of Doctor of Philosophy.

James D. Winefordner
Graduate Research Professor of Chemistry

I certify that I have read this study and that in my opinion it conforms to acceptable standards of scholarly presentation and is fully adequate, in scope and quality, as a dissertation for the degree of Doctor of Philosophy.

Benjamin A. Horenstein
Assistant Professor of Chemistry

I certify that I have read this study and that in my opinion it conforms to acceptable standards of scholarly presentation and is fully adequate, in scope and quality, as a dissertation for the degree of Doctor of Philosophy.

Thomas W. Vickroy
Associate Professor of Veterinary Medicine

This dissertation was submitted to the Graduate Faculty of the Department of Chemistry in the College of Liberal Arts and Sciences and to the Graduate School and was accepted as partial fulfillment of the requirements for the degree of Doctor of Philosophy.

December, 1997

_____

Dean, Graduate School